THE UNIVERSITY
of EDINBURGH

THE UNIVERSITY
of EDINBURGH

CSPG4 in Osteosarcoma: Functional Roles and Therapeutic Potential

HARRISON WORRELL

Doctor of Philosophy
Experimental and Genomic Medicine
University of Edinburgh

2018

ABSTRACT

Osteosarcoma is the most common primary malignancy of bone. 5-year survival has remained stable at around 60-70% for 40 years. However, a number of patients will suffer from recurrent and/or metastatic disease representing a large unmet clinical need. CSPG4 is a transmembrane protein which is expressed on a number of progenitor cells and tumour types. Preliminary work had found CSPG4 present in osteosarcoma tumour samples.

In this study, CSPG4 mRNA and protein expression was demonstrated in clinical samples and model cell lines. CSPG4 mRNA is overexpressed in osteosarcoma samples compared to mature osteoblast cells, the putative cell of origin for osteosarcoma. In a cohort of patients, CSPG4 protein expression was found on 86% of samples. Furthermore, CSPG4 expression was demonstrated in U2OS, MG63, HOS, HOS-MNNG and 143B osteosarcoma cell lines.

CSPG4 protein expression was successfully deleted in 143B cells using CRISPR/Cas9 technology. Two stable CSPG4-negative cell lines were produced. CSPG4 expression was then reintroduced into negative cell lines, as well as the parental 143B cell line. This created a panel of 6 cell lines with differing CSPG4 expression. Furthermore, siRNA treatment of U2OS, MG63, 143B and U87MG cell lines reduced CSPG4 expression. These cells provided another panel with varying CSPG4 expression for in vitro investigation.

In vitro experiments failed to demonstrate a role for CSPG4 in osteosarcoma tumorigenesis. The CRISPR/Cas9 cell panel found that CSPG4 expression did not influence cell proliferation, adhesion and spreading on fibronectin or collagen-I, cell migration, chemosensitivity or

anchorage-independent growth. Similarly, the siRNA cell panel found that CSPG4 expression did not influence cell proliferation or anchorage-independent growth. In vivo experimentation did not demonstrate a role for CSPG4 in mediating osteosarcoma tumour growth or metastatic spread. Treatment with a sc-Fv antibody fragment failed to demonstrate specific toxicity of CSPG4-positive cell lines.

These results indicate that CSPG4 plays no role in osteosarcoma tumour cell behaviour. However, due to its wide expression pattern it represents a viable therapeutic option for drug targeting.

LAY SUMMARY

Osteosarcoma is the most common type of bone cancer. Survival has remained stable for 40 years and no new treatments have emerged in this time. Osteosarcoma is an aggressive tumour which is prone to spreading to distant parts of the body and failing to respond to chemotherapy. CSPG4 is a molecule found on the cell surface. It can be found throughout development and on a number of tumour types. Preliminary work had identified CSPG4 in osteosarcoma patient samples.

In this study, CSPG4 has been identified on a larger set of clinical samples. CSPG4 is overexpressed compared to healthy bone cells that are thought to give rise to osteosarcoma. Therefore, CSPG4 could act as a diagnostic tool in the future. Furthermore, 86% of samples featured CSPG4, making it an attractive target for new drugs.

In order to investigate how CSPG4 alters osteosarcoma cell behaviour, cell lines were created which were CSPG4-positive and CSPG4-negative. CSPG4 did not appear to influence osteosarcoma growth, movement or response to therapy. Using an animal model, CSPG4 also did not influence tumour growth or spread.

Therefore, CSPG4 does not appear to play a role in osteosarcoma behaviour. Due to its presence in clinical samples, CSPG4 remains a viable option for the targeting of new drugs.

DECLARATION

I declare that this thesis was composed by myself, that the work contained herein is my own except where explicitly stated otherwise in the text, and that this work has not been submitted for any other degree or professional qualification except as specified.

Harrison Worrell

September 2017

CONTENTS

ACKNOWLEDGEMENTS

I am grateful to my supervisors Professor Donald Salter and Professor Val Brunton for their help and support throughout my PhD, for allowing me to develop my own ideas and for giving me the space to direct my own research. I have learned a great deal over the course of this project, I am grateful to them for giving me that opportunity.

I would like to thank Helen Caldwell for assistance with histology samples, Morwenna Muir for assistance with animal experiments and performing intratibial surgery experiments, John Dawson for assistance with in vitro assays and Incucyte and Tesh Patel for general advice and assistance. I would like to thank them all for their continual advice and assistance over the past three years. I would like to extend this gratitude to all members of the Bone and Brunton groups for helpful discussion and input in lab meetings.

This thesis would have not possible without my parents, whose love and support over the course of my education has enabled me to succeed to this level. Special thanks to Eve for listening to my (often lengthy) hypothesises, experimental ideas and complaints for three years and for making my time in Edinburgh more special. Thanks also to all of my family and friends whose encouragement was greatly appreciated.

I would also like to thank Marley the whippet for ensuring my PhD was not the most stressful thing in my life.

LIST OF ABBREVIATIONS

3D	Three dimensional
Ack-1	Activated CDC42 kinase 1
ADP	Adenosine diphosphate
AKT	Protein kinase B
Amp	Ampicillin
BCL-2	B-cell lymphoma 2
bFGF	Basic Fibroblast Growth Factor
BLM	Bloom Syndrome RecQ Like Helicase
bp	Base pair
BRAF	B-Rapidly Accelerated Fibrosarcoma
BrdU	Bromodeoxyuridine
BSA	Bovine serum albumin
CAR	Chimeric antigen receptors
Cas9	CRISPR associated protein 9
Cdc42	Cell Division Control Protein 42
cDNA	complementary DNA
cm	Centimetre
CO2	Carbon dioxide
COL VI	Collagen 6
CREB	cAMP response element-binding protein
CRISPR	Clustered regularly interspaced short palindromic repeats
CS	Chondroitin sulphate
CS A	Placental chondroitin sulphate A
CSPG4	Chondroitin sulphate proteoglycan 4
CT	Computerised tomography
CTGF	Connective tissue growth factor
D1	Domain 1
D2	Domain 2
D3	Domain 3
DAPI	4',6-diamidino-2-phenylindole
dbSNP	Single Nucleotide Polymorphism Database
ddH_2O	Double-distilled dihydrogen monoxide
DKK-3	Dickkopf-3
DMSO	Dimethyl sulfoxide
DNA	Deoxyribonucleic Acid
DNase	Deoxyribonuclease
dNTP	Deoxyribonucleotide triphosphate
E2F	E2 transcription factor
ECM	Extracellular matrix
EDTA	Ethylene Diamine Triacetic Acid
eEF-2	Eukaryotic elongation factor 2
ERK	Extracellular Signal-Regulated Kinase
ETA	Exotoxin A
FACS	Fluorescence Activated Cell Sorting

FAK	Focal Adhesion Kinase
FAM	Fluorescein amidite
FBS	Fetal bovine serum
FFPE	Formalin fixed paraffin embedded
FGF	Fibroblast growth factor
FGF-2	Fibroblast growth factor 2
FGFR	Fibroblast growth factor receptor
FN	Fibronectin
GABA	Gamma-Aminobutyric acid
GAG	Glycosaminoglycan
GAPDH	Glyceraldehyde-3-Phosphate Dehydrogenase
gDNA	Genomic DNA
GFP	Green fluorescent protein
GRIP1	Glucocorticoid Receptor Interacting Protein 1
gRNA	Guide RNA
GTPase	Guanosinetriphosphatase
H&E	Haematoxylin and eosin
H_2O	Dihydrogen monoxide
HCL	Hydrochloric acid
HDAC	Histone Deacetylase
HER2	Human epidermal growth factor receptor 2
HGF	Hybridoma Growth Factor
HMBS	Hydroxymethylbilane synthase
HMW-MAA	High Molecular Weight-Melanoma Associated Antigen
HNSCC	Head and neck squamous cell carcinoma
HRP	Horseradish peroxidase
IF	Immunofluorescence
IGF	Insulin growth factor
IGFR1	Insulin growth factor receptor 1
IGMM	Institute of Genetic and Molecular Medicine
IHC	Immunohistochemistry
IPTG	Isopropyl β-D-1-thiogalactopyranoside
ISEMF	Intestinal subepithelial myopfibroplasts
IVC	Inferior vena cava
kb	Kilobase
kDa	Kilodalton
KO	Knock-out
kV	Kilovolt
LB	Liquid broth
mAb	Monoclonal antibody
MCSP	Melanoma chondroitin sulphate proteoglycan
MEK	MAPK/ERK kinase
mel-CSPG	Melanoma-chondroitin sulphate proteoglycan
mL	Millilitre
mM	Milimolar
mm	Millimetre
MMP-13	Matrix Metalloproteinase 13

MMP2	Matrix Metalloproteinase 2
mRNA	Messenger RNA
MSC	Mesenchymal stem cells
MSCSP	Melanoma-specific chondroitin sulphate proteoglycan
MT1-MMP	Membrane type 1 matrix metalloproteinase
MT3-MMP	Membrane type 3 matrix metalloproteinase
Na3Vo4	Sodium orthovanadate
NaCl	Sodium chloride
NAD	Nicotinamide adenine dinucleotide
NaF	Sodium fluoride
NCBI	National Centre for Biotechnology Information
ng	Nanogram
NG2	Neural glia antigen 2
NHS	National Health Service
nm	Nanometre
nM	Nanomolar
OB	Osteoblast
OMI-HtrA2	HtrA Serine Peptidase 2
OPC	Oligodendrocyte Precursor Cell
OS	Osteosarcoma
p130CAS	Crk-associated substrate p130
PAI-1	Plasminogen activator inhibitor-1
PBS	Phosphate Buffered Saline
PCR	Polymerase chain reaction
PDGF	Platelet derived growth factor
PDGF-BB	Platelet derived growth factor-B
PDGFaa	Platelet derived growth factor-A
PDGFR	Platelet derived growth factor receptor
PDK1	3-phosphoinositide-dependent protein kinase 1
PE	Phycoerythrin
PI	Propidium iodide
PI3K	Phosphoinositide 3-kinase
PKCalpha	Protein kinase C
PMSF	Phenylmethylsulfonyl fluoride
pRB	Retinoblastoma protein
PTHR	Parathyroid hormone 1 receptor
qPCR	Quantative PCR
Raf	Rapidly Accelerated Fibrosarcoma protein
Ras	Rat sarcoma protein
RCF	Relative centrifugal force
RECQ	RecQ helicase
RIPA	Radioimmunoprecipitation assay buffer
RNA	Ribonucleic acid
RNase	Ribonucleases
rpm	Rotations per minute
RT-PCR	Real time PCR
rVAR2	Recombinant VAR2CSA

sc-Fv	Single chain fragment variable
SCID	Severe Combined Immune Deficient
SEM	Standard error of the mean
siRNA	Small-interfering
SNP	Single-nucleotide polymorphism
SOC	Super optimal broth
SS RT	Single strand reverse transcriptase
TBE	Tris/Borate/EDTA
TBS	Tris-buffered saline
TBST	Tris-buffered saline tween
TGF-BETA	Transforming growth factor-
TGS	Tris-glycine-SDS
Thr	threonine
TMA	Tumour microarray
TP53	Tumour protein p53
tRNA	Transfer RNA
U	Unit
uA	Microamp
ug	Microgram
uL	microlitre
μM	Micromolar
V	Volt
WRN	Werner Syndrome RecQ Like Helicase
X-GAL	5-bromo-4-chloro-3-indolyl-β-D-galactopyranoside

LIST OF FIGURES

LIST OF TABLES

Chapter 1

Introduction

.

1.1 Osteosarcoma

Osteosarcoma is a high-grade mesenchymal malignancy and the most common primary malignant tumour of bone (Durfee et al. 2016, Whelan et al. 2012). It has a bimodal incidence peak, with the first peak rising between the ages of 10-14 and a second smaller peak occurring over 65 years of age (Whelan et al. 2012, Mirabello et al. 2009). It is a rare cancer with 3.1 cases diagnosed per million, representing only 1% of cancer cases in the US (Durfee et al. 2016, Mirabello et al. 2009). This rises to 3-5% of cases diagnosed in children (Mirabello et al. 2009). Osteosarcoma predominantly develops in relationship to the epiphyseal growth plate of the long bones and is composed of malignant osteoblast-like cells (Allison et al. 2012, Miller et al 2013). The deposition of immature osteoid matrix by these cells is essential for diagnosis (Durfee et al. 2016).

1.1.2 Molecular pathogenesis and risk factors

The aetiology of osteosarcoma is unknown and the identification of early events in tumorigenesis is frustrated by the high levels of genetic aberration that exist between individual cells and individual tumours (Allison et al. 2012). Investigations into osteosarcoma tumour karyotypes have indicated that chromosomal alterations, such as chromosomal loss, amplification and copy number gains are numerous (Martin et al. 2012). Genetic instability has also been observed in vitro with osteosarcoma cell lines displaying altered gene expression and chromosomal alterations whilst in culture (Muff et al. 2015).

A suggested mechanism behind this genomic instability is chromothripsis, a phenomenon

characterised by a single catastrophic event that results in hundreds of genomic changes (Stephens et al. 2011). While chromothripsis has been suggested to occur in only 2-3% of all cancers, it has been found that a third of osteosarcoma cases have evidence of chromothripsis (Stephens et al. 2011). There is also evidence of localised hypermutation (kataegis) in 50% of osteosarcoma samples. These events could contribute to chaotic intratumoural heterogeneity (Chen et al. 2014).

1.1.2.1 Growth and development

Whilst causative mutations are unknown, evidence of risk factors that increase the likelihood of developing osteosarcoma have been identified. One phenotypic trait that has been associated with osteosarcoma is rapid bone growth during puberty.

Babies who have shorter birth length or have a higher birth weight are more likely to develop osteosarcoma (Troisi et al. 2006). Another study reported that patients diagnosed during adolescence tend to be taller than their peers, whilst those diagnosed in adulthood did not differ significantly in height to their peers. (Longhi et al. 2005). This finding suggests bone growth is associated with risk of developing osteosarcoma. However, as a whole, evidence is mixed on the association between osteosarcoma and height with different studies drawing differing conclusions (Gianferante et al. 2017).

Stronger evidence relates osteosarcoma to growth and development during puberty. The fact that females, who undergo puberty earlier, develop osteosarcoma at a younger age than males; further implicates the risk association to puberty. Osteosarcoma is more

common in males with the male:female incident ratio being 1.5:1 cases (Mirabello et al. 2009). It is argued that this is due to greater bone growth and therefore greater chance of oncogenic insult or mitotic error. Osteosarcoma often occurs in areas of the bone responsible for bone growth during puberty.

1.1.2.2 Genetic predisposition syndromes

Whilst the genetic alterations behind osteosarcoma development usually arise sporadically, several cancer predisposition syndromes are associated with its incidence (Durfee et al. 2016).

Li-Fraumeni syndrome is a highly penetrant autosomal disorder caused by a germline mutation in the *TP53* gene and predisposes to a number of different cancer types. 30% of patients with Li-Fraumeni syndrome develop osteosarcoma (Zhang et al. 2015, Bougeard et al. 2015). Somatic loss of p53 is also important in sporadic cases (Miller et al. 1981). Loss of p53 is critical for cells to avoid cell cycle arrest and programmed cell death. Genes that regulate p53 are altered in osteosarcoma also.

Another autosomally dominant predisposition syndrome associated with osteosarcoma is familial retinoblastoma syndrome, which is caused by germline mutations in *RB1*. Through regulation of E2F transcription factors, pRB controls progression through the cell cycle (Harbour and Dean 2000). Alteration of this mechanism allows cells to progress through the cell cycle unchecked leading to elevated cell proliferation. Familial retinoblastoma syndrome patients have an incidence of osteosarcoma that is ~500 times higher than incidence in the

general population (Wong et al. 1997). Inactivation of pRB is found in 50% of osteosarcoma tumours (Lohmann 2010). Osteosarcoma is also the most common secondary tumour in patients with hereditary retinoblastoma (Lohmann 2010).

Hereditary syndromes associated with mutations in the RECQ helicase family are associated with osteosarcoma development. The RECQ helicases are involved in unwinding DNA and have roles in DNA replication, transcription and repair (Sittonen et al. 2008). Rothmund-Thompson syndrome, Baller-Gerold syndrome and Rapadilino syndrome result from mutations in the *RECQ4* gene and predispose individuals to osteosarcomas (Sittonen et al. 2008). Around one-third of patients with Rothmund-Thompson develop osteosarcoma (Wang et al. 2001). However, less than 5% of sporadic OS cases feature a RECQL4 mutation. Two other syndromes associated with RECQ mutations, Bloom (*BLM* mutation) and Werner (*WRN* mutation) syndromes are also associated with osteosarcoma with 10% of patients developing the disease (Goto et al. 1996, Sanz et al. 2016).

1.1.2.3 Molecular pathway and signalling pathways

Sequencing of whole genomes and whole exomes from sporadic osteosarcoma patient samples suggest a high prevalence of mutations in genes associated with cancer predisposition syndromes (Gianferante et al. 2017). Outside of rare inherited genetic susceptibility, a number of common single nucleotide polymorphisms (SNPs) have been discovered in a number of genes that may contribute to osteosarcoma aetiology. These genes exist in biological pathways associated with bone homeostasis, DNA-repair, apoptosis, the cell cycle, detoxification of reactive oxygen species and tumour immunity pathways

(Gianferante et al. 2017).

A number of biological pathways have been studied for their contribution to osteosarcoma development and have potential as therapeutic targets. These pathways are summarised below:

Notch pathway – Proteins involved in the Notch pathway are important for bone development and homeostasis (Zanotti and Canalis 2016). Notch proteins suppress differentiation of mesenchymal stem cells into osteoblasts, maintaining a stem cell niche (McManus et al. 2014). *HEY1*, *HES* and *NOTCH2* genes have been found overexpressed in osteosarcoma samples compared to healthy bone (Engin et al. 2009, Mu et al. 2013). There has also been correlation between Notch pathway overexpression and metastatic osteosarcoma (Zeng et al. 2016). Activation specifically in mouse osteoblasts in vivo increased osteosarcoma incidence suggesting Notch could represent a driver mutation and osteoblasts are the cell of origin (Tao et al. 2014).

Wnt pathway – The Wnt pathway has a multitude of physiological roles including bone development and cellular growth (Cai et al. 2014). Activation of the canonical pathway in osteoblast progenitors results in cellular proliferation and differentiation. In vitro studies have found that the Wnt pathway and its endogenous inhibitor, DKK-3, are upregulated and down-regulated in osteosarcoma cell lines respectively (Modder et al. 2011, Lin et al. 2013, Ma et al. 2013). However, one study found that 90% of conventional high-grade osteosarcoma samples had an absence of nuclear beta-catenin suggesting an activated Wnt pathway (Cai et al. 2010).

PI3K-mTOR pathway – The PI3K pathway is a growth-factor stimulated pathway that has important roles in the cell cycle, growth and development (Laplante and Sabatini, 2012). It is altered in a number of different cancer types as well as in 24% of osteosarcoma cases (Perry et al. 2014). Inhibition of the pathway in vitro and in vivo has shown growth suppression (Perry et al. 2014, Zhao et al. 2015). The pathway may also play a role in pulmonary metastasis. Activated Akt levels are increased in osteosarcoma tumours in patients with metastatic disease (Zhu et al. 2014). SNPs in the Akt gene demonstrated a susceptibility towards metastasic spread in one set of patients (He et al. 2013)

Ezrin – Ezrin is a protein that connects the cell cytoskeleton to the cell membrane allowing signal transduction, adhesion and motility (Sato et al. 1992). Ezrin expression has been associated with shorter survival time and larger, more aggressive osteosarcoma tumours (Lugowska et al. 2016, Li et al. 2013, Lun et al. 2014). Preclinical work has found that ezrin expression correlates with metastatic spread to the lungs and may help with early colonisation (Khanna et al 2004).

Growth factor pathways – Osteosarcoma has been shown to express a number of growth factor receptors, including IGF, PDGF, HER2, FGF, ErbB-4, PTHR, HGF, TGF-beta and CTGF (Gorlick 2009). However, it has been suggested that these pathways tend to be redundant and may represent a bystander effect, rather than being related to tumour behaviour. A recent study has shown that overexpression of PDGF in osteosarcoma may not represent a therapeutic target, as imatinib mesylate produced no benefit (Kubo et al. 2008).

1.1.2.4 Environmental factors

Osteosarcomas do not develop through an obvious multi-step progression model, as has been shown for adult tumours with an epithelial origin. Although there is no known premalignant dysplastic lesion or carcinoma in situ for osteosarcoma, incidence is known to be increased in people suffering from pre-existing bone disorders (Gorlick 2009). This is often referred to as secondary osteosarcoma. Secondary osteosarcomas can arise from bone changes that arise from fibrous dysplasia, radiation, osteochondromas, enchondroma, Ollier disease, chronic osteomyelitis, osteonecrosis and sites of prostheses or internal fixation (Ottaviani and Jaffe 2009). Paget's disease of bone, characterised by disorganized bone remodelling following excessive destruction is strongly associated with osteosarcoma, with 1% of Paget's patients developing the disease (Mirabello et al. 2009). It is more common in older patients and 20% of osteosarcomas in patients older than 40 years of age are attributed to Paget's disease.

Aside from genetic and host factors that contribute to osteosarcoma risk, there are a limited number of recognised environmental factors. Exposure to radiation is thought to be responsible for 2% of osteosarcoma cases (Picci 1978). Administration of radiotherapy is a common route through which radiation increases the risk of developing osteosarcoma (Ottaviani and Jaffe 2009). Increasing dose of radiation has a linear relationship with risk of osteosarcoma incidence (Le Vu et al. 1998).

Exposure to alkylating agents has also been found to contribute to the development of osteosarcoma (Ottaviani and Jaffe 2009). Ewing sarcoma survivors are at high-risk of

developing osteosarcoma as a secondary neoplasm due to treatment involving alkylating agents and radiotherapy (Le Vu et al. 1998). Anthracyclines, in particular, decrease the interval for the development of osteosarcoma (Newton et al. 1991). Risk of osteosarcoma rises with increasing drug exposure (Henderson et al. 2007).

1.1.3 Anatomic and histological types

Osteosarcoma has the potential to develop in any bone, however, it most often develops in the long bones of the extremities. The most common sites include the distal femur, proximal tibia and proximal humerus with less common sites including the skull, jaw and pelvis (Luetke et al. 2014). Long bones of the lower extremities account for 75% of adolescent osteosarcoma cases and are the most common site for patients over the age of 60 (Durfee et al. 2016). However, after this age, tumour sites diversify with craniofacial and axial tumours increasing in frequency (Durfee et al. 2016).

Osteosarcoma comprises of a number of different histological sub classifications (Kundu 2014) These sub classifications are described below:

Conventional – Conventional osteosarcoma is the most common type and can be further divided depending on the predominant type of extracellular matrix (ECM) produced within the tumour (Klein and Siegal 2006). These subdivisions are: osteoblastic (50%), chondroblastic (25%) and fibroblastic (25%) (Klein and Siegal 2006). Tumour cells appear spindled with pleomorphic and hyperchromatic nuclei (Klein and Siegal 2006). All

conventional osteosarcomas are assigned as high grade (Yi et al. 1991). No survival difference or difference in treatment exists between the sub-types.

Low-grade central – Low-grade central osteosarcomas are rare and account for 1-2% of cases (Griend et al. 1996). Histologically, it has variable cellularity with its matrix arranged in parallel fibrous bands (Bertoni et al. 1993). Patients have a prognosis that is significantly better than conventional osteosarcoma (Klein and Siegal 2006).

Surface – Surface osteosarcomas develop outside of the centre of the bone with little or no involvement of the medullary cavity (Klein and Siegal 2006). Most are low-grade tumours with little capacity for metastatic spread to distant sites but commonly reoccur locally (Klein and Siegal 2006). There are two main types of surface osteosarcoma:

- Parosteal – Parosteal osteosarcoma accounts for less than 5% of cases and most commonly arises on the distal posterior femur (Klein and Siegal 2006). They appear as radiopaque masses, with parallel orientation of bone trabeculae resembling periosteal bone formation. Key to diagnosis is the presence of cellular fibrous tissue within intertrabecular spaces.

- Periosteal – Periosteal osteosarcoma is less common than parosteal and usually arises in the diaphysis of the femur or the tibia (Klein and Siegal 2006). The tumours are characterised by a cartilaginous matrix arranged in to lobulated islands with spindle-cells present on the periphery (Matsuno et al. 1976).

Telangiectatic – Telangiectatic osteosarcoma is an uncommon variant that resembles a lytic bone cyst (Matsuno et al. 1976). It is defined by radiolucent bone destruction and blood-filled spaces separated by septa with malignant cells (Liu et al. 2013). Survival has been found to be better than conventional osteosarcoma in some studies (Dorfman and Czerniak 1998).

Small cell – Small cell osteosarcoma constitutes between 1-2% of cases and resembles a combination of Ewing's sarcoma and osteosarcoma histologically (Nakajima et al. 1979). Tumour cells are round and small with hyperchromatic nuclei and produce little matrix (Klein and Siegal 2006).

Extra-skeletal – Osteosarcoma that occurs outside of the skeleton accounts for 2% of soft-tissue sarcomas (Klein and Siegal 2006). Patients are usually older with most being between the ages of 50-70. Common sites include deep soft tissues such as the thigh, buttocks, upper extremities and retroperitoneum (Chung and Enzinger 1987). Extra-skeletal osteosarcomas include all the histological types that arise in bone (Klein and Siegal 2006).

A number of unusual sub-types also exist that are considered rare sub-types of conventional osteosarcoma (Kunda et al. 2014).

1.1.5 Treatment and survival

The presence of few consistent alterations results in a high level of inter- and intra-tumour

heterogeneity. This has made molecular targeting difficult, unlike in other tumours, which have seen huge strides in terms of molecular-based treatments.

Localised OS is treated through surgical resection of the primary tumour partnered with chemotherapy (Luetke et al. 2014). Radiotherapy is not often used as osteosarcoma is considered to be a radio-resistant tumour (Schwarz et al. 2009). Surgery has seen a shift towards limb salvage surgery and away from amputation (Luetke et al. 2014). Metastasectomy is also used for treatment of pulmonary metastasis (Luetke et al. 2014).

The standard chemotherapy regime consists of a combination of methotrexate, doxorubicin, cisplatin and/or ifosfamide with various protocols being used for these drugs (Luetke et al. 2014). Preoperative chemotherapy is administered for 8-10 weeks and following surgery adjuvant chemotherapy is administered for 12-29 weeks (Luetke et al. 2014). Approximately 35-45% of patients have chemoresistant tumours that arise initially or during the course of treatment. Numerous mechanisms have been proposed including increased drug efflux, increased DNA damage repair and overexpression of survival signalling pathways (Luetke et al. 2014).

30-40% cases will relapse, with metastatic spread to the lungs accounting for two-thirds of these cases. 5-year survival rates for localised disease stands at around 60-70% (Whelan et al. 2012). This level drops to ~20% for patients with metastatic disease (Whelan et al. 2012). Indeed, pulmonary metastases (the most common site for secondary tumours) are the main cause of mortality (Whelan et al. 2012, Allison et al. 2012). Metastasis can also occur in the bone but rarely in the lymph nodes. Poor survival rates are compounded by the fact that a

large number of patients present at diagnosis with metastatic disease (with many more predicted to have micrometastatic lesions).

Due to the long-term side effects associated with current treatments, poor targeting of the primary tumour and poor survival rates associated with recurrent/metastatic disease, finding novel, more-targeted therapeutic agents is paramount. Preliminary work suggests CSPG4 could represent a novel target in osteosarcoma.

1.2 CSPG4

CSPG4 is a single type I transmembrane protein which exists as a 250-300kDa core protein or a chondroitin sulphated >400kDa proteoglycan (Nishiyama et al. 1991). It was first discovered on rat neural progenitor cells and named 'Neural-Glia Protein 2' (NG2) (Nishiyama et al. 1991). The human ortholog was discovered as an antigen present on malignant melanoma cells around the same time (Wilson 1981). Due to its size and expression it was named High Molecular Weight Melanoma-Associated Antigen (HMW-MAA). Other names have included: Melanoma Cell Surface Proteoglycan (MCSP) and Melanoma-associated proteoglycan (mel-CSPG).

Cloning of the rat ortholog linked it to the human gene named Chondroitin Sulphate Proteoglycan 4 (CSPG4) and the mouse gene *AN2* (Pluschke et al. 1996, Schneider et al. 2001). The rat and mouse share 80% of their amino acid sequence with CSPG4, suggesting the gene has undergone very little change through evolution (Stegmuller et al. 2002).

The gene exists on chromosome 15:24q2 (Pluschke et al. 1996). It encodes for an 8.9kb transcript with an open reading frame of 8,071 nucleotides. This translates into a core protein of 2,326 residues (Pluschke et al. 1996). It is regulated by a promoter upstream of the translation initiation site and is 1,585 base pairs long (Sellers et al. 2009). The promoter contains sites for p300 and CREB binding proteins (Sellers et al. 2009).

The gene contains 10 exons and no spliced variants have been discovered (Nicolosi et al. 2015, Trotter et al. 2010). Using the dbSNP NCBI and ENSEMBL databases, a number of SNPs

are located in the CSPG4 gene. Five SNPs resulting in premature stop codons appear in the N-terminal part of the protein and could produce a shorter protein (Dallatomasina 2013). No genetic alterations have been found involving the CSPG4 gene, including chromosomal amplification, translocation or deletion (Nicolosi et al. 2015).

CSPG4 has undergone very little change throughout evolution, and studies on the rat protein have helped elucidate a number of its structural and functional characteristics. This expression in rat neural stem cells and melanoma has since been expanded to a number of different developmental contexts and adult tissues as well as a diverse range of tumour types (Stallcup and Huang 2008).

1.2.1 Structure

CSPG4 is unique amongst proteoglycans and cannot be grouped into structurally similar families, such as the syndecans or the aggrecans, due to a lack of common structural motifs (Nishiyama et al. 1991). Structurally, CSPG4 consists of a very large extracellular domain and a short 76 amino acid cytoplasmic domain, separated by a 25 amino acid transmembrane domain (Nishiyama et al. 1991).

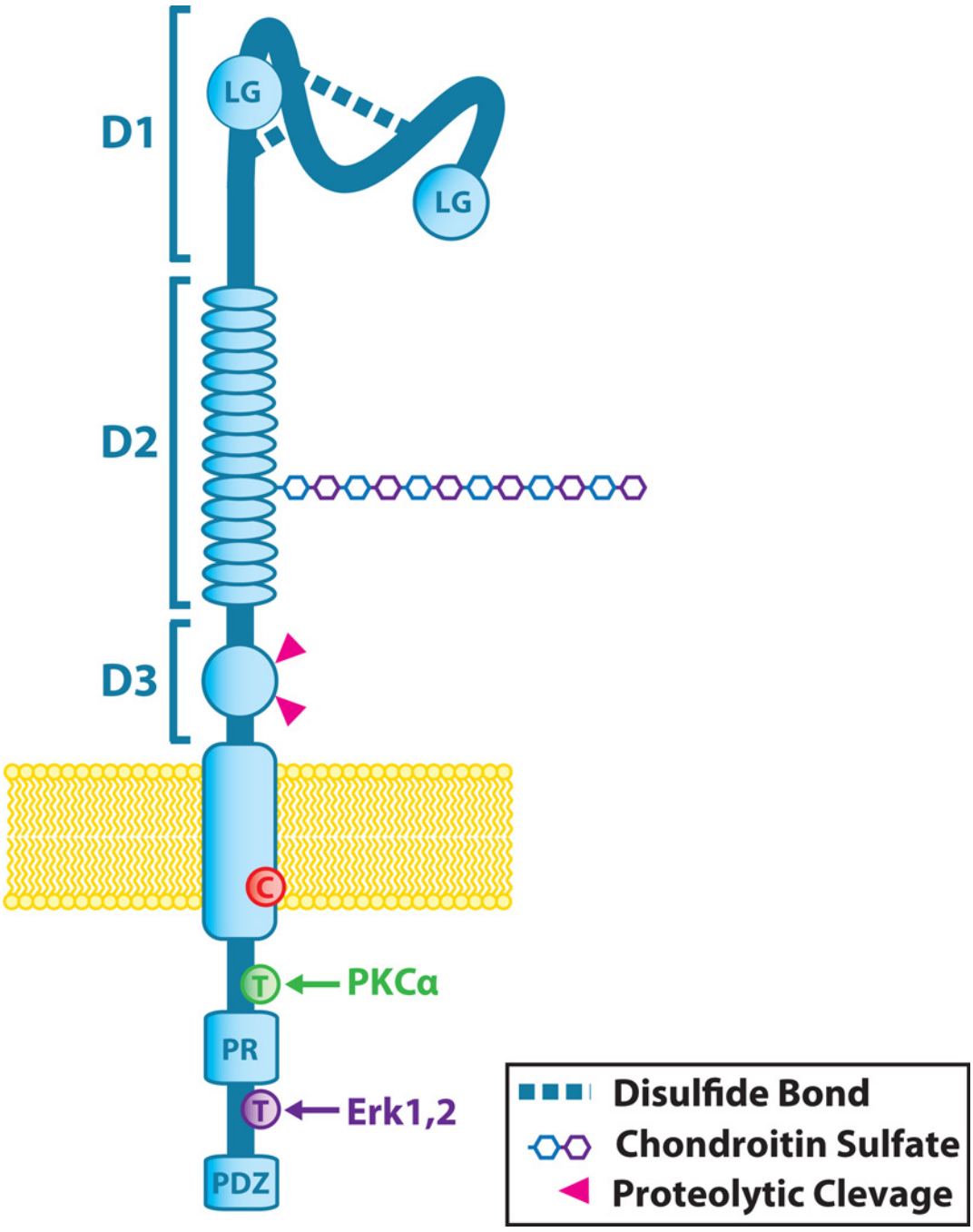

Figure 1.1 – Structure of CSPG4. The extracellular portion is comprised of three domains (D1-D3). A small transmembrane domain through the extracellular membrane (yellow). A cysteine residue (C) is found here and is thought to be critical for loicalisation to the membrane. The intracellular domain contains a proline-rich region (PR) and a PDZ-binding motif (PDZ). The intracellular domain also contains two threonine residues (T) which interact with PKC and Erk1,2. Figure taken from Price et al. (2011).

1.2.1.1 Extracellular structure

The extracellular domain of the CSPG4 protein is further split into three domains named D1-D3 (Nishiyama et al. 1991). The secondary structure (based on amino acid sequence) predicted that D1 and D3 are globular domains connected by D2, the more central extended domain (Tillet et al. 1997). This has been demonstrated by electron microscopy (Tillet et al. 1997). D1 contains two laminin G-type motifs and is stabilised by intermolecular disulphide binding. This stabilises the protein giving it a characteristic dumbbell shaped structure.

A number of surface ligands interact with CSPG4. MT3-MMP acts as a cell surface ligand for CSPG4 and leads to the formation of a complex that allows melanoma cells to destroy type I collagen, facilitating invasion into the extracellular matrix (Iida et al. 2001). Other surface ligands include plasminogen and angiostatin, through which the CSPG4 ectodomain interacts with kringle domains in the proteins. The complex formed between plasminogen and CSPG4 accelerates the activation of plasminogen by urokinase forming plasmin (Goretzki et al. 2000). This may facilitate plasmin's role in degradation of the ECM, which is essential for cellular migration. CSPG4 was shown to bind to the kringle domains of angiostatin (Goretzki et al. 2000). Angiostatin is an anti-angiogenic protein that halts endothelial proliferation. Through binding to angiostatin, CSPG4 inhibits the anti-proliferative effect of angiostatin (Goretzki et al. 2000).

CSPG4 has also been found to bind soluble ligands such as PDGFaa and bFGF (Goretzki et al. 1999). It then acts as a co-receptor and presents the ligands to their cognate receptors (Stallcup and Huang 2008).

The D2 domain has an alpha helical domain that has been shown to directly bind collagens V and VI, providing an important mechanism through which CSPG4 binds to the ECM (Stallcup and Dahlin-Huppe 2001, Burg et al. 1996, Burg et al. 1997). The D2 domain contains the attachment site (ser-999) for chondroitin sulphate (CS) chain modification (Stallcup and Dahlin-Huppe 2001). Attachment of GAG chains is cell-type specific and depends on developmental context (Schneider et al. 2001). The role the glycosylation pattern of CSPG4 plays, and indeed the role of the chain itself is relatively unknown. However, it has been suggested to control intracellular localisation and interaction with specific membrane-bound proteins (Stallcup and Dahlin-Huppe 2001, Iida et al. 1992, Iida et al. 2001, Iida et al. 2007). It has also been shown to be involved in CSPG4 attachment to α4β1 and fibronectin (Price et al. 2011). The CS chain has also been demonstrated to facilitate the activation of proMMP2 by matrix metalloproteinases present in the membrane (Iida et al. 2007).

The third domain, D3, contains carbohydrate domains that have been implicated to be responsible for CSPG4 binding to galectin-3, p-selectin and beta-1 integrin (Fukushi et al 2004, Wen et al 2006). The D3 domain also contains putative proteolytic sites, allowing CSPG4 to be shed from the cell surface (Nishiyama et al. 1991). Three molecular forms of different sizes are expressed by different cell lines and present in the tissue culture supernatant of the cells (Nishiyama et al. 1995). Shed CSPG4 has been found in large amounts within the central nervous system (CNS), this increases following injury to the cerebral cortex (Asher et al. 2005). It was suggested in this study CSPG4 was cleaved from the cell surface in order to limit cell proliferation, as shredded CSPG4 increased with increasing cell density (Asher et al. 2005). CSPG4 has also been found in a number of pathological settings, such as spinal cord injuries and multiple sclerosis (Jones et al. 2002, De

Castro et al. 2005). Fragments of CSPG4 have also seen found in the sera of normal patients and those with metastatic disease (Price et al. 2011). Soluble CSPG4, when bound to endothelial cells, has been found to increase cell motility and angiogenesis using a corneal pocket assay (Wen et al. 2006, Fukushi et al. 2004). Whilst a number of studies have investigated the tryptic products, no definitive physiological or pathological functions have been described (Nicolosi et al. 2015).

Attachment or association with extracellular components such as integrins and matrix proteins alongside functional intracellular domains allows CSPG4 to mediate the cells relationship to its environment and to influence cellular behaviours such as cell migration, cell proliferation, invasion, extra-cellular remodelling and angiogenesis.

1.2.1.2 Intracellular structure

CSPG4 contains a number of intracellular domains, which are important for its function. A PDZ-domain is present at the extreme C-terminus end and mediates attachment to scaffolding proteins such as synthetin-1 (involved in oligodendrocyte migration), MUPP-1 (a multivalent scaffold protein) and GRIP1 (a scaffold protein) (Stallcup 2008). It is through these scaffolding proteins, as well as proteins such as ezrin and cofilin-1 that CSPG4 is linked to intracellular signalling pathways and the actin cytoskeleton (Stallcup 2008).

CSPG4 co-localises with actin and myosin containing microfilamentous stress fibres (Lin et al. 1996a). It was suggested it used these fibres to anchor itself to the cytoskeleton (Lin et al. 1996a). CSPG4's location on the cell membrane depends on the ECM component the cell is

in contact with. Whilst spreading on fibronectin-coated plates, which engages integrins, CSPG4 associates with stress fibres. Cells spreading on poly-L-lysine coated dishes results in CSPG4 localising in radial processes that emanate from the cell periphery (Lin et al 1996b). CSPG4 localises with a distinct set of radial processes that are fascin-negative and appear to be filopodia (Lin et al 1996b). Fascin-containing processes are located at the opposite pole of the cell in lamellipodia (Lin et al 1996b). The cytoplasmic tail of CSPG4 is critical for correct migration of cells (Fang et al. 1999). A CSPG4 mutant that lacks the cytoplasmic domain cannot relocalise, explaining the incorrect migratory response (Fang et al. 1999).

CSPG4's cytoplasmic tail has a role in recruiting and activating downstream mediators in order to induce cytoplasmic rearrangement. In melanoma cell lines activation of CSPG4 and clustering of the protein caused the activation of Rho-family GTPase Cdc42 converting it to a GTP-bound site (Eisenmann et al. 1999). Cdc42 is a protein responsible for the formation of filopodia (Eisenmann et al. 1999). CSPG4 then recruits Cdc42 and Cdc42-associated tyrosine kinase, Ack-1, into a signalling complex which activates and recruits $p130^{cas}$ (Eisenmann et al. 1999).

CSPG4 also contains two important threonine phosphoacceptor sites, Thr^{2256} and Thr^{2314} (Makagianar et al. 2007). Following PDGF-BB stimulation, PKCα and ERK phosphorylate the Thr2256 and Thr2314 sites respectively (Makagianar et al. 2007). Phosphorylation at these sites has been found to be critical in balancing between cell motility and cell proliferation, with PKCα promoting motility and ERK stimulating cell proliferation (Makagianar et al. 2007).

Analysis of CSPG4's primary sequence found a putative D-domain docking site, where ERK 1,2 binds and explains how CSPG4 could potentiate downstream signalling. Proline-rich regions present within the cytoplasmic tail may also facilitate further protein interactions and influence signalling pathways, however, no information yet exists on this site (Stallcup and Huang 2008).

Therefore, CSPG4 has a complex structure that allows it to regulate a number of different functions within the cell, making it an important protein within development but also in tumorigenesis.

1.2.2 Tissue distribution

CSPG4 is present on a number of different cell types throughout growth and development (Stallcup and Huang 2008). CSPG4 is recognised as being a marker of an activated cell type. While not present on multipotent stem cells, it is upregulated on motile and mitotic progenitors before being downregulated again during the onset of terminal differentiation (Stallcup and Huang 2008). However, expression persists following terminal differentiation on a select number of cell types. It has been suggested that CSPG4 is expressed in >10 organs in the human adult body, including the brain, gastrointestinal tract and endocrine organs (Nicolosi et al. 2015). Expression is also upregulated in pathological conditions, most notably in a number of tumour types.

1.2.2.1 Distribution in the central nervous system

CSPG4 has been most studied in the central nervous system. It is associated with glial precursor cells. It was initially recognised as a marker for precursor cells of oligodendrocyte lineage (Nishiyama 1996). In development, oligodendrocytes populate the entire CNS and myelinate neurons (Stallcup and Huang 2008). Oligodendrocyte progenitor cells undergo asymmetrical mitosis with CSPG4 expression confined to just one daughter cell (Sugiarto et al. 2011). The CSPG4-negative cells differentiate into mature oligodendrocytes whilst the CSPG4-positive cells maintain the progenitor stock (Sugiarto et al. 2011). A breakdown in this asymmetry is thought to result in a premalignant state with tumour-initiating potential (Sugiarto et al. 2011). A population of these CSPG4-positive cells persists in to adulthood.

CSPG4-positive precursor cells have been shown to develop into protoplasmic astrocytes (Zhu et al. 2008). Protoplasmic astrocytes are found predominantly in the white matter; however, protoplasmic astrocytes developing from CSPG4-positive progeny are found in the grey matter of the spinal cord and central forebrain (Miller and Raff 1984). This research suggests the differentiation path that CSPG4-positive pluripotent cells take depends on the microenvironment in which they are present (Stallcup and Huang 2008). In vitro, the differentiation of CSPG4-positive pluripotent cells can be determined by culture environment (Zhu et al 2008).

CSPG4-positive cells are antigenically distinct from the classical glial cell types (Nishiyama et al. 2002). The name ‘polydendrocyte’ has been proposed to describe all CSPG4-expressing positive cells within the CNS (Nishiyama et al. 2002). These cells have a branched

morphology and are present in the grey and white matter (Nishiyama et al. 2009). Polydendrocytes have also been found to interact with neurons, receiving synaptic input (Nishiyama et al. 2009).

Historically, CSPG4-positive cells were thought to be distinct from neuronal stem cells and only gave rise to mature glial cells. An early study demonstrated through immunofluorescent double-labelling experiments that tetanus toxin (a marker specific to neurons) expression was found on a subpopulation of cells with NG2-positivity in cultured rat brain samples (Stallcup 1981). More recent evidence has demonstrated that CSPG4-positive progenitor cells differentiate into GABAergic neurons within the mouse hippocampus (Belachew et al. 2003). However, the ability to acquire a neuronal fate may depend on epigenetic mechanisms. Treatment of CSPG4-positive oligodendrocytes with HDAC inhibitors enabled activation of a neuronal gene expression programme (Liu et al. 2009).

1.2.2.2 Distribution in the musculoskeletal system

CSPG4 expression has also been studied in musculoskeletal system. CSPG4 has been found in the developing limb bud of rat. Whilst not present on early stem cells within the limb bud, it is upregulated as precursors make the initial commitment to chondrocyte lineage and organise into mesenchymal condensations (Nishiyama et al. 1991). CSPG4's expression continues to increase as differentiation occurs but is then downregulated following hypertrophic maturation of chondrocyte cells (Nishiyama et al. 1991). CSPG4 expression has also been demonstrated on foetal and adult chondrocyte cells (Midwood and Salter 1998).

Once chondrocytes reach the hypertrophic stage, the extracellular matrix starts to calcify and cells invade the microenvironment with blood vessels (Fukushi et al. 2003). The invading cells represent progenitor cells that develop into osteoblasts (Fukushi et al. 2003). CSPG4's presence has been found on immature osteoblasts which line newly formed bone as well as secondary ossification centres within the epiphysis (Fukushi et al. 2003). Its expression is downregulated once ossification takes place (Fukushi et al. 2003). CSPG4 was also found at osteogenic bone fronts and in the cellular suture matrix during intramembranous ossification (Fukushi et al. 2003). CSPG4 co-localises with tenascin-c on preosteoblast cells within ossification centres (Fukushi et al. 2003). Tenascin-c is responsible for alkaline phosphatase production and is thought to be involved in bone cell differentiation. It is proposed that CSPG4 could act as a cell-surface receptor for tenascin-c and mediate its role in differentiation (Fukushi et al. 2003). A role for CSPG4 directing osteoblast differentiation has been demonstrated through an association with collagen VI in the periosteum of rat femoral diaphysis (Kohara et al. 2015). CSPG4-positive cells migrate into the groove of Ranvier where they interact with collagen VI (Kohara et al. 2016). Mature osteoblasts with osterix-positivity, migrate away from the groove and Ranvier and start producing bone within the epiphyseal region of the cortical bone (Kohara et al. 2016).

Elsewhere within the adult musculoskeletal system, CSPG4 expression is found within the sarcolemma and neuromuscular junction. This expression is present postnatally but decreases with age (Petrini et al. 2003).

1.2.2.3 Distribution in the integumentary system

CSPG4 has been shown to be expressed present in human skin. In samples of non-palmoplantar skin samples from the scalp, breast, finger and foreskin, CSPG4 expression was found in the epidermis but not the dermis (Legg et al. 2003). CSPG4 is also present on the surface of hair follicle progenitor cells (Ghali et al. 2004). Within the interfollicular epidermis, CSPG4 immunoreactivity is seen on a subset of basal keratinocytes, predominantly within the tips of dermal papillae (Legg et al. 2003). These keratinocytes were Ki67-negative suggesting they are slow-cycling stem cells (Legg et al. 2003). Whilst research has focused on using adult human skin samples, developing skin in the mouse has also been investigated for CSPG4 expression. Prenatal mouse skin is negative for CSPG4, but at post-natal day one, CSPG4 expression can be found within the dermis, the outer root sheath of the hair follicles and the basal layer of keratinocytes (Kadoya et al. 2008). By postnatal day 7, expression remained in the keratinocytes but was gone from the bulge region and the dermis, in parallel with human adult skin (Kadoya et al. 2008). CSPG4 expression was also found within developing adipocytes in the subcutis (Kadoya et al. 2008).

1.2.2.4 Distribution in the vasculature

A role for CSPG4 has been established in the vasculature. During development, cardiomyocytes within the embryonic mouse heart and mural cells within the microvasculature and smooth muscle cells associated with blood vessels, are positive for CSPG4 (Ozerdam et al. 2001, Grako and Stallcup 2001). Expression within vasculature continues postnatally but is restricted to pericytes involved in vasculogenesis or

angiogenesis (Schlingemann et al. 1990). No staining is found on endothelial cells during these stages (Schlingemann et al. 1990). CSPG4 is also present on angiogenic pericytes involved in abnormal or pathological angiogenesis. Studies inducing angiogenesis through retinal hyperoxia and exogenous angiogenic growth factor placement in the cornea show CSPG4 expression on pericytes (Ozerdam et al. 2001). CSPG4 is also expressed during wound healing and tumour angiogenesis (Schlingermann et al. 1990). In vitro studies have found CSPG4 present on pericytes can affect availability of anti-angiogenic proteins such as angiostatin, increase endothelial cell proliferation and induce tube sprouting (Goretzki et al. 2000, Chekenya et al. 2002, Fukushi et al. 2004).

1.2.2.5 Distribution in the gastrointestinal system

CSPG4 expression has also been found in the adult small and large intestine. Intestinal subepithelial myofibroplasts (ISEMFs) are positive for CSPG4 and play a role in wound healing (Terada et al. 2006). These cells form a layer in the lamina propria under epithelial cells, CSPG4 is expressed on the ISEMFs through the crypt to the villi (Terada et al. 2006).

1.2.2.6 Distribution in tumours:

CSPG4 has been most extensively studied in melanoma and glioblastoma, however it has also been discovered on a number of other tumour types (Wang et al. 2011). CSPG4 has been found in chondrosarcoma (Jamil et al. 2016); head and neck squamous cell carcinoma (Warta et al. 2014); breast carcinomas (Wang et al. 2010, Hsu et al. 2013); soft-tissue sarcomas (Cattaruzza et al. 2013, Benassi et al. 2009); chordoma (Schoenfeld et al. 2016);

mesothelioma (Rivera et al. 2012); rhabdomyosarcoma (Brehm et al. 2014); endometrial epithelial cancer (Winship et al. 2017); hepatocellular carcinoma (Lu et al. 2015); pancreatic cancer (Keleg et al. 2014); acute myeloid leukaemia (Smith et al. 1996, Petrovici et al. 2010); acute lymphoblastic leukaemia (Behm et al. 1996) and mixed lineage leukaemia (Mauvieux et al. 1999). CSPG4 has a number of predicted roles in tumorigenesis, such as increased proliferation, migration, adhesion, invasion, metastasis and chemoresistance.

1.2.4 Role in proliferation

As previously mentioned, CSPG4 plays a major role in proliferative behaviour of progenitor cells, as well as tumour cell populations. Evidence suggests that the protein has no catalytic activity of its own and that it potentiates cellular proliferation by acting as a co-receptor for FGFR and PDGFR and influencing Erk 1,2 signalling downstream (Price et al. 2011). Research has demonstrated that the CSPG4 core protein can bind PDGFaa and FGF, with high affinity (Goretzki et al 1999). CSPG4 may have a role in organising and presenting growth factors to their cognate receptors (Goretzki et al 1999).

CSPG4 co-localises with PDGFR on O2A cells in the developing rat brain and on cells in culture (Nishiyama et al. 1996a). Indeed, immunoprecipitation experiments demonstrated that CSPG4 and PDGFR form a molecular complex in vivo (Nishiyama et al. 1996b). Expression of both proteins decrease as the cells differentiate. If differentiation is blocked via bFGF treatment, both CSPG4 and PDGF expression is increased, suggesting they are co-ordinately regulated (Nishiyama et al. 1996b). Reduction of CSPG4 reduces the proliferative ability of O2A cells and correlates with a reduction in PDGFR expression (Nishiyama et al.

1996b). CSPG4 also potentiates proliferation of smooth muscle cells when treated with PDGF-aa (Grako et al. 1995). CSPG4-negative pericytes respond to PDGFbb as wild-type cells do, but fail to proliferate when treated with PDGFaa, as wild-type pericytes do (Grako et al. 1999). This supports the idea that CPSG4 acts in conjunction with PDGFR in order to direct cellular proliferation.

Similarly to PDGFaa, CSPG4 sequesters FGF-2, thereby increasing the ligands accessibility and availability to its receptor (Cattaruzza et al. 2013). CSPG4-negative pericytes and smooth muscle cells fail to proliferate when treated with FGF-2 (Ozerdam and Stallcup 2004, Cattaruzza et al. 2013). The CSPG4 ectodomain can compensate for low FGFR expression and increases mitosis of pericytes (Cattaruzza et al. 2013).

The interaction of CSPG4 with PDGFaa and FGF activates ERK 1,2 signalling downstream. ERK is a constituent member of the Ras-Raf-MEK-Erk pathway. This pathway is activated by a number of proteins, such as integrins and receptor tyrosine kinases, on the cell surface that contribute to growth and differentiation. Once a signal has been initiated and transduced down the protein cascade, ERK is activated and translocated into the nucleus to activate genes responsible for proliferation (Price et al. 2007). CSPG4-negative smooth muscle cells fail to activate ERK in response to PDGFaa, whereas CSPG4-positive cells can phosphorylate ERK and increase proliferation (Grako et al. 1999). Expression of CSPG4 activates ERK in melanoma cell lines (Yang et al. 2004). Melanoma cell lines with the BRAFV600E mutation require CSPG4 for maximal ERK activation (Yang et al. 2009).

Extracellular signalling can regulate the phosphorylation of the intracellular domain of

CSPG4. PDGF-BB and constitutively activated MEK-DD activate ERK 1,2 which phosphorylates CPSG4 at Thr^{2314} and increases proliferation (Makagiansar et al. 2007). Phosphorylation of the cytoplasmic Thr^{2314} domain causes CSPG4 re-localisation to apical membrane protrusions, where it co-localises with β1 integrins (Makagiansar et al. 2007). Phosphorylation of different threonine sites causes different re-localisation but CSPG4 still co-localised with β1 integrins. Therefore, CSPG4 could influence proliferation downstream in conjunction with integrins when localised in discrete cellular compartments. Cells featuring a mutation in the Thr^{2314} domain of CSPG4 cannot proliferate and show reduced ERK signalling (Makagiansar et al. 2007). This was shown in A375 melanoma cell line, which endogenously expresses CSPG4 and U251 glioblastoma cell line in which CSPG4 was transfected (Makagiansar et al. 2007). Interestingly, U251 CSPG4-positive cells exhibited high basal proliferation rates suggesting CSPG4 could influence proliferation independently of extracellular cues (Makagiansar et al. 2007).

This CSPG4-dependent impact on proliferation is seen in glioblastoma clinical samples and glioblastoma cell lines in culture (Al-Mayhani et al. 2011). Glioblastoma cells sorted through FACS for CSPG4 expression exhibit higher proliferation levels than those with low CSPG4 expression. This is mirrored in cell samples taken from patients with glioblastoma, where CSPG4 expression denotes an actively proliferating subset of cells (Al-Mayhani et al. 2011). The proliferative advantage of CSPG4-positive cell lines was shown to be cell autonomous and does not depend on extracellular cues (Al-Mayhani et al. 2011). Inhibition of CSPG4 delays soft-tissue xenograft growth and reduced cell proliferation by 50% (Hsu et al. 2017).

1.2.5 Role in migration and adhesion

CSPG4 also plays a major role in the migratory behaviour of a number of different cell types. This is in addition to a number of other aspects that are critical for the metastatic cascade, such as adhesion and invasion. Indeed, targeting CSPG4 with monoclonal antibodies reduces melanoma cell attachment and spreading (Bumol et al. 1984).

CSPG4 has been shown to play a role in adhesion to a number of different components of the extracellular matrix. It is thought that these attachments promote motility via downstream signalling emanating from the intracellular tail following engagement of the extracellular domain by the ECM. CSPG4's association with collagen VI (Col VI) has been comprehensively studied. CSPG4 binds to Col VI directly via the central domain of its structure (Tillet et al 1997). This interaction is seen on the surface of several cell lines as well as on the surface of arteries in the rat spinal cord and within the rat intervertebral disc (Stallcup 1990). Alteration of CSPG4's location on the cell surface results in a different variation of Col VI's distribution (Stallcup 1990). CSPG4 is important in retaining Col VI at the cell surface (Nishiyama and Stallcup 1993). This relationship has been shown to result in greater migratory potential for cells. Interaction of CSPG4 and Col VI results in extensive cell spreading and morphological change (Tillet et al. 2002). The spreading that occurs after CSPG4 and Col VI association is mediated by α3β1 integrin (Cattaruzza et al. 2013). Glioma cell lines expressing CSPG4 have a greater potential to migrate on Col VI-coated plates than CSPG4 negative cells (Burg et al. 1997). Migratory behaviour has also been found to depend on the α3β1 integrin, as well as downstream signalling of the PI3K pathway (Cattruzza et al. 2013).

The interaction of CSPG4 and Col VI and subsequent increase in migratory behaviour may be important in tumour metastasis. CSPG4 and Col VI expression has been demonstrated through qPCR analysis in both primary and metastaic lesions from soft-tissue sarcoma patients (Cattaruzza et al. 2013). Higher expression of the two proteins correlated with the worst disease course present in the sub-set of patients studied and an abundance of both in primary tumours was common in patients who developed metastatic disease (Cattruzza et al. 2013).

CSPG4 has been found to bind a number of other ECM components such as collagens II and V, tenascin, laminin and fibronectin (Burg et al. 1996). CSPG4's interaction with fibronectin has been shown to be important for melanoma cell adhesion and migration, therefore contributing to their tumorigenicity. CSPG4 mediates melanoma cell lines adhesion to fibronectin in conjunction with α4β1 integrin (Iida et al. 1992). Melanoma cell lines are able to achieve a fully spread morphology on a substrate chimera consisting of CSPG4 antibodies and the fibronectin region, FN IIICS (Iida et al 1995). This is not achieved for substrate chimera consisting of CSPG4 antibodies and other components of the extracellular matrix, such as collagen VI (Iida et al 1995). CSPG4 transfected into MW1552C, a melanoma cell line, enhanced the phosphorylation of FAK and ERK 1,2 (Yang et al. 2004).

CSPG4 also plays a role in migration that is potentiated through growth factor signalling. As previously mentioned, CSPG4 intracellular tail contains two distinct phosphoacceptor sites which, when activated, differentially alter cell behaviour. PDGF-BB treatment activates PKCα, which phosphorylates CSPG4 at Thr^{2256} resulting in increased cell motility

(Makagiansar et al. 2007). Once phosphorylated, CSPG4 relocalises to lamellipodia alongside β1. Both are present at the leading edge of the cell when migrating (Makagiansar et al. 2007). Whilst migration in response to PDGF-BB occurs through mechanisms unrelated to CSPG4, when endogenously expressed, it enhances the migratory effect above that seen by CSPG4-negative cells (Makagiansar et al. 2007). Variants of the protein that mimic a phosphorylated Thr^{2256} site enhance migration independent of growth factor treatment (Makagiansar et al. 2007).

CSPG4 shed from the cell surface has also been shown to influence the migratory behaviour of cells it interacts with. The formation of a molecular complex consisting of galectin-3, α4β1 and CPSG4 influences motility of endothelial cells (Fukushi et al. 2004). This encourages sprouting and formation of new blood vessels during angiogenesis. The shedding of CSPG4 occurred from the surface of the pericyte cells lining the vessels (Fukushi et al. 2004).

As well as transducing signals from the ECM, CSPG4 has also been shown to actively modify the ECM through proteases. Studies from melanoma have demonstrated it mediates invasion through collagen I via activation of MT1-MMP and MMP2 (Iida et al. 2001; Iida et al. 2007). It is important to note that collagen I is a major component of the bone ECM (Viguet-Carrin et al. 2006).

CSPG4 helps regulate the internal architecture of the cell in response to signals from its environment, allowing the cell to migrate. CSPG4-positive cells can attach and spread on surfaces coated with CSPG4 antibodies, highlighting its involvement in these processes (Fang et al. 1999). This illustrates that engagement of CSPG4 must be able to alter the

cytoskeleton, thereby facilitating spreading to occur. Different antibodies targeting different epitopes on the protein produce different forms of actin rearrangement (Fang et al. 1999). Migration requires the cytoplasmic tail of CSPG4. Mutated forms of the protein that contain the ectodomain only, can spread but cannot migrate with the cells forming abnormal arrays of radial actin filaments (Fang et al. 1999).

CSPG4 co-localises with actin and myosin positive stress fibres allowing it to anchor to the cytoskeleton (Lin et al. 1996a). As well as being present on lamellipodia, CSPG4 has also been shown in filopodia (Lin et al. 1996b). Its interaction with the actin cytoskeleton is mediated through small GTPases. During cytoskeleton reorganisation, CSPG4 recruits $p130^{cas}$ and activates Cdc42 and Ack-1 allowing a signalling cascade starting the process (Eisenmann et al. 1999). The GTPase rac also interacts with CSPG4 and may help form the lamellipodia structure (Majumandar et al. 2003).

The above roles in adhesion, motility and invasion are also seen alongside an increase in metastasis in cells bearing CSPG4 (Benassi et al. 2009, Cooney et al. 2011). Indeed, this is underlined by studies on patient samples where expression has been found to be higher in metastatic lesions (Cooney et al. 2011, Benassi et al. 2009, Cattaruzza et al. 2013). This has been comprehensively shown in soft-tissue sarcoma. Through qPCR analysis, high expression in primary tumours can predict metastatic spread and is associated with lower metastasis-free survival (Benassi et al. 2009). CSPG4 has also been shown to be overexpressed in metastatic breast cancer tissues (Cooney et al. 2011). Research has found that CSPG4's GAG chain may function as a receptor for P-selectin, which may aid survival during metastatic dissemination through the circulation (Cooney et al. 2011). Removal of

the GAG chain from cells, diminished metastatic tumour development in the lungs of mice, suggesting CSPG4 may play a role in tumour colonization (Cooney et al. 2011).

1.2.6 Role in cell survival and chemoresistance

An emerging problem within cancer treatment is resistance to chemotherapy and other targeted drugs. CSPG4 is overexpressed by a number of tumour types that fail to respond to chemotherapy (Price et al. 2011).

In glioblastoma cell lines, CSPG4 has been found to offer a protective effect and helps mitigate apoptosis in response to cellular stress (Chekenya et al. 2008). TNF-alpha treatment, a pro-apoptotic mediator, produced lower cell death in U251 cells that exogenously expressed CSPG4 than wild-type CSPG4 negative U251 cells (Chekenya et al. 2008). This resistance is also seen when cells are treated with chemotherapy. U87 glioblastoma cell lines which endogenously express CSPG4, are resistant to doxorubicin. U87 cells treated with CSPG4 shRNA become sensitive to doxorubicin, demonstrating that the cell line is dependent on CSPG4 for drug resistance and survival (Chekenya et al. 2008). In order to attenuate apoptosis following drug treatment, CSPG4 interacts with α3β1, which subsequently activates the PI3K/Akt pathway. The PI3K/Akt promotes cell survival and its inhibition diminishes the cell survival effect seen in CSPG4-positive cells (Chekenya et al. 2008). Glioblastoma cell spheroids derived from biopsy samples also demonstrated a correlation between chemoresistance and CSPG4 expression (Chekenya et al. 2008).

Short-lived responses to molecular therapies are common as patients develop resistance to

the drugs. CSPG4 has also been found to increase resistance to BRAF-selective inhibitors in melanoma cell lines. Melanoma cell lines are more resistant to dabrafenib-induced cell toxicity if they express CSPG4 (Washura et al 2013). CSPG4 expression potentiates survival signalling through the PI3K pathway and through phosphorylation of Akt (Washura et al. 2013). Antibodies directed to CSPG4 enhanced the initial effects of BRAF-selective inhibitors and prolonged their effect compared to control conditions (Yu et al. 2011). CSPG4's contribution to survival depends on the PI3K/Akt axis, if the pathway is abrogated; CSPG4 expression has no effect on cell survival (Javaid et al. 2015).

Outside of PI3K signalling, CSPG4 has been shown to mitigate the effects of oxidative stress through binding of pro-apoptotic serine proteases (Maus et al. 2015). CSPG4 expression on oligodendrocyte progenitor cells binds OMI-HtrA2. OMI-HtrA2 is a protein released from damaged mitochondria following cellular stress in order to degrade anti-apoptotic factors (Maus et al. 2015). This interaction reduces the cytosolic activity of OMI-HtrA2, making the cell less sensitive to oxidative stress. CPG4-null and CPSG4 knock-down OPC cells are more sensitive to oxidative stress and experience higher levels of apoptosis (Maus et al. 2015). The study also demonstrated that glioma cell lines with high CSPG4 expression were less sensitive to oxidative stress. This is reversed through siRNA treatment of CSPG4 (Maus et al. 2015).

CSPG4 expression has been linked to the up-regulation of drug transporter proteins in mixed-lineage leukemia (MLL) cells making them less sensitive to chemotherapy treatment (Nicolosi et al. 2015).

1.2.8 Therapeutic targeting

CSPG4 has been investigated as a potential molecular therapy for targeting cancer. Its expression on a number of tumour types, limited distribution in normal tissues and location on the cell surface make it an attractive target. Studies disrupting CSPG4 expression have found that tumour viability and behaviour is altered underlining CSPG4's potential as an anti-cancer target. Wang et al. (2011) found that shRNA directed towards CSPG4 reduced tumour growth and angiogenesis in melanoma and glioblastoma models. This impact on angiogenesis may be mediated through CSPG4 expression on pericytes, offering the potential that CSPG4 could be used as a dual-targeting approach to target the tumour stroma as well as cancer cells.

Antibody-based treatments have shown to improve the clinical course of a number of solid and haematological tumours (Scott et al. 2012). Antibody-based therapeutics can act through a number of mechanisms. Monoclonal antibodies (mAb) can be used to alter the function of the tumour antigen by causing endocytosis or blocking its interactions. This may decrease oncogenic signalling pathways the antigen interacts with (Scott et al. 2012). Antibodies can be used to modulate the immune system, attracting cytotoxic immune cells to the site of the tumour where they are able to recognise, previously unrecognisable tumour cells through the antibody-antigen complex and induce cytolysis of tumour cells (Scott et al. 2012). Antibodies have also been developed that are conjugated to cytotoxic drugs. Through the antibody binding to the tumour, cytotoxic drugs can be delivered to the tumour directly (Scott et al. 2012). These approaches have been used to target CSPG4 in vitro and in vivo.

Due to CSPG4's role in influencing oncogenic signalling pathways implicated in tumorigenesis, naked antibodies have been investigated to block CSPG4's function for therapeutic gain. The monoclonal antibodies, TP41.2 and 225.28 have been used to target mesothelioma and breast cancer respectively (Rivera et al. 2012, Wang et al. 2010). Both antibodies reduced adhesion, migration and growth in vitro. TP41.2 further showed reductions in invasiveness alongside increased apoptosis (Rivera et al. 2012, Wang et al. 2010). Tested in vivo, TP41.2 reduced mesothelioma tumour growth in mice and increased their survival (Rivera et al. 2012). mAb 225.28 was shown to cause the regression of breast cancer metastasis in the lungs as well as inhibiting spontaneous metastasis from primary tumours in the mammary fat pad (Wang et al. 2010). In another study, mAb 225.28 extended the duration and effect of BRAF inhibitors in melanoma cell lines. The antibodies effect was suggested to occur through the abrogation of several signalling pathways related to tumorigenesis (Yu et al. 2011).

Another strategy for delivering function-blocking proteins to tumours is the use of single-chain fragment variable (sc-Fv). The Fv subunit of the antibody molecule is the smallest part concerned with antigen-binding function (Wang et al. 2011). sc-Fv fragments are advantageous to whole antibody molecules due to the fact their smaller size could offer deeper penetration into tumour tissues, resulting in greater therapeutic benefit (Wang et al. 2011). They also avoid off-target Fc receptor mediated uptake by non-cancerous cells (Schwenkert et al. 2008).

An sc-Fv directed to CSPG4 was found to bind with melanoma, glioma, basal breast carcinoma, mesothelioma, chondrosarcoma and osteosarcoma cells (Wang et al. 2011). As

with studies that investigated whole antibodies, the anti-CSPG4 sc-Fv reduced growth in vitro, as well as inhibiting metastatic spread of melanoma cells in vivo (Wang et al. 2011). The inhibition of metastasis coincided with reduced mitosis and sv-Fv treatment reduced Erk 1,2 signalling which could contribute to this growth inhibition.

Naked antibodies that block the function of single molecules have the potential to become redundant through acquired drug resistance (Shefet-Carasso and Benhar 2015). Shift of dependence to other signalling pathways unaffected by the drug or increased target degradation may limit therapeutic effectiveness (Shefet-Carasso and Benhar 2015). The combination of mAbs with potent drugs may help deliver a more effective cytotoxic strike (Diamantis and Banerji 2016). Conjugated antibodies have been studied for CSPG4 with a number of different drugs.

Classical chemotherapy drugs have been linked to antibodies therefore avoiding systemic side effects of the drugs. Anti-CSPG4 antibodies conjugated to methotrexate have been found to reduce tumour burden in mice with melanoma xenografts (Ghose et al. 1991). Antibody bound methotrexate was three times more potent than unconjugated drug (Ghose et al. 1991).

Immunotoxins have also been utilised for drug conjugates. *Pseudomonas* extotoxin A (ETA') from the gram-negative bacterium *Pseudomonas aerugionsa* has been used to target different cancer types conjugated to anti-CSPG4 antibodies and antibody fragments (Wolf and Elsasser-Beile 2009, Nicolosi et al. 2015). When ETA' was conjugated to an anti-CSPG4 mAb, it was shown to induce apoptosis in four rhabdomyosarcoma cell lines, after being

internalised by the cell (Brehm et al 2014). In glioblastoma, the conjugated CSPG4 antibody, 9.2.27-ETA', prolonged survival in rats injected with the U87MG cell line (Hjortland et al. 2004). The sc-Fv strategy has also been utilised with conjugated ETA' (Schwenkert et al. 2008). Melanoma cell lines, A2058 and A375M underwent apoptosis, with up to 80% of cells being killed with a single dose of the drug (Shwenkert et al. 2008). Primary cultured cells from patients with advanced disease were also sensitive to the drug with 70% of cells undergoing apoptosis within 96 hours of treatment (Schwenkert et al. 2008).

Radiolabelled mAbs have also been studied. Alpha emitting Bismuth-213-conjugate killed micrometastatic melanoma lesions (Rizvi et al. 2005). Critically, pharmacokinetics demonstrated no retention of the drug in the brain (Rizvi et al. 2005). This is an important consideration for off-target effects on healthy CSPG4-positive cells present in the brain. However, its efficacy reduced with increasing tumour burden (Rizvi et al 2005). This could be due to poor penetration of the whole antibody molecule.

CSPG4's association with angiogenic pericytes makes it is possible that antibodies targeting the protein could be used as an anti-angiogenic treatment, or as a dual treatment if the patient's tumour is CSPG4-positive. Guan et al. (2014) created a nanoparticle drug delivery system based on an anti-CSPG4 peptide conjugated to nanoparticles loading docetaxel. Through internalisation of the nanoparticles, pericyte migration and viability was inhibited (Guan et al. 2014). It was also established that pericytes associated with lung metastasis could be targeted. This targeting resulted in pericyte apoptosis and tumour regression due to a reduction in microvessel density (Guan et al. 2014). Mice experienced significantly prolonged survival with no obvious side effects from the treatment (Guan et al. 2014).

Another therapeutic strategy that utilises antibodies is activation of the immune system. The use of the host immune system in cancer therapy has the potential to achieve long-lasting regression. Through genetic engineering it is possible to direct lymphocytes to target tumour antigens (Beard et al. 2014). Receptors that recognise tumour antigens can be expressed in to lymphocytes and then reintroduced into patients. Chimeric antigen receptors (CARs) are comprised of a sc-Fv fragment and intracellular T-cell signalling domains. This complex can instruct T cells to recognise tumour antigens and kill the tumour cells (Beard et al. 2011). CARs that target CSPG4 have been developed and demonstrate the potential of this treatment. CARs constructed from anti-CPSG4 sc-Fv fragments and expressed in peripheral blood lymphocytes recognise several CSPG4-positive cells lines from a number of different cancer types (Beard et al. 2011). The types included melanoma, breast cancer, mesothelioma, glioblastoma and osteosarcoma. The lymphocytes produced cytokines and could cause lysis of cancer cells when co-cultured (Beard et al. 2011). Another study has shown that T cells expression anti-CSPG4 CARs controlled tumour growth in vitro and in vivo for melanoma, HNSCC and breast carcinoma (Geldres et al. 2014). Furthermore, anti-CSPG4 CARs have demonstrated 40% cell lysis of 143B osteosarcoma cell line when co-cultured with lymphocytes (Tschernia et al. 2014)

Other immune cells have also demonstrated efficacy. The use of natural killer cells in combination with anti-CSPG4 antibody 9.2.27 affected tumour cell proliferation, reducing tumour growth in vivo (Poli et al. 2013). This was seen in conjunction with increased apoptosis and prolonged animal survival (Poli et al. 2013). This effect was greater than vehicle or monotherapy.

The preclinical use of anti-CSPG4 demonstrates that it may constitute an attractive therapeutic target for use in a number of different cancers. A small number of clinical trials have been undertaken using a mouse anti-idiotypic monoclonal antibody (MK2-23) with an internal image of anti-CSPG4 mAb (Mittelman et al. 1992). The aim was to use MK2-23 to activate specific immunotherapy. Patients with stage IV melanoma were immunised with MK2-23 over four weeks of therapy. Three patients developed anti-CSPG4 antibodies and experienced a partial response (Mittelman et al. 1992). As the anti-CSPG4 antibodies were of the IgG class, it suggests the immune response elicited by MK2-23 is dependent on T-cell activity (Mittelman et al. 1994). The three patients saw a decrease in the size of metastatic tumours (Mittelman et al. 1992). The development of anti-CSPG4 antibodies preceded the reduction, suggesting the acquired immunity can have a positive effect on metastatic melanoma (Mittelman et al. 1994). Overall, survival of 14 patients who developed anti-CSPG4 immunity had significantly longer survival than the 9 patients without humoral anti-CSPG4 development (Mittelman et al. 1992). Anti-CSPG4 immunity has been shown to be an important variable through multivariate analysis by Cox development (Mittelman et al. 1995).

1.3 Hypothesis and scientific aims

The roles for CSPG4 that have been described provide an insight into how CSPG4 could function in osteosarcoma. Importantly for treating osteosarcoma in the clinic are CSPG4's potential roles in chemoresistance and metastasis, as well as primary tumour growth. Preliminary work has indicated that CSPG4 is present on patient samples, as well as model osteosarcoma cell lines.

Hypothesis:

CSPG4 contributes to osteosarcoma tumorigenicity and therefore represents a therapeutic target for the disease.

Scientific aims:

1. To confirm that CSPG4 is expressed in human osteosarcoma tumours.

2. To create osteosarcoma cell lines that are both CSPG4-deficient and CSPG4-positive for use in in vitro and in vivo assays

3. To investigate the functional role that CSPG4 plays in osteosarcoma cell behaviour through in vitro assays measuring:

- Proliferation
- Migration

- Adhesion
- Cell spreading
- Chemotherapy sensitivity
- Cell survival under stressful conditions

4. To investigate whether CSPG4 expression contributes to tumour growth and/or metastatic spread in vivo

5. Provide proof-of-principle data that CSPG4 could be targeted for therapeutic gain in osteosarcoma

Chapter 2

Materials and Methods

2.1 CSPG4 expression in vivo

2.1.1 Clinical material

Fixed frozen osteosarcoma sections and fixed formalin paraffin embedded (FFPE) osteosarcoma tumour microarrays were obtained from Scottish NHS tissue governance. Soft tissue sarcoma samples were obtained as positive controls from Scottish NHS tissue governance.

Mouse tumours and lungs were obtained following animal sacrifice. Animal tissues were placed in formalin overnight, before being embedded in paraffin and cut into 4μm thick sections by Helen Caldwell (Division of Pathology, IGMM). Slides were placed at -20^{o}C for storage before use. All samples were decalcified in a saturated solution of EDTA at 37^{o}C.

2.1.2 Expression of CSPG4 mRNA expression through RT-PCR

2.1.2.1 RNA extraction from FFPE samples

RNA was extracted from FFPE osteosarcoma samples following the RNeasy FFPE kit protocol (Qiagen). Four 10μm sections were cut onto slides per patient sample. Tissue was scraped off of the slide using a scalpel and placed in a fresh RNase free reaction tube to minimise the presence of wax.

320μl of deparaffinisation solution (Qiagen) was added to samples and vortexed for 10 seconds prior to incubation for 3 minutes at 56^{o}C. Samples were allowed to cool at room temperature. 240μL of buffer PKD was added and mixed by vortex then centrifuged for one

minute at 11,000 x g. 10μL of Proteinase K was added to the lower clear phase and mixed through gentle pipetting. Samples were then incubated for 15 minutes at 56^{o}C and then at 80^{o}C for a further 15 minutes on a heat block. Samples were kept at room temperature whilst heat block changed temperature. Solution was transferred to a 2mL reaction tube and incubated on ice for 3 minutes before being centrifuged for 15 minutes at 20,000 x g. The supernatant was transferred to a new tube with care as to not to disturb the pellet. 25μl of DNase booster and 10μl of DNase I stock was added, mixed through inverting the tube several times and then centrifuged for 30 seconds.

Sample was incubated for 15 minutes at room temperature. 500μl of buffer RBC was added mixed through pipetting. 1200μL of 100% ethanol was then added to sample and mixed. The sample was then passed through a spin column after 15 seconds of centrifugation at 11,000 x g. 500μL of buffer RPE was added to the column and centrifuged at 11,000 x g twice, firstly for 15 seconds and secondly for 2 minutes. The collection tube was replaced and centrifuged at 13,500 x g for 5 minutes. The collection tube was then replaced for a 1.5mL reaction tube. 20μL of RNase free water was added to samples to centre of the spin column in order to elute the RNA – samples were centrifuged for 1 minute at 13,5000 x g.

RNA concentration was then read with a NanoDrop1000 v3.7.0 (Thermo). Samples were frozen at -80^{o}C for later use.

2.1.2.2 cDNA production

RNA was used to produce cDNA using the Sensiscript Reverse Transcriptase kit (Qiagen). Protocol was followed according to manufactures instructions. Kit was thawed at room temperature while RNA and random primers (NEB) were thawed at 4^{o}C. Reaction was set on ice using a 0.2mL RNase free reaction tube following reagent constitution detailed in Table 2.1. Sample was run at 37^{o}C for 60 minutes (Bio-Rad). cDNA was then stored at -20^{o}C for later use.

Table 2.1 – Reagent concentrations for Sensiscript Reverse Transcriptase kit

Reagent	**Volume (μL)**
10x Buffer	2
dNTP	2
Random primer mix	2
Dnase inhibitor	1
SS RT	1
RNA	3
ddH_20	9
Total:	20

2.1.2.3 Real time PCR protocol

Real-time PCR reactions were carried out using TaqMan technology (Life Technologies). Reaction was set up on ice with minimal lighting in order to protect fluorescent bleaching. Reagent constitution and thermocycling conditions were followed as per the manufacturer's instructions detailed in Table 2.2 and Table 2.3.

cDNA and 20x TaqMan assays were thawed fully on ice before being mixed with 2x TaqMan MasterMix. Samples were added in triplicate to an Armadillo 96-well PCR plate (Thermo-Fisher). Fluorescence detection was performed by a LightCycler 480 thermocycler. All PCRs were run for 40 cycles with data acquisition taken during the extension step. The LightCycler 480 software calculated relative expression. Healthy adult human osteoblast cDNA was used as a calibrator and given a value of 1. Samples with an expression >1 were considered to be over expressed, those with an expression <1 were considered to be under expressed.

Table 2.2 – Reagent concentrations for RT-PCR reactions

Reagent	Volume (μL)
20x TaqMan CSPG4 - FAM	1
20x TaqMan HMBS - VIC	1
2x TaqMan MasterMix	10
cDNA	4
Range free H_2O	4
Total:	**20**

Table 2.3 – Thermocycling conditions for RT-PCR reactions

Parameter	Temperature (^oC)	Time (mm:ss)
Polymerase activation	95	10:00
PCR (40 cycles):		
Denature	95	00:15
Anneal / Extend	60	01:00

2.1.3 Expression of CSPG4 mRNA expression through end-point PCR

2.1.3.1 Primer design

All primers were purchased from Sigma-Aldrich (UK). Primers for sequencing of CSPG4 were designed using the human sequence data and primer design tool Primer3 v.0.4.0. Primers to be used with cDNA extracted from clinical material were designed to generate amplicons of 97 base pairs. This was to ensure gene amplification following heavy fragmentation of RNA that occurs during FFPE fixation process. Primers for GAPDH were pre-designed and appropriate for cDNA from FFPE samples.

Primers to be used to detect CRISPR/Cas9-mediated mutation were designed to be at least ~200 base pairs apart. A high stringency filter was applied in the case of primers that fell within introns to ensure specificity for CSPG4 DNA sequence. Primers for GAPDH were pre-designed and appropriate for cDNA from FFPE samples.

2.1.3.2 cDNA production PCR

Patient cDNA was produced from RNA extracted from FFPE tissue sections using FFPE RNaeasy kit (Qiagen) by members of the osteoarticular research group.

cDNA production for use in end-point PCR was performed using qScript cDNA Supermix (5x) (Quanta Biosciences). RNA samples (1μg/μL) were added to nuclease-free H_2O and qScript

cDNA SuperMix (5x) (Quanta Biosciences) at concentrations in Table 2.4. Solutions were mixed and briefly centrifuged and run on the Bio-Rad T-100 Thermal Cycler (Bio-Rad). Thermocycling conditions used are listed in Table 2.5.

Table 2.4 Reagent concentrations for cDNA production

Reagent	Volume (μL)
RNA (1ug/uL)	Variable
qScript Supermix	4
H_2O	Variable
Total:	20

Table 2.5 Thermocycler conditions for qScript cDNA production

Temperature (^{o}C)	Time (mm:ss)
25	05:00
42	30:00
85	05:00
4	Hold

2.1.3.3 End-point PCR protocol

cDNA was amplified using the Taq MasterMix kit (Qiagen). Two reactions were run in parallel for CSPG4 amplification and for GAPDH amplification. Reactions were prepared on ice to a total volume of 25μL. Reactions were run alongside a negative control where RNA was substituted for dH_2O. Reaction concentrations shown in Table 2.6. All end-point PCR's were run for 35 cycles. Samples were run on the Bio-Rad using thermocycling conditions listed in Table 2.7.

Table 2.6 Reagent concentrations for end-point PCR

Reagent	Volume (μL)
Taq MasterMix (2x)	12.5
Forward primer	1
Reverse primer	1
Control dye	2.5
dH_2O	3
Total:	20

Table 2.7 Thermocycler conditions for end-point PCR reactions

Temperature (°C)	Time (mm:ss)
95	03:30
60	30:00
70	05:00
72	05:00
4	Hold

2.1.3.4 Gel electrophoresis and visualisation

In order to investigate expression from the PCR, samples were loaded on a 2% agarose (Invitrogen) tris/borate/ethylenediaminetetraacetic acid (EDTA) (TBE) (1X) gel containing 0.01% SYBR Safe (InvitrogenTM). Samples were run alongside a low molecular weight marker (NEB). Samples were run for 1 hour at 100V and 50mA. Gel was removed and imaged using a UV imager.

2.2 CSPG4 expression in vitro

2.2.1 Cell line culture

Human osteosarcoma cell lines U2OS, MG63, HOS, HOS-MNNG, 143B and human Ewings sarcoma cell line TC71 were purchased from ATCC (Manasass, VA). U2OS cells were grown in McCoys 5A medium (Sigma), MG63 cells were grown in Dulbecco's Modified Eagles Medium (Gilbco) and HOS, HOS-MNNG and 143B cells were grown in Modified Eagles Medium with Earles salts (Sigma). TC71 cells were grown in Iscove's Modified Dulbecco's Medium.

All media was supplemented with FBS (10%) and penicillin/streptomycin (1μl/ml). HOS, MNNG and 143B cells were further supplemented with 2mM L-glutamine and 5% non-essential amino acids. Additionally, 15μg/mL BrdU was added to 143B media. All cells were maintained at 37^{o}C in 5% CO_2.

2.2.2 Resuscitation of cell lines

Cell aliquots were removed from liquid nitrogen and allowed to defrost for 2 minutes in a water bath at 37^{o}C. Once defrosted cell freezing medium was added to 10mL of culture medium and centrifuged for 5 minutes at 150 x g. The supernatant was removed and the cell pellet was resuspended in 10mL of culture medium. Cells were then seeded in a 75cm^2 flask and grown over night in the incubator at 37^{o}C with 5% CO_2.

2.2.3 Passaging of cell lines

Once cells reached 70-80% confluence, culture medium was removed and cells were incubated with 2mL of TripleE Trypsin Replacement Enzyme (Gilbco) until they detached from the flask (approximately five minutes). Cells were then washed in PBS and centrifuged at 800 x g for 5 minutes. The supernatant was removed and the cell pellet was resuspended in culture medium and transferred to a new 75cm^2 flask.

2.2.4 Freezing of cell lines

Cells were passaged as above before being resuspended in cell freezing medium comprised of DMSO (10%) and FBS (90%). Cells were then stored overnight in Mr. Frosty at -80^{o}C (Sigma) before being transferred to liquid nitrogen for long term storage.

2.2.5 CSPG4 mRNA expression through end-point PCR

2.2.5.1 RNA extraction

One 75cm^2 flask of cells was used for RNA extraction. Cells were passaged and resuspended in PBS. Once the supernatant was removed, 1mL of TRIzol (Life technologies) was used to resuspend cells and transfer to a 1.5mL reaction tube. Cells were left for 20 minutes. In a hood, 200μL of chloroform was added and then vortexed until thoroughly mixed and incubated for 3 minutes. The sample was centrifuged at 13,500 rpm on a table top micro centrifuge at 4^{o}C for 20 minutes. After centrifugation, the RNA exists in a clear liquid

separated from pink protein containing solution by a white ring. The clear RNA solution was transferred to a fresh reaction tube without disturbing the white ring. Propanol, of an equal amount to the RNA solution, was added and mixed by inverting the tube ~15 times. The solution was incubated at room temperature for 10 minutes and centrifuged at 10,000 x g for 10 minutes. The supernatant was discarded. The pellet was washed twice in 500μL of 70% ethanol and centrifuged at 10,000 x g for 5 minutes. All excess ethanol was removed and the pellet was to air dried for 5 minutes. The RNA was suspended in 30μL of RNase free H_2O and stored at -20^{o}C for later use.

2.2.5.2 RNA concentration determination

RNA concentration was measured using the Nanodrop 1000 spectrophotometer (Thermo Scientific). 1.5μL of RNAse free water was used as a blank before 1.5μL of samples were measured. Only RNA samples with a 260/280 reading of 0.8-1 and a 230/260 reading of 2.0-2.2 were used to ensure purity.

End-point PCR protocol was followed as detailed in section 2.1.2.3.

2.2.6 CSPG4 protein expression through western blotting

2.2.6.1 Protein extraction

RIPA buffer (Sigma) was supplemented with protease and phosphatase inhibitors and used for protein extraction as listed in Table 2.6.

Table 2.8 – Reagent concentrations for complete RIPA buffer

Reagent:	Volume per 1ml of RIPA buffer (μL):
Sodium orthovanadate (Na_3VO_4)	2
Sodium Fluoride (NaF)	2
Aprotinin	7
Phenylmethylsulfonyl fluoride (PMSF)	12.5

For cell lysis and protein extraction, cells were washed twice in PBS and resuspended in complete RIPA buffer for 15 minutes on ice. Cell lysates were then ultracentrifuged for 15 minutes at 13,500 rpm at 4^{o}C. The supernatant was transferred to a clean 1.5mL reaction tube with care taken not to disturb the pellet.

2.2.6.2 Protein concentration determination using Bradford reagent

Bradford reagent (Sigma) was used to determine cell lysate protein concentration. 295μL of Bradford reagent was pipetted in triplicate wells of a 96-well plate per sample. 5μL of lysate was pipetted and mixed in each triplicate well. Bradford reagent-only wells were used as a blank reading. Samples were incubated at room temperature for five minutes prior to absorbance at 495nm being read using the BMG LabTech plate reader. The concentration was taken as an average across the triplicate wells.

2.2.6.3 Chondroitinase ABC treatment

Chondroitinase ABC is an enzyme that deglycosylates chondroitin-sulphated proteoglycans. Addition of this enzyme to cell lysates results in expression of the chondroitin-sulphate free core protein segment of the CSPG4 proteoglycan only. Chondroitinase ABC (1U/mL) was added to cell lysates and incubated for 45 minutes at room temperature. Chondroitinase ABC was only added to samples where noted.

2.2.6.4 Running procedure

The TETRA-PROTEAN mini-gel system was used for gel electrophoresis and blotting steps and all reagents and materials were purchased from Bio-Rad unless otherwise stated. The protocol was set-up according to the manufacturer's instructions.

Unless otherwise stated, 20μg of protein was solubilized in 2x Lamelli sample buffer (800μl betamercaptoethanol, 1.3ml 1M Tris pH 6.8, 2ml glycerol, 5ml 10% SDS, 0.9mL dH_2O, drop of bromophenol blue) and loaded on to a 12% Bis-Tris gel in 10% TGS running buffer. Gel was run for 90 minutes at 160V. Protein size was determined using the Precision-Plus Protein Standard Dual Colour protein ladder (Bio-Rad).

2.2.6.5 Blotting procedure

Transfer buffer (10% TGS, 5% methanol and 85% distilled H_2O) was prepared in advance and cooled to 4^{o}C. Sponges, filter paper and nitrocellulose membrane were soaked in transfer buffer for 5 minutes prior to assembly of transfer sandwich. The transfer sandwich was set up with the following configuration: sponge, filter paper, nitrocellulose membrane, gel, filter paper and sponge. Transfer was run at 100V for 60 minutes at 4^{o}C.

2.2.6.6 Blocking and antibody dilution

After blotting, the nitrocellulose membrane was briefly washed in TBS-T (10% TBS, 0.1% Tween-20) and blocked with 5% Marvel TBS-T for one hour at room temperature. Antibodies were either diluted in 5% (w/v) BSA TBS-T or 5% (w/v) Marvel TBST. Membrane was incubated with antibody overnight at 4oC on a shaker. The membrane was washed three times with TBS-T for five minutes before incubation with anti-mouse or anti-rabbit HRP-linked secondary antibodies diluted in 5% (w/v) Marvel TBS-T for 60 minutes at room temperature on a rocker. The nitrocellulose membrane was washed 3 times with TBS-T for five minutes prior to imaging.

For chemiluminescent protein detection, the nitrocellulose membrane was incubated in ECL for one minute prior to visualisation with the ChemiDoc MP imager (Bio-Rad).

2.2.7 Direct flow cytometry

Cells were washed and resuspended in 1mL of Cell staining buffer (Promega). 20μL of cell suspension was loaded on to a cell counting chamber (Nexcelom Bioscience) and counted using the Cellometer Mini Auto T4 (Nexcelom Bioscience). 3 x 10^5 cells were used per condition. Cells were added to 100μL of cell suspension buffer. In order to reduce non-specific background staining, samples were incubated with 5μL of TruStain Human FcX (Promega) for 5 minutes on ice. Cells were incubated with anti-NG2 (LHM-2, PE conjugated) (SantaCruz), PE-conjugated Rabbit IgG isotope control (Santa Cruz) or Cell Staining buffer for unstained controls, for 60 minutes in darkness on ice. Cells were washed three times with 1mL cell staining buffer and centrifuged at 400 x g for 5 minutes. Samples were diluted in 500μL of cell staining buffer and analysed using the Accuri C6 flow cytometry reader (BD Biosciences).

2.2.8 Indirect immunofluorescence

10mm glass coverslips were sterilised in 70% ethanol, air dried for 10 minutes then added to 6-well plates. 5 x 10^3 cells were used per well and once seeded grown overnight. Cells were then washed in ice-cold PBS three times for five minutes. Cells were then fixed with ice-cold methanol for 15 minutes at -20^{o}C. In order to reduce non-specific background staining cells were incubated with PBS 3% BSA solution for 20 minutes. Cells were incubated with anti-NG2 (Abcam 86067) 1:100 or anti-His tag (CST) 1:100 diluted in PBS 1% BSA for one hour. Cells were washed three times for five minutes with PBS.

AlexaFluor 488 and AlexaFluor 594 (Thermo) antibodies were diluted in PBS 1% BSA solution and added to cells for one hour in darkness. Cells were washed three times for five minutes with PBS. Coverslips were then removed, washed in distilled H_2O and mounted on to microscope slides using Diamond Anti-Fade with DAPI (Dako) and dried overnight. Images were obtained using the Olympus V100 confocal microscope and software.

2.3 Modulation of CSPG4 expression

2.3.1 CRISPR/Cas9 mediated deletion

2.3.1.1 Plasmid preparation

CRISPR/Cas9 plasmids were a gift from Horizon Discovery. Four unique constructs were used initially, with constructs 21 and 23 taken forward. Plasmids included sequences for Cas9 expression, Kanamyosin resistance and DasherGFP.

Table 2.9 - Sequences of gRNA constructs in CRISPR/Cas9 plasmids

Construct	gRNA sequence
19	GGACTGCATCCCGGCGGGCT
20	CAAAGCCAAGGCCAGGCCGG
21	AAGTCTGGCCAACATAGTCA
23	TGGCCACAGGCACCTCCAGG

2.5ng of lyphodised plasmid was added to 10μL of TOP10 cells (Thermo) and incubated for 10 minutes on ice. 200μL SOC media (Thermo) was added and tubes were incubated at 37^{o}C for 60 minutes on a rocker. The bacteria was then added to 200mL LB broth with Kanomycin and left to grow overnight at 37^{o}C on a rocker.

The Plasmid Maxi Kit (Qiagen) was used to purify plasmids according to the manufacturer's instructions. Bacteria was then centrifuged at 20,000 RCF for 20 minutes and the supernatant was removed. Bacteria pellets were re-suspended in 10mL of Buffer P1, supplemented with RNase A and LyseBlue at 1:1000. 10mL of Buffer P2 was added and was inverted 6 times and left to incubate at room temperature for 5 minutes, at which point the solution turns blue. 10mL of Buffer P3 was added, inverted six times and incubated on ice for 20 minutes. The solution was centrifuged at 10,000 x g for 10 minutes at 4^{o}C. At the same time a Qiagen tip was equilibrated with 10mL Buffer QBT and allowed to empty by gravity flow. The supernatant was removed from the sample into a Qiagen syringe, which was used to dispense the sample into the Qiagen tip and remove any suspended pellet that remained. The sample was allowed to flow through the tip and was washed twice with 30mL of Buffer QC. The Qiagen tip was moved to a new 50mL falcon tube and the DNA was eluted with 10mL of Buffer QF. The tip was then discarded and the eluted DNA was precipitated with 10.5mL isopropanol and mixed. The sample was centrifuged at 15,000 x g for 30 minutes at 4^{o}C. The supernatant was removed and 5mL of 70% ethanol was added to resuspend and wash the pellet. The sample was then centrifuged at 10,000 x g for 5 minutes. The pellet was redissolved in ~100μL of ddH_2O. DNA concentration was measured using the NanoDrop 1000 spectrophotometer.

2.3.1.2 Transfection of plasmids

1x10^4 cells were plated per well of a six well plate. DNA plasmids from each construct (5μg/mL) and Lipofectamine 2000 (Life technologies) (0.3μl/mL) were incubated separately in OptiMem Reduced Serum Media (Gilbco) for 5 minutes. The two tubes were then mixed

and incubated for 20 minutes. Prior to transfection, cell culture media was removed and cells were washed 3 times with PBS. The plasmid, Lipofectamine 2000 and OptiMem Reduced Serum Media solution was added to cells and incubated for 4 hours. After the incubation period, the wells were washed with PBS 3 times and normal serum-containing media was added. Cells were grown until 80% confluent and then passaged with some being used for protein extraction in order to observe CSPG4 expression in pooled cells via western blotting.

2.3.1.3 Single-cell clone growth

24 hours post transfection, cells were washed and resuspended in 300μL of PBS 3% FBS. The cells were then sorted on the basis of DasherGFP expression using the Jazz FACS machine. This was kindly done by Elizabeth Freyer, IGMM.

2.3.2 Mutation of genomic DNA confirmation

2.3.2.1 gDNA extraction

For extraction of genomic DNA from knock-out cells, the Blood and Tissue Cuture gDNA kit (Qiagen) was used following the manufacturers protocol. 5 x 10^6 cells were harvested and washed in PBS before being centrifuged at 400 x g for 5 minutes. Cells were resuspended in 0.5mL of Buffer C1 and 1.5mL of ice-cold H_2O, mixed and incubated on ice for 10 minutes. The sample was centrifuged at 1300 x g at 4^oC for 15 minutes. The supernatant was discarded and the nuclear pellet was washed with 250μL Buffer C1 and 750μL of H_2O. The sample was then vortexed and centrifuged again at 1300 x g at 4^oC for 15 minutes. The supernatant was discarded and the pellet was resuspended thoroughly through vortexing in 1mL of Buffer G2. 25μL of Qiagen protease was added and the sample was incubated at 50^oC for 60 minutes by which point the lysate appeared clear. The Qiagen genomic tip was equilibrated with 1mL of Buffer QBT and the sample was vortexed and loaded to the tip. Once the sample had passed through, the tip was washed with 1mL of Buffer QC three times. The DNA was eluted with 2mL of Buffer QF (pre-warmed to 50^oC) in to a new falcon tube. 1.4mL of isopropanol was added to the sample, mixed and centrifuged at 5000 x g for 15 minutes at 4^oC. The supernatant was then removed and the pellet was washed with 1mL of cold 70% ethanol. The sample was vortexed and centrifuged at 5000 x g for 10 minutes at 4^oC. The pellet was then air-dried for 5 minutes. The pellet was dissolved in 200μL of TE buffer at 55^oC for 1-2 hours.

DNA concentration was read by the NanoDrop 1000 v3.7.0 (Thermo). All samples used for DNA sequencing had A260/A280 rations of ≥2.0 to ensure sufficient purity.

2.3.2.2 PCR and PCR clean-up

The PCR protocol was followed as previously described in section 2.1.3.1.

25μL of the PCR sample used for PCR clean-up performed with the QIAquick PCR purification kit (Qiagen). 125μL of Buffer PB was added to the sample and loaded into a QIAquick spin column. This was centrifuged in a microcentrifuge at 13,500 rpm for 60 seconds and the flow-through was discarded. The spin column was washed with 750μL of Buffer PE and centrifuged again for 60 seconds at 13,500 rpm. The flow-through was discarded and then centrifuged again before being placed in a new 1.5mL reaction tube. In order to elute the DNA, 40μL of H_2O was added to the spin column for 60 seconds and then centrifuged for 60 seconds.

The DNA concentration was then read by the NanoDrop 1000 v3.7.0 (Thermo).

2.3.2.3 Ligation

Ligation of the gDNA fragment into a vector was performed using the pGEM-T Easy Vector system (Promega) following the manufacturer's instructions. The formula used to calculate

the amount of insert DNA needed was: (**kb of insert / kb of vector)** x ng of vector. The ratio of vector to insert used was 1:3. The ligation was set up in Table 2.10 with both positive and background controls. The reaction was left for 24 hours at 4^{o}C.

Table 2.10 – Reagent concentration for ligation reactions

Reagents	Standard reaction (μL)	Positive control (μL)	Background control (μL)
2X Rapid Ligation Buffer, T4 DNA Ligase	5	5	5
pGEM-T Easy vector (50ng)	1	1	1
PCR product	Variable	-	-
Control Insert DNA	-	2	-
T4 DNA Ligase 2	1	1	1
dH_2O	Variable	1	3
Total	10	10	10

2.3.2.4 Bacterial selection

The bacterial transformation was performed according to the protocol summarised in section 2.1.3.1. 2μL of the ligation reaction was added to the reaction and once incubated for an hour, bacteria were plated on to LB/Amp/ IPTG/X-Gal plates.

The plates were produced by spreading 80uL of X-Gal (20mg/mL) followed by 80μL of IPTG (100mM) on to pre-made LB/Ampicillin plates.

2.3.2.5 Sequencing

Single white bacterial colonies were picked off of the plate and placed in a 96-well bacteria growth plate containing 1mL of ampicillin containing LB media. The samples were then sent to the IGMM sequencing department who sequenced vectors in both directions. The sequences were checked against CSPG4 DNA sequence using online BLAST software.

2.3.3 Re-expression of CSPG4 in knock-out cell lines

2.3.3.1 Plasmid preparation and freeze down

Expression of CSPG4 in cells was achieved using the expression vector pEF6-CSPG4-myc-his, which was a gift from Wensheng Wei (Addgene plasmid # 69037). Single colonies were isolated from the bacterial stab by touching the bacterial growth on the stab with a pipette tip and spreading the bacteria across one third of a pre-made LB/Amp plate. A second pipette tip was used to smear the bacteria across another third of the plate and a third pipette tip was used to spread the bacteria over the final third of the plate. This was left to grow for 16-18 hours.

A single colony was picked off and grown up in 10mL of LB/ampicillin and allowed to grow over night. 500μL was then taken and gently mixed with 50% glycerol in order to create a glycerol stock. This allowed long-term storage of the plasmid at -80^{o}C. The rest of the growth media was grown up further so that enough material was available for a MaxiPrep, the protocol of which was described in section 2.3.2.1.

2.3.3.2 Blasticidin kill-curve

Blasticidin-HCL (Corning) was dissolved in 50mL of ddH_2O giving a stock concentration of 10μg/μL. In order to set up a kill-curve assay, 7000 cells were seeded in triplicate for 8 different blasticidin concentrations in a 96-well plate and left overnight. The concentrations tested were 0, 2.5, 5, 7.5, 10, 12.5, 15 and 20μg/mL.

The selection media containing Blasticidin was added to cells and was changed every three days until 100% of cells had undergone apoptosis in the lowest concentration condition.

2.3.3.3 Transfection

The parental 143B line and CRISPR knock-out cell lines were transfected with the pEF6-CSPG4-myc-his vector using the same protocol as described in section 2.3.1.2. 24 hours after transfection, cell media was replaced with selection media containing 2.5μg/mL blasticidin. This was replaced every 3 days.

2.3.3.4 Single-cell clone growth

Once cells reached confluence, they were harvested and sorted into single cell clones based on their level of CSPG4 expression. Expression was determined through FACS analysis using the same protocol as described in section 2.2.7. Parental 143B was used as the control expression level for overexpressed condition, with only clones exhibiting double the level of expression being sorted. Knock-out cells were used as control expression level for re-expression conditions, with cells exhibiting CSPG4 expression sorted. Single clones were then seeded into a 96-well plate. Elizabeth Freyer, IGMM, kindly performed FACS analysis.

2.3.4 siRNA mediated knock-down of CSPG4

siRNA-mediated knock-down was used as an alternative method to CRISPR and so modulation of CSPG4 could be investigated in other osteosarcoma cell lines. SMARTpool ON-TARGETplus CSPG4 siRNA was purchased from Dharmacon. siRNA was reconstituted in H_2O to a concentration of 20μM. The final concentration of siRNA used to transfect cells was 25nM.

The manufacturer's protocol for siRNA transfection was followed. Briefly, siRNA and Lipofectamine 2000 were mixed with OPTIMEM in separate tubes and incubated for 5 minutes. The two tubes were then mixed and incubated for a further 20 minutes. They were then both added to culture medium before being added to the cells.

Cells were left to incubate for 48 and 72 hours before they were harvested. CSPG4 protein expression was measured through western blotting technique.

2.4 Functional roles of CSPG4 in vitro

2.4.1 Proliferation assay using Alamar Blue

2.4.1.1 Optimisation

In order to calculate proliferative rates of cell lines, a cell number is required which displays a sigmoid growth curve over 5 days. In order to establish this number, cells were plated at 25,000 cells in doubling down dilutions to ~350 cells in a 96-well flat-bottom microtitre plate. These were grown for 5 days. AlamarBlue® (Life Technologies) was added (1:10 concentration) and incubated for 4 hours. The background florescence was then measured. This was plotted on a graph establishing the saturation point and therefore a cellular concentration to use for each cell line.

2.4.1.2 Protocol

The optimised cell concentration for each cell line was plated out in sextuplicate in 5 separate 96-well plates and left overnight. At days 1-5 the plates were incubated with Alamar Blue (1:10 concentration) for four hours and then fluorescence was read. The average of the triplicate wells was taken.

2.4.2 Cell spreading and adhesion assay

Cell spreading and cell adhesion assays were run in unison with cell area used as a measurement of spreading and cell number used as a measurement of cell adhesion. Cells were plated on collagen-I and fibronectin coated plates for 15, 30, 60 and 120 minutes before being taken for measurement.

Firstly, 96-well plates are coated with collagen-I and fibronectin matrices. Collagen-I is diluted to a stock of 300μg/mL in 20mM acetic acid and 50μL added to wells and left overnight at 4^{o}C. Fibronectin is diluted to 3μg/mL in PBS and 50μL is added to wells and left overnight at 4^{o}C. Before use, the wells were washed three times with PBS. 2000 cells were added per well and separate plates were left for 15, 30, 60 and 120 minutes. At time points, wells were washed three times with PBS before cells were fixed with 4% paraformaldehyde (4% paraformaldehyde, PBS) for 30 minutes at room temperature. Wells were then washed again three times with PBS. Plates were then left at 4^{o}C until all time points are ready. Cells were permeabilised with 0.2% TRITAN-X (PBS) for 5 minutes. Cells were then washed three times with PBS. Cells were then stained with CytoPainter Phalloidin-iFluor 488 Reagent (Abcam) at a concentration of 1:500 in 1% BSA/PBS and with Hoechst at a concentration of 1:5000, for 90 minutes at room temperature in darkness. Cells were then washed three times with PBS before being stored at 4^{o}C until imaged.

2.4.3 Scratch-wound assay

2.4.3.1 Optimisation

To obtain reliable results from scratch wound assay, cells had to be plated at a concentration that would ensure 100% confluency at the time of performing the assay. 50,000 cells, in doubling down dilutions to 781 cells, were plated per well in a 96-well plate. Cells were then grown overnight. A cell dilution of 20,000 was sufficient to ensure 100% confluency the following day; therefore, this concentration was taken forward.

2.4.3.2 Protocol

Cells were plated at a concentration of 20,000 cells in sextuplicate in an Essen wound-maker 96-well plate, and left overnight. Wounds were produced using the Essen WoundMaker tool to ensure scratches were reproducible. Once wounds were produced, medium was removed and cells were washed three times in PBS, before fresh media was added. Cells were placed in the Incucyte (Essen) for 48 hours. Images were taken every three hours to monitor cellular migration. Wound density (as calculated by Incucyte software) from time point 0 to the end of the assay was used as a measure of cellular migration.

2.4.5 Chemosensitivity assay using Alamar Blue

Chemosensitivity was investigated in cell lines using doxorubicin and cisplatin, both of which were purchased from Sigma (European Pharmacopoeia Reference Standard). Doxorubicin was dissolved in DMSO, whereas cisplatin was dissolved in 0.9% NaCl.

For the assay 5000 cells were plated in sextuplicate for each of the 8 dilutions of drug tested and a non-treatment control and a drug vehicle control. The cells were left to attach overnight. The media was then removed and replaced with either no treatment media, drug containing media or drug vehicle containing media - a concentration which matched the concentration highest drug condition.

The cells were then left for 20 hours before adding AlamarBlue (1:1000) and left for four hours. The plates were then read at 24 hours post-treatment. The average of the six wells were taken and then normalised to the vehicle control.

In order to investigate cell recovery after treatment, cells were washed with PBS three times before being incubated for 48 hours. The plates were measured as detailed above.

2.4.6 Measurement of apoptosis following chemotherapy treatment

In order to assess whether reduced viability following drug treatment has occurred due to programmed cell death, apoptotic markers were measured.

50,000 cells were grown over night before being treated with 7.5μM of either cisplatin or doxorubicin. For 24 hours. Cells were then taken for flow cytometry analysis using the Cell MeterTM APC-Annexin V Binding Apoptosis Assay Kit (AAT Bioquest). Protocol was followed according to manufacturer's instructions. Cells were centrifuged and resuspended in 200μL of assay buffer. 2μL of 100X APC-Annexin V stock solution and 2μL of 100X propidium iodide was added to cells for 60 minutes in darkness. 200μL of assay buffer is then added to cells before analysis. Annexin V and PI staining was measured using a Accuri C6 flow cytometry machine.

2.4.7 Anoikis assay

In order to assess whether CSPG4 contributed to anchorage-independent growth, apoptosis was measured with cells grown in low attachment conditions.

50,000 cells were plated in ultra-low attachment plates and grown for 72 hours. Cells and media was then taken for flow cytometry analysis. Using the Cell MeterTM APC-Annexin V Binding Apoptosis Assay Kit (AAT Bioquest). The protocol described in section 2.4.6.

2.5.8 Cytotoxic antibody treatment

In order to assess cytotoxicity of the sc-Fv anti-CSPG4-ETA antibody, cells were treated for 72 hours and then their viability was measured.

5000 cells were plated per well in triplicate and left to grow overnight. The antibody was diluted in fresh media at a maximum concentration of 81ng/μL. Media was removed and cells were washed once with PBS before antibody-treated media was added. The antibody was serially diluted in doubling down concentrations across the plate. Non-treatment control had media added only. The cells were then left for 72 hours. Viability of the cells was then measured using AlamarBlue (Thermo) reagent for four hours and measured using an automated plate reader.

2.5 Functional roles of CSPG4 in vivo

2.5.1 Animals used

In each experiments female CD-1 athymic nude mice of 6 weeks of age were used. Athymic nude mice lack T-cells and therefore allow human tumour xenografts to be used without any host immune response. Mice were housed in IVC cages and tumours were measured twice-weekly using callipers.

An equation was used to determine tumour volume from these measurements. Once any human end-point was reached animals were terminated using Schedule 1 methods. Once culled, the tumour and lungs were removed from the mouse, placed in formalin overnight and then fixed in Paraffin by Helen Caldwell.

The Animal Welfare and Ethical Review Body of the University of Edinburgh approved all animal experiments. Animal experiments were performed in accordance with the United Kingdom Animals (Scientific Procedures) Act 1986.

All animal experiments were conducted with assistance and supervision from Morwenna Muir, BRF.

2.5.2 Subcutaneous injection of tumour cells

2.5.1.1 Model optimisation

In order to assess whether 143B cells could grow subcutaneously in vivo, two mice were injected with $2x10^6$ cells subcutaneously into each flank. Mice were culled when the tumours reached over 1.5cm in any dimension.

2.5.3 Intratibial injection of tumour cells

2.5.3.1 Protocol

The surgical procedure for intratibial injections was kindly carried out by Morwenna Muir.

General anaesthesia was induced through administration of Isoflurane (IsoFlo, Abbott Laboratories) at a concentration of 3-5% in oxygen through an anaesthetic circuit with the use of a nose cone. Mice were also administered subcutaneously Buprenorphine (Vetergesic) at a concentration of 0.3mg/ml in sterile water. Anaesthesia was maintained through Isoflurane at a concentration of 1-2% delivered through the nose cone. Lacrilube was used to ensure eyes stayed lubricated throughout the procedure. Mice were placed on their back and the leg due to be operated on was pinned to a cork-board. Povidone-iodine was used to sterilise the leg. Using a sterile size 15 scalpel a unilateral incision was made along the tibia. The muscle and connective tissue was moved aside to reveal the bone. Two holes were drilled using a 27G needle in the dark channel of the bone marrow in the tibia.

The holes were drilled to 0.4mm in diameter through the bone cortex. The area was swabbed clean and sterile saline was injected into one of the holes flushing the bone marrow out the other side. Tumour cells were injected via a bent 37G needle into the space created by ablation of the bone marrow. Approximately 20μL was injected into the proximal section of the bone shaft until cells flow freely from the upper hole. The holes were then sealed using pre-warmed bone wax on the head of a pin. Once filled the area was flushed with sterile water to avoid growth of cancer cells in surrounding soft tissues. The edges of the skin were closed and the wound was sutured using three absorbable sutures. The mice recovered from anaesthesia in an incubation chamber at 25^{o}C. Mice were returned to clean cages. For 48 hours post-surgery, Carprofen containing water was used for the mice. For one-week post-surgery, the mice were closely monitored for signs of local infection.

2.5.3.2 Model optimisation

We wanted to investigate 143B cell growth and metastasis within an orthotopic model. In order to observe growth and metastasis, mice were injected with 143B cells intratibially. Two mice received 1x10^{6} cells and two mice received 2x10^{6} cells. Palpable tumours were measured twice weekly with callipers. Mice were culled when their normal behaviour repertoire was limited through lameness of the foot.

2.5.3.3 Comparison of CSPG4-negative and –positive cell line behaviour in an orthotopic mouse model

In order to assess growth differences and metastatic spread in cell lines with different CSPG4 expression in vivo, $1x10^6$ cells were injected intratibially in athymic nude mice as detailed in section 2.5.1.2. Five mice were used per cell line. Tumours were measured twice weekly until a humane end-point was reached. Tumour growth, metastatic spread and survival were measured.

2.5.3.4 MicroCT scanning

MicroCT analysis was conducted in order to assess osteolytic damage to the bone following tumour cell injection. MicroCT was performed using a Skyscan 1172 instrument (Bruker). The machine was set to the following parameters 12.38uM, 70kV, 139uA and 0.5mm. Construction of microCT images and measurement of bone characteristics were kindly carried out by the Bone group, IGMM. MicroCT images were reconstructed with Skyscan NRecon software and analysed using Skyscan CTAn software. Image number and image contrast threshold were constant for all samples. Reconstructed images were analysed for bone density. Analysis of the microCT scans was kindly performed by the Bone group, IGMM.

2.5.2.4 Lung tumour burden model

In order to assess the tumour burden, the lungs were removed and fixed as earlier described. Prior to this, the lung surface was observed for evidence of macroscopic tumour growth. Once fixed lung sections were taken at levels 1,3,5,10,12,15,20 they were stained with H&E and imaged on the Nanozoom Slide Scanner (Hamamatsu). The Hamamatsu was then used to calculate the area of tumour compared to area of the lung providing a percentage of tumour burden.

2.6 Statistical analysis

Each experiment was conducted three times except where stated. The average, standard deviation and standard error of the mean (SEM) were calculated from triplicate experiments. GraphPad prism was used for all statistical analyses. Student unpaired t-test was used to test between two independent variables.

2.7 Antibodies used

Tables 2.11 and 2.12 detail antibodies used throughout the study:

Table 2.11 – List of primary antibodies used

Antibody	Supplier	Catalogue number	Experiment (Concentration)
NG2	Abcam	ab86067	IHC (1:200) Western blot (1:2000)
NG2 (LHM2-PE)	Santa Cruz	Sc-53389PE	Flow cytometry (20ug/mL)
NG2 (LHM2)	Santa Cruz	Sc-53389	Immunofluorescence (4ug/mL)
b-actin	Cell signaling	8H10D10	Western blot (1:5000)
His-tag	Cell signaling	D3I1O	Immunofluorescence 1:500
Goat anti-rabbit IgG-PE	Santa Cruz	Sc-3739	Flow cytometry (20ug/mL)

Table 2.12 – List of secondary antibodies used

Antibody	Supplier	Catalogue number	Experiment (Concentration)
anti-rabbit-HRP	Cell signaling	7074	Western blot (1:5000)
anti-mouse-HRP	Cell signaling	7076	Western blot (1:5000)
Goat anti-rabbit Alexa Fluor 488	Thermo	A-11034	Immunofluoresence (10ug/mL)
anti-mouse Alexa Fluor 594	Thermo	A-11032	Immunofluoresence (10ug/mL)

2.8 Primers used

Table 2.13 details the primers used throughout the study and the experiment they were used in.

Table 2.14 – List of primers used

Gene	Primer sequence (3'-5')	Size (bp)	Experiment	Supplier
CSPG4	F: GGCTGTCAAAACCAGGGT R: CTTCCTTCTCCTTGCCCTCT	131	In vitro and in vivo expression	Invitrogen
CSPG4 (exon 1)	F: GACACCCGGAGCCGGCCC R: GCCAGGCTGGGTCGGGGT	235	CRISPR mutation	Sigma
CSPG4 (exon 2)	F: AGAACCATGAGGGTGCGC R: AATCCCGCCCAGATCTCA	318	CRISPR mutation	Sigma
GAPDH	F: TTGTCCTCCTCCTGTCTCTCGC R: TGTAGCGAGTCTGTCGGTACC	81	In vitro and in vivo expression	Invitrogen

Chapter 3

In vitro and in vivo expression of CSPG4 in osteosarcoma

3.1 Summary

The aim of this chapter was to demonstrate CSPG4 expression in osteosarcoma. CSPG4 has been demonstrated in a number of different tumour types previously. Its presence is implicated in augmenting several different processes that contribute to tumorigenesis. These processes include cell proliferation, migration, adhesion and cell survival. CSPG4 expression was investigated in clinical osteosarcoma samples through RT-PCR and immunohistochemistry and in osteosarcoma model cell lines through RT-PCR and western blotting.

CSPG4 expression was found in clinical samples and model cell lines. CSPG4 mRNA expression was found in 100% of samples studied. CSPG4 mRNA was overexpressed in 20 patient samples when compared to normal human osteoblasts, a suggested cell of origin for osteosarcoma development. CSPG4 protein expression was demonstrated in clinical samples. Protein expression was found on the vast majority of cases. Staining was seen round the cell membrane. This included cases from a number of osteosarcoma subsets and metastatic lesions. CSPG4 mRNA and protein expression was found in all the model cell lines studied, including U2OS, MG63, HOS, HOS-MNNG and 143B.

This expression profile provides good evidence that CSPG4 could represent a modulator of osteosarcoma tumorigenesis. Its presence on the majority of cases demonstrates how CSPG4 could be used as a potential therapeutic target for osteosarcoma treatment. CSPG4 expression on osteosarcoma cell lines provides a

number of model cell lines to use for in vitro and in vivo studies.

3.2 Aims:

The aims of the experiments detailed in this chapter were to:

1. Demonstrate expression of CSPG4 mRNA in patient samples expression through end-point and real-time PCR experiments
2. Quantify expression of CSPG4 mRNA level compared to healthy human osteoblast cells
3. Identify anti-CSPG4 antibodies that can be utilised for immunohistochemistry experiments
4. Demonstrate expression of CPSG4 protein expression through immunohistochemistry
5. Identify extent of CSPG4 expression in a cohort of patient samples through immunohistochemistry

3.4 CSPG4 expression through end-point PCR

Initial results from within Osteoarticular group (IGMM) had demonstrated that CSPG4 mRNA expression was present in osteosarcoma patient samples. In order to confirm this, I created cDNA from FFPE extracted RNA from 20 osteosarcoma samples. Ying Zhou has previously extracted RNA from FFPE samples. cDNA was used for reverse-transcriptase polymerase chain reaction to investigate CSPG4 mRNA expression. GAPDH was used as a loading control.

The RT-PCR reaction demonstrated that CSPG4 mRNA was present in all 11 (100%) clinical samples (Figure 3.1a). CSPG4 expression varied across the samples. Negative control reactions containing no RNA produced no visible bands (data not shown).

3.4.1 CSPG4 expression through real-time PCR

In order to investigate expression of CSPG4 and level of expression compared to healthy osteoblast cells, RNA was extracted from osteosarcoma FFPE samples for real-time PCR experiments.

CSPG4 expression was calculated using the $2^{-\Delta\Delta ct}$ comparative method whereby CSPG4 was normalised to HMBS, used as an endogenous control, and relative to a calibrator, healthy human osteoblast cDNA. A value of >1 ± SEM denotes overexpression of the gene whereas a value of <1 ± SEM would denote under expression of the gene.

All 20 (100%) of the osteosarcoma samples demonstrated CSPG4 expression and amplification of mRNA levels compared to healthy osteoblast cells (Figure 3.1b). The overexpression was heterogeneous within the patient population. Patient details for the investigated samples can be found in Table 3.1. All samples were high grade osteosarcomas.

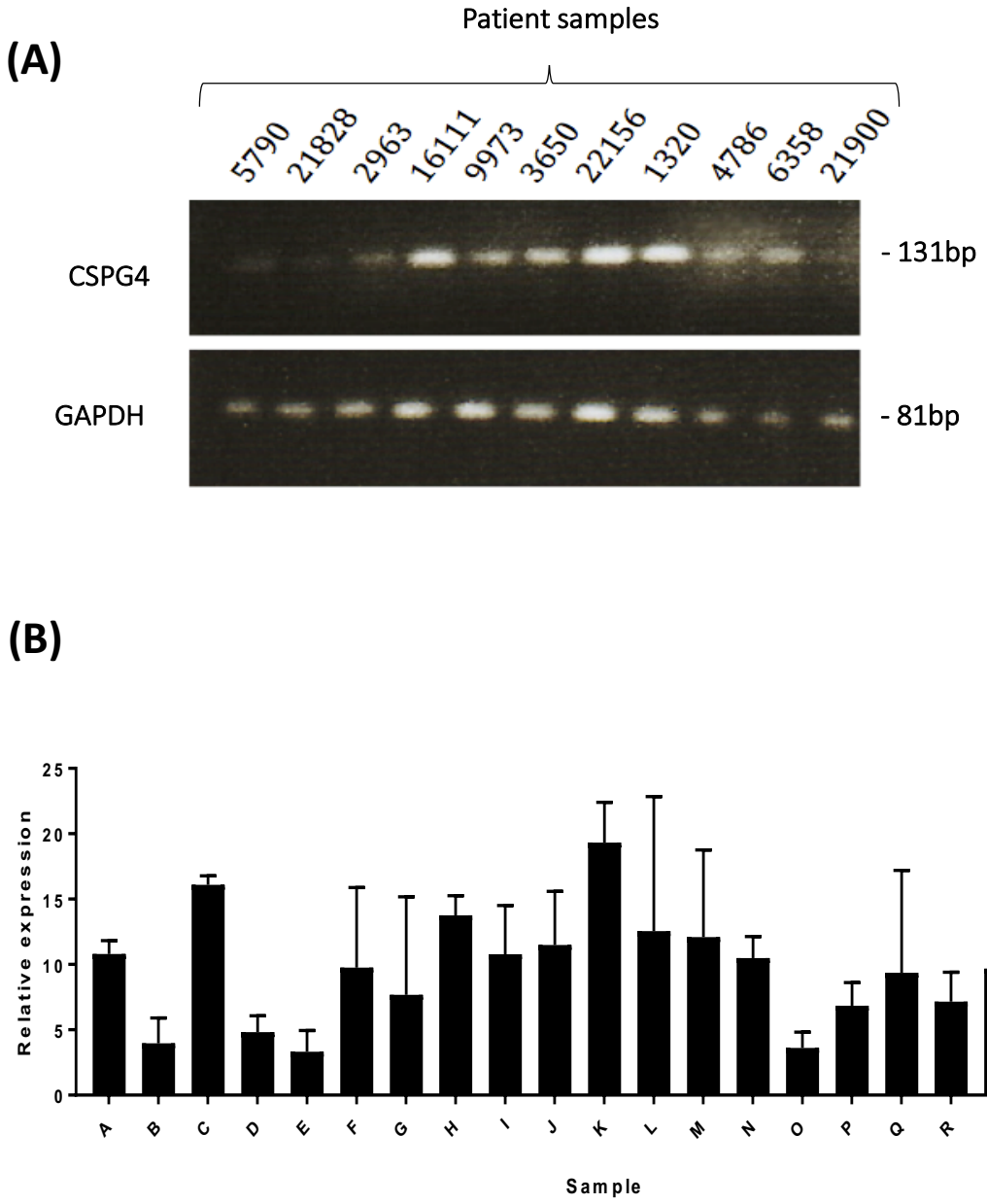

Figure 3.1: CSPG4 mRNA expression in osteosarcoma clinical samples: (A) Representative gel image of RT-PCR reaction for CSPG4 expression in 11 human osteosarcoma samples. GAPDH was used as a loading control. 131bp and 81bp were the product sizes of CSPG4 and GAPDH respectively. **(B)** qPCR results for CSPG4 mRNA expression in human osteosarcoma samples normalised to HMBS, used as an endogenous control and compared to a healthy osteoblast calibrator (OB) using the $2^{-\Delta\Delta ct}$ comparative method. Values shown represent the mean (n=3) ± SEM.

Sample	Patient Identification no.	Patient details	RNA extracted (ng/μl)	260/280	260/230
A	2G632UB08	30M Telangiectatic OS chest wall	27.5	1.83	2.4
B	026936AUB13	16M metastatic OS to lung	317.5	1.93	2.13
C	018344AUB14	26M OS R ilium	126.9	2.08	2.57
D	UB003650/11	15M OS L fibula	233.4	2	2.24
E	2234UB041B	F57 post irradiation OS L humerus	50.3	2.06	4
F	15327UB052	Unknown	62.9	1.74	1.47
G	019083BUB13	16 M OS R tibia	461.7	1.78	1.9
H	495801FUB06	Unknown	11611.6	1.94	2.11
I	027790UB13	M85 Pagets OS biopsy**	117.2	2	1.61
J	028977BUB13	M85 Pagets OD resection	404.5	1.87	2
K	21687AUB07	F70 post-irradiation OS scapula	407.8	1.9	1.95
L	0242302UB14	F68 R tibia OS	203.1	1.92	2.04
M	014665UB14	19M L tibia OS	131.5	1.91	1.9
N	026748BUB14	F68 resection OS R tibia – no chemotherapy	325.3	1.83	1.91
O	020619AUB14	M9 R humerus	74	1.89	1.78
P	004550UB15	26M recurrent OS post chemotherapy	91.8	1.9	1.75

Q	0255177UB14	M19 metastatic OS to pleura	884.5	2.03	2.14
R	310UB081L	M 62 Extraskeletal OS	1116.9	1.99	2.07
S	025020LUB14	M 19 post-chemotherapy OS 80% viable	30.9	1.73	1.32
T	UB005790/111A	M59 metastatic OS to Lung	1036.6	1.98	2.1

Table 3.1 – **Patient details of human osteosarcoma sections used for RT-PCR analysis.** Details of human osteosarcoma samples used in RT-PCR samples to investigate CSPG4 expression. Patient details include age, gender (male or female), site of tumour and details of treatment.

3.4.3 Antibody optimisation for immunohistochemistry

In order to assess CSPG4 protein expression through immunohistochemistry, it was essential to establish a reliable antibody. Three separate antibodies were investigated, two gifted by Roberto Perris (University of Parma). Antibodies 2161F9 and 2161D3 have both demonstrated CSPG4 positivity on a number of cell lines (Girolamo et al. 2013). The third antibody was purchased commercially from Abcam.

To investigate staining of the antibodies, three soft-tissue sarcomas previously found to be CSPG4-positive were stained with three separate primary anti-CSPG4 antibodies. All three antibodies demonstrated CSPG4 immunoreactivity (Figure 3.2). The three antibodies also demonstrated a similar pattern of staining. The majority of tumour cells were stained positive, with staining focused around the cellular membrane (Figure 3.2). A negative control was obtained through omission of the primary antibody and demonstrated no positive staining.

Due to the ready supply of ab86067 and its congruent staining pattern with the other antibodies, this was taken forward and used for immunohistochemical staining of the CSPG4 protein.

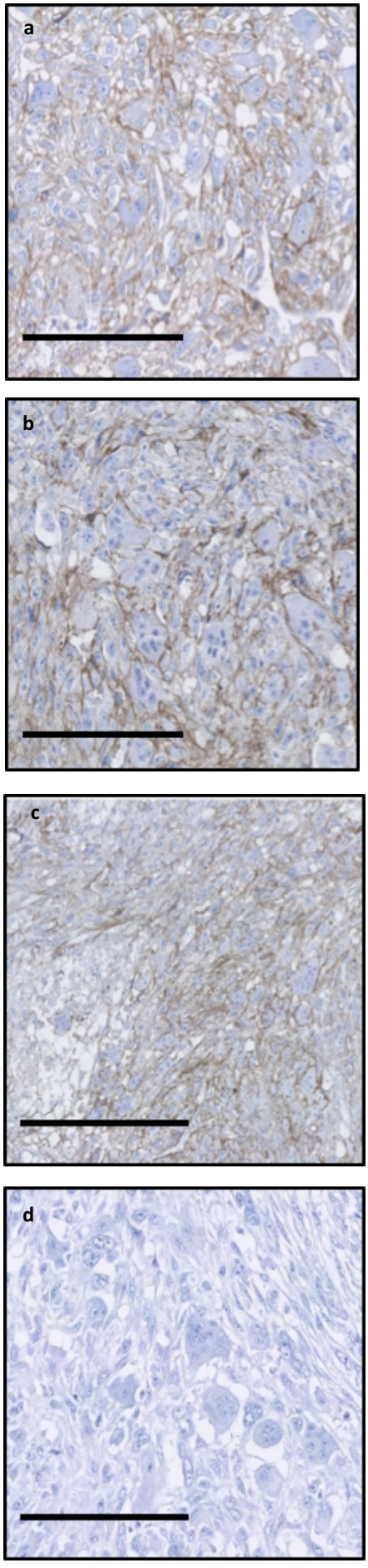

Figure 3.2: Optimisation of anti-CSPG4 antibodies for osteosarcoma FFPE samples. Representative images of soft-tissue sarcoma sections positively stained for CSPG4 using three separate antibodies; **a.** 2161F9 (University of Parma), **b.** 2161D3 (University of Parma)**, c.** Ab86067 (Abcam), **d.** negative control (no primary antibody). Scale bar = 100µm.

3.4.4 CSPG4 expression through immunohistochemistry

CSPG4 protein expression was investigated through immunohistochemistry using both fixed-frozen and FFPE samples. Results for the fixed frozen sections showed positive immunoreactivity for all 12 samples. A representative image is shown in Figure 3.3 (A). A negative control was obtained through omission of the primary antibody.

Due to the nature of freezing sections, cellular morphology is not preserved well and staining may not localise to specific structures, such as the cell membrane. In order to observe the cellular location of positive CSPG4 protein expression, FFPE samples were used. A tumour microarray (kindly provided by NHS Grampian) containing 47 samples belonging to 30 patients, the details of which can be seen in Table 3.2, was investigated for CSPG4 protein expression.

86% of the samples demonstrated positive immunoreactivity for CSPG4 protein expression. A sample was deemed positive if >50% of cells were positive. CSPG4 positivity was found in different sub-types of osteosarcoma, including parosteal, chondroblastic, fibroblastic and osteoblastic tumours (Figure 3.3b). CSPG4 expression was also found on all metastatic samples present in the lung. However, the number of metastatic samples was low and more samples would be needed to suggest any association between metastasis and CSPG4 expression. CSPG4 expression was found predominantly on the cell surface with some intracellular staining.

A number of healthy controls were included on the TMA and shown to be negative for CSPG4 expression, such as skeletal muscle, smooth muscle, vascular tissue, nerve tissue and lung tissue. A representative tissue is shown in Figure 3.3B(f).

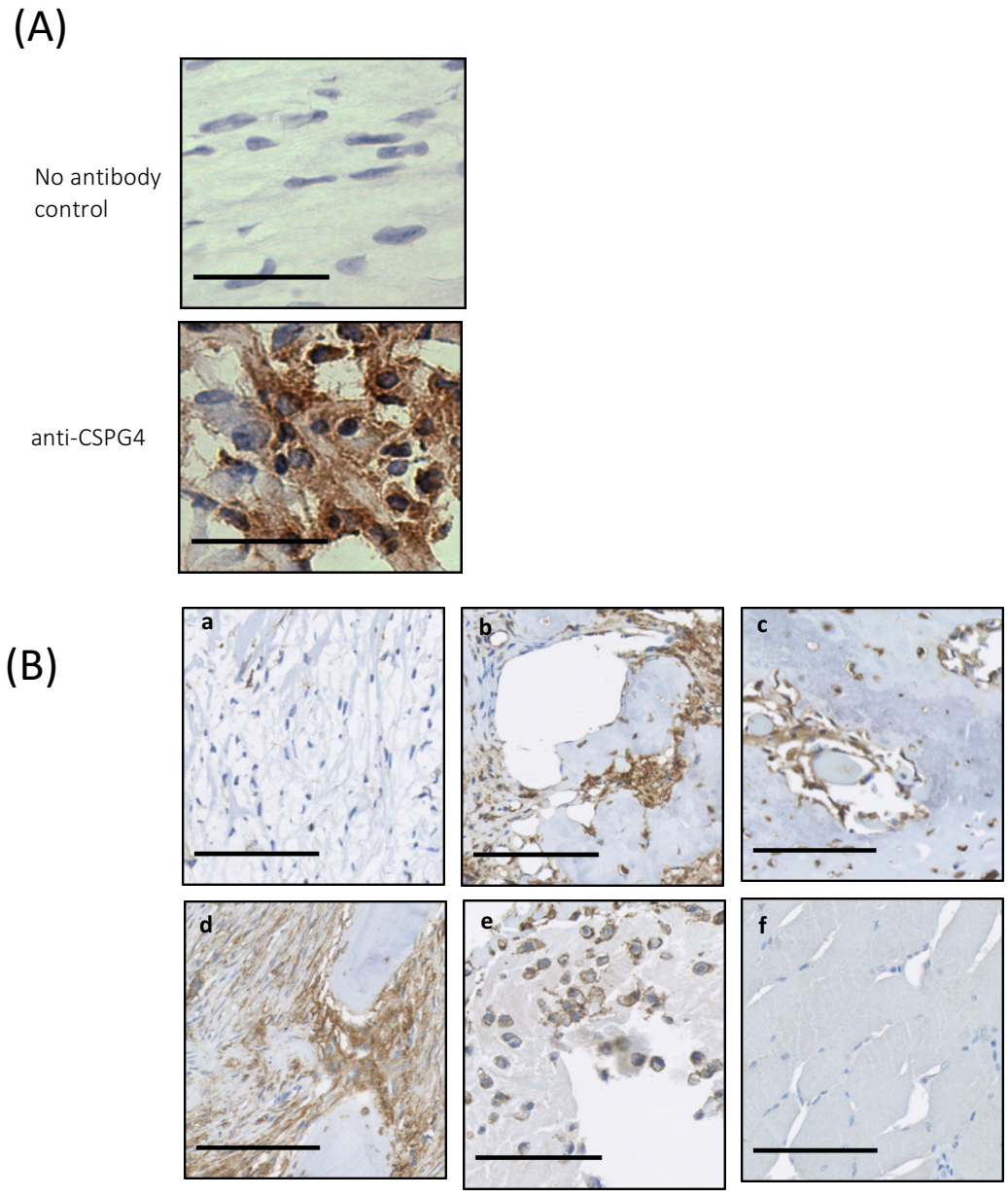

Figure 3.3: CSPG4 protein expression in osteosarcoma FFPE clinical samples. (A) Representative image for CSPG4 immunoreactivity in frozen osteosarcoma sections. Negative control obtained through omission of the primary antibody. Scale bar = 25µm. **(B)** Images of osteosarcoma cases from a tumour micro-array (NHS Grampian); **a.** negative osteoblastic, **b.** parosteal, **c.** chondroblastic, **d.** fibroblastic, **e.** osteoblastic, **f.** skeletal muscle. Scale bar = 100µm.

Table 3.2 – **Patient details of human osteosarcoma samples from a TMA cohort used for FFPE IHC analysis.** Details of human osteosarcoma samples from the tumour microarray used for immunohistochemistry experiments to investigate CSPG4 expression in vivo.

Patient number	Sex	Date of birth	Sample number	Positivity (Y/N)	Biopsy stage	Gross pathological features
1	**M**	**15/01/42**	6929/91	Y	Pre-treatment	Hip
2	**M**	**16/03/34**	4331/92	Y	Pre-treatment	Proximal femur
			7401/92	Y	Post-treatment	Proximal femur
3	**M**	**22/05/47**	22560/92	Y	Post-treatment	Proximal tibia
4	**F**	**27/08/08**	1092/93	Y	Pre-treatment	Extra-skeletal OS present in soft tissue in lower right leg
5	**M**	**29/04/77**	15886/95	Y	Pre-treatment	Humerus
			19846/95	N	Post-treatment	Humerus
6	**M**	**27/01/66**	9205/96	Y	Pre-treatment	Parosteal OS present in femur

			12089/96	Y	Post-treatment	Parosteal OS present in femur
7	**F**	**12/01/63**	23764/96	N	Pre-treatment	Unusual tumour reported as primary OS in lung tissue
8	**Unknown**	**Unknown**	27209/96	N	Pre-treatment	Low grade in scapula
9	**Unknown**	**Unknown**	27212/96	N	Pre-treatment	Tibia
10	**M**	**12/05/81**	5228/98	Y	Pre-treatment	Unknown
11	**M**	**19/10/86**	13220/98	Y	Pre-treatment	Femur
12	**M**	**21/05/39**	29711/99	Y	Pre-treatment	Tibia
			7519/00	Y	Post-treatment	Recurrent disease present in soft-tissue in thigh
13	**F**	**11/08/23**	15721/01	Y	Pre-treatment	Femur
			17214/01	Y	Post-treatment	Femur after surgical treatment

14	**F**	**18/03/77**	8348/02	Y	Pre-treatment	Femur
15	**F**	**26/01/91**	20660/02	Y	Pre-treatment	Femur
16	**F**	**27/07/31**	4089/03	Y	Pre-treatment	Unknown
17	**F**	**10/09/87**	18047/03	Y	Pre-treatment	Tibia
			24894/03 D	Y	Post-treatment	Tibia
			24894/03 G	Y	Post-treatment	Unknown site of tumour spread
18	**F**	**19/03/88**	9422/05	Y	Pre-treatment	Femur
19	**M**	**06/02/90**	28026/05	Y	Pre-treatment	Femur
			5199/06	Y	Pre-treatment	Femur
20	**M**	**26/04/90**	29324/05	Y	Pre-treatment	Proximal tibia
			31619/07	Y	Pre-treatment	Metastatic disease present in the spine

21	**Unknown**	**Unknown**	11114/77	Y	Pre-treatment	Chondroblastic disease present in unknown site
22	**F**	**04/01/89**	6236/08	Y	Pre-treatment	Metastatic disease present in the vena cava
23	**M**	**19/08/44**	7213/08	Y	Pre-treatment	Tibia
24	**F**	**14/04/35**	1320/09	Y	Pre-treatment	Scapula
			5399/09	N	Post-treatment	Scapula
25	**F**	**22/05/42**	8216/09	Y	Pre-treatment	Maxilla
			21570/09	Y	Post-treatment	Maxilla
26	**M**	**28/08/78**	15611/09	Y	Pre-treatment	Fibroblastic tumour present in distal femur
			22259/09	N	Post-treatment	Fibroblastic tumour present in distal femur
			18837/10	Y	Pre-treatment	Metastatic fibroblastic tumour present in lungs
			6811/11	Y	Post-treatment	Metastatic fibroblastic tumour

						present in lungs
27	**F**	**21/05/37**	16790/09	N	Pre-treatment	Chondroblastic OS present in ribs
			22257/09	Y	Post-treatment	Chondroblastic OS present in ribs
			4567/10	Y	Pre-treatment	Recurrent chondroblastic OS present in chest wall
			32400/10	Y	Post-treatment	Metastatic chondroblastic OS present in lung
28	**M**	**02/12/22**	27824/09	Y	Post-treatment	Humerus
29	**M**	**24/03/43**	11275/09	Y	Post-treatment	Extra-skeletal OS present in unknown site
30	**F**	**25/01/97**	23235/11	Y	Pre-treatment	Femur
			34770/11	Y	Post-treatment	Femur

2.5 CSPG4 expression in osteosarcoma in vitro

After establishing that CSPG4 mRNA and protein expression was present in human osteosarcoma samples, it was important to establish if it was present in in vitro osteosarcoma cell models. The osteosarcoma cell lines investigated were U2OS, MG63, HOS, HOS-MNNG and 143B.

2.5.1 CSPG4 mRNA expression in vitro through end-point PCR

In order to assess CSPG4 mRNA expression, RNA was extracted from each of the cell lines and underwent RT-PCR reaction. GAPDH was used as a loading control. All five cell lines demonstrated CSPG4 mRNA positivity (Figure 3.4a).

2.5.2 CSPG4 protein expression in vitro through western blotting

Cell lines were lysed and protein was collected using RIPA buffer. CSPG4 exists as a ~250kD core protein and a ~400kD proteoglycan. In order to test specificity of the bands, chondroitinase ABC, an enzyme that cleaves chondroitin sulphate chains was added to lysates from each of the cell lines. This would result in the expression of the chondroitin sulphate free core protein only.

Each of the five cell lines demonstrated CSPG4 expression (Figure 3.4b). Although this is only just visible in the HOS cell line. The expression of CSPG4 differed between the five cell lines investigated (Figure 3.4b). Chondroitinase ABC treatment resulted

in core protein expression only. β-actin was used as a loading control and was consistent across cell lines.

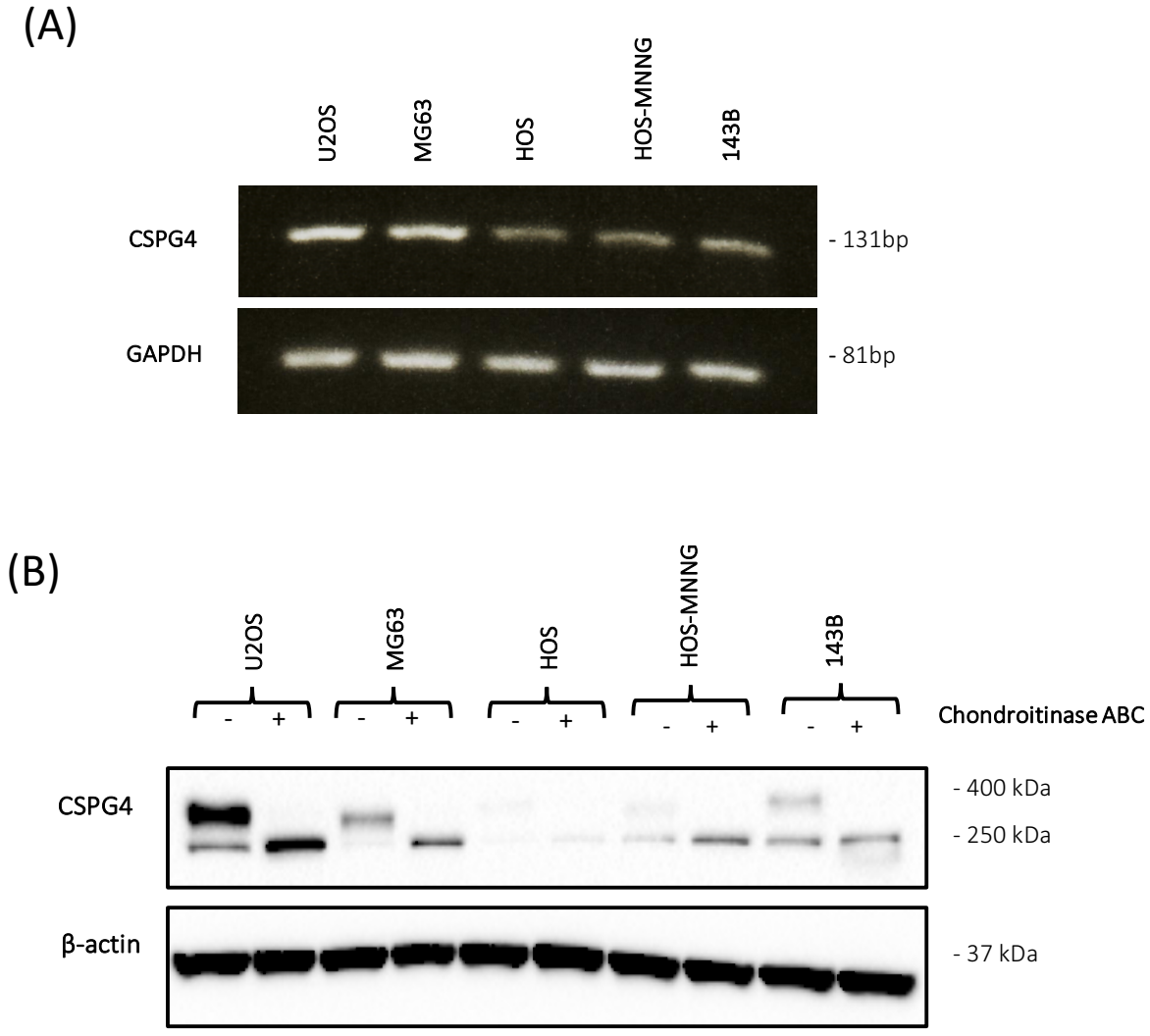

Figure 3.4 CSPG4 expression in osteosarcoma cell lines. (A) Representative gel image of end-point PCR reaction investigating CSPG4 expression in model osteosarcoma cell lines; U2OS, MG63, HOS, HOS-MNNG and 143B. GAPDH was used as a loading control. 131bp and 81bp were the product sizes of CSPG4 and GAPDH respectively. **(B)** Representative blot showing CSPG4 protein expression in cell lysates with, and without chondroitinase ABC pre-treatment. B-actin was used as a loading control.

3.4 Discussion

The purpose of this chapter was to demonstrate the expression of CSPG4 expression in osteosarcoma. Osteosarcoma patient samples were assessed for CSPG4 mRNA and protein expression. The extent of CSPG4 expression in osteosarcoma was assessed within a cohort of tumour samples. Levels of mRNA expression were compared to healthy adult osteoblast cells, the purported cell of origin for osteosarcomas. It was also the aim of this chapter to investigate CSPG4 expression in a number of model osteosarcoma cell lines. CSPG4-positive cell lines would be taken forward for in vitro experiments. Both mRNA and protein expression were examined in U2OS, MG63, HOS, HOS-MNNG and 143B cell lines.

This chapter has demonstrated that CSPG4 expression is present in osteosarcoma in vitro and in vivo. Observable evidence of CSPG4 mRNA expression was found in all patient samples (Figure 3.1a). However, the expression was variable between samples. This is reflected in the GAPDH expression level and could be a result of poor RNA quality.

mRNA levels in further patient samples analysed through qPCR, were heightened in comparison to healthy osteoblast cells (Figure 3.1b). These samples also display heterogeneity of expression. Due to its overexpression compared to healthy osteoblasts, CSPG4 could function as a prognostic tool in osteosarcoma.

A study by Benassi et al. (2009) investigated CSPG4 expression in relation to clinicopathological features in soft-tissue sarcomas. They found high CSPG4 mRNA levels increase the risk of secondary lesions within 12 months post-surgery (Benassi et al 2009). Patients were stratified into high and low CSPG4 expression groups and correlated to disease progression and existence of metastatic spread. Patients with high CSPG4 mRNA expression were significantly more likely to have developed metastatic disease (Benassi et al. 2009). Separately, it was shown that CSPG4 has an 81-fold amplification in metastatic lesions (Benassi et al. 2009).

If clinical data was sought for the osteosarcoma patients, a similar analysis could be run, giving insight into whether CSPG4 could predict metastasis or disease-free survival in osteosarcoma. Future experiments should analyse this point using a greater cohort of patient samples.

For the experiment, cDNA from healthy osteoblast cells were used as a calibrator, as they have been described as the cell of origin for osteosarcoma development (Durfee et al. 2016). Therefore, the results demonstrated that CSPG4 mRNA is overexpressed in osteosarcoma compared to healthy osteoblast cells. If osteoblasts represent the cell of origin for osteosarcoma development, this result would imply that CSPG4 is upregulated during the onset of tumorigenesis and therefore, could suggest that CSPG4 is playing a role in osteosarcoma tumorigenesis.

Other studies have suggested other cell types are the cell of origin for osteosarcoma development. As well as committed osteoblasts, intermediate cell lines along the

osteogenic lineage have been suggested (Abarrategi et al. 2016). Mesenchymal stem cells (MSCs) have been suggested as a cell of origin for osteosarcoma (Mutsaers and Walkley 2014). MSCs can develop pleomorphic sarcomas in vivo (Xiao et al. 2013). Their transformation also rests on the deregulation of many signalling pathways mutated in osteosarcomas (Xiao et al. 2013).

Pericytes are thought to be related to mesenchymal stem cells and may represent the same cell population identified in vivo (de Souza et al. 2016). They both have perivascular localisation and feature corresponding molecular markers (de Souza et al. 2016). However, the evidence is not settled on their connection – some studies demonstrate that pericytes do not harbour plasticity in vitro or after transplantation into mice (Guimaraes-Camboa et al. 2017).

Pericytes express CSPG4 both during development and post-natally (Sato et al. 2016). When angiogenic, pericytes upregulate the expression of CSPG4 (Sato et al. 2016). Pericytes with a mutation in the *Trp53* gene can give rise to osteosarcomas (Sato et al. 2016). Pericytes were confirmed as the cell of origin through lineage tracing using CSPG4 protein expression (Sato et al. 2016). 76% of mice with pericyte conditional knock-out of *Trp53* developed osteosarcoma. These results suggest that pericytes can be a cell of origin for osteosarcoma development. As CSPG4 is endogenously expressed on pericytes throughout life, its upregulation compared to osteoblasts may be a false comparison. This has implications for whether CSPG4 is involved in tumorigenesis, or whether its overexpression represents a passenger mutation.

CSPG4 protein expression was demonstrated through IHC analysis (Figure 3.3). This expression was found on the cell surface (Figure 3.3). High levels of CSPG4 transcript is poorly correlated with membrane-expressed protein. This suggests that given osteosarcoma samples express CSPG4 mRNA and protein, CSPG4 could be a primary event of tumour formation (Nicolosi et al. 2015).

One aim of the chapter was to identify an anti-CSPG4 antibody for use in various experiments. Using two antibodies previously characterised by Girolamo et al. (2013). In their study, they produced a number of different monoclonal antibodies with the aim of identifying different isoforms of the CSPG4 protein (Girolamo et al. 2013). Forty eight immunologically distinct CSPG4 isoforms were identified using various mAbs (Girolamo et al. 2013). The first antibody, 2161F9, identified the core protein and glycosylated protein. 2161F9 also demonstrated positivity on A375 and 143B cells in vivo, as well as pericytes in in vivo glioblastoma samples (Girolamo et al. 2013). The 2161D3 antibody identified a smaller variant of the protein and was discovered on a number of tumour cells in vitro (Girolamo et al. 2013). Alongside these two antibodies we also, compared a commercially available antibody from Abcam, ab86067.

When tested on soft-tissue sarcoma samples, known to be positive for CSPG4, each antibody demonstrated similar staining pattern (Figure 3.2). Tumour cells were positively stained around the cell membrane, as would be expected. As the commercial antibody was consistent with the mAbs, ab86067 must either recognise a portion of the protein consistent across isoforms or different isoforms of CSPG4

exist within one sample and were recognised by the antibodies. Due to the consistency of staining and ready availability of ab86067, this was taken forward as the antibody of choice for future experiments.

The isoform of CSPG4 present on cells may differ depending on context. For example, tumour samples may express one isoform whereas developmental tissues express a different isoform. This would be important when considering treatment options. Drugs could be developed that would only recognise tumour-specific isoforms of the protein. This could be therapeutically useful if different tumour types expressed differing isoforms of the protein. Tumour-specific drugs could also protect healthy adult cells that express CSPG4 from cytotoxicity. This is an important consideration for CPSG4-positive pericyte cells. Targeting pericyte depletion in hypoxic tumours can result in increased lung metastasis (Keskin et al. 2015). On the contrary, targeting CSPG4- positive pericytes at the same time as CSPG4-positive tumour cells could act as a dual-treatment, working on the tumour directly as well as the tumour microenvironment (Kelly-Goss et al. 2014).

CSPG4 has been demonstrated in 100% of fixed-frozen osteosarcoma samples and 86% of FFPE osteosarcoma samples from a tumour micro array (Figure 3.3). New therapeutic targets have been rare in osteosarcoma due to its heterogeneous nature (Hattinger et al. 2015). There have been no new treatments for osteosarcoma since the early 1980s (Behjati et al. 2017). The clinical need for new treatments is also compounded by the short- and long-term toxicity associated with the use of chemotherapy (Taran et al. 2017). The finding that CSPG4 is present in 86% of cases

is important and in excess of what is presented in other studies. For example, another study has found IGFR1 amplification observed in 14% of tumours (Bejati et al. 2017).

This experiment also demonstrated that CSPG4 is present in a number of different osteosarcoma sub-types, such as osteoblastic, parosteal, chondroblastic and extra-skeletal (Figure 3.3b). This suggests that CSPG4 may not be restricted to one type of osteosarcoma, however the sample size would need to be increased in future experiments. The same is true for metastatic tumours. All 5 metastatic tumour samples were positive for CSPG4.

Another aim of this chapter was to establish whether commonly used osteosarcoma cell line models were positive for CSPG4. RNA was extracted from cell lines U2OS, MG63, HOS-MNNG and 143B demonstrated CSPG4 expression (Figure 3.4a). The loading control (GAPDH) was consistent across samples (Figure 3.4a). U2OS and MG63 displayed higher expression levels than HOS, HOS-MNNG and 143B.

This was reflected in CSPG4 protein expression across samples (Figure 3.4b). The cell lines differed in their expression pattern of CSPG4, with each having a different combination of the core protein and proteoglycan (Figure 3.4b). The significance of the GAG chain is unknown for CSPG4 and it has not been found to influence cell behaviour (Nicolosi et al. 2015).

These results confirm that CSPG4 expression exists in osteosarcoma cell lines. This

allows a number of cell lines to be used for further experiments investigating the role of CSPG4 in osteosarcoma tumorigenesis.

Chapter 4

Modulation of CSPG4 expression in vitro

4.1 Summary

In order to assess the effect CPSG4 plays in osteosarcoma cell behaviour, it was essential to modulate its expression. Two approaches were taken to achieve this aim.

Firstly, CRISPR-Cas9 was used to produce CSPG4-deficient cells. The 143B osteosarcoma cell line, which expresses CSPG4 endogenously, was used as the parental cell line. Two negative cell lines, H10-KO and H7-KO were produced. Genetic analysis confirmed the CSPG4 gene had undergone mutation and protein analysis confirmed these two cell lines were negative for CSPG4 expression. The parental cell line as well as the negative cell lines were transfected with a CSPG4 expression plasmid in order to express CSPG4 exogenously. Therefore, from the 143B cell line, a panel of experimental cell lines was produced with varying levels of CSPG4 expression.

Secondly, siRNA was used as an alternative mechanism to reduce CSPG4 expression, rather than abolish it. siRNA treatment was used on three osteosarcoma cell lines, U2OS, MG63 and 143B. The glioblastoma cell line, U87MG, was used as a positive control. siRNA treatment over 72 hours successfully reduced CSPG4 expression in all cell lines used.

These two sets of cell lines provide a model for use in in vitro assays.

4.2 Aims

The aims of the experiments detailed in this chapter were to:

1. Create CSPG4 knock-out cell lines using the CRISPR/Cas9 system
2. Exogenously express CSPG4 in CSPG4-negative CRISPR/Cas9 cell lines
3. Use small interfering RNA to reduce CSPG4 expression

4.3 CRISPR/Cas9 mediated knock-out of CSPG4 in 143B cells

In order to investigate CSPG4's biological function in osteosarcoma, it was important to create cell lines with modulated CSPG4 expression levels. This was achieved through the use of the CRISPR/Cas9 system. The experimental technique has been summarised in Figure 4.1.

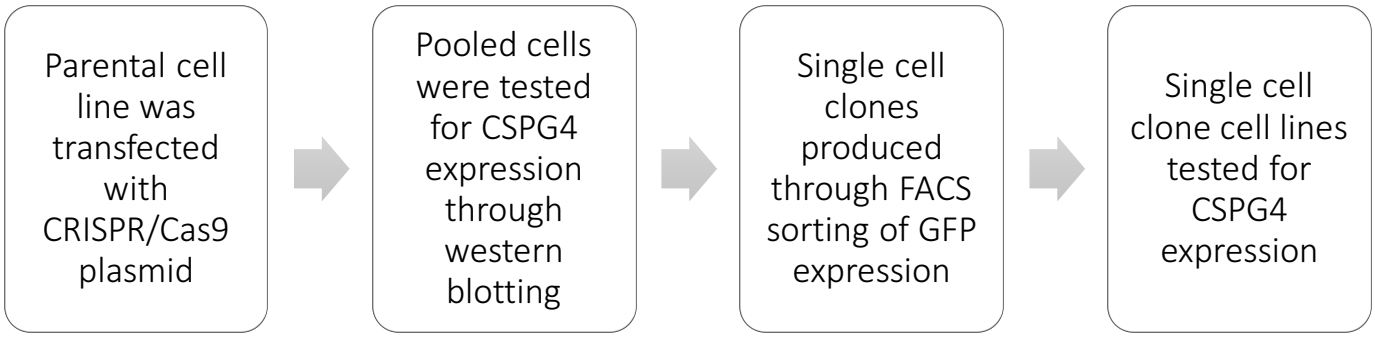

Figure 4.1 – **Experimental work flow to create CRISPR/Cas9 knock-out cell line.** Schematic diagram outlining the experimental steps and protocols used to establish CSPG4 knock-out cell lines from the 143B parental cell line.

4.3.1 CSPG4 expression in pooled cells through western blotting

In order to test the efficacy of the CRISPR/Cas9 plasmid, pooled cells were tested for CSPG4 expression, before single cell cloning. All plasmids received from Horizon discovery contain gRNA complimentary to sequences present in CSPG4 exon 1 and 2 were used. All four plasmids, featuring separate gRNA sequences, resulted in no detectable CSPG4 protein expression as investigated through western blotting (Figure 4.2). β-actin was used as a loading control.

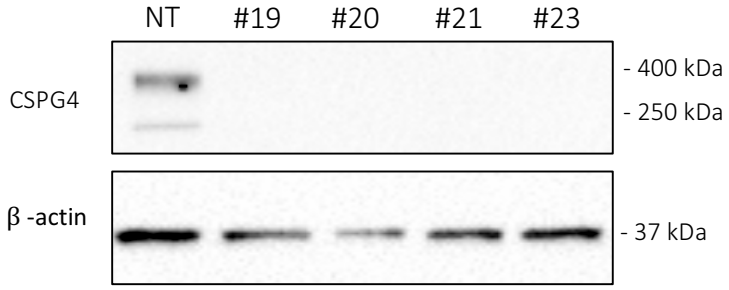

Figure 4.2 – **Initial expression of CSPG4 protein following CRISPR/Cas9 plasmid transfection.** Four plasmids (#19, #20, #21 and #23) were transfected into separate cell populations and compared to a non-treatment control (NT) for CSPG4 protein expression.

4.3.2 Characterisation of knock-out cell lines

Following initial expression testing, cells were sorted via FACS for GFP expression. GFP expression indicated the CRISPR/Cas9 plasmid had been transfected into the cell and was being expressed. Cells were sorted into single cell clones and grown until confluent. Surviving cells were screened for CSPG4 expression through western blotting and then flow cytometry.

After screening for CSPG4 protein, two cell lines, H10-KO and H7-KO consistently displayed no CSPG4 expression as shown through western blotting (Figure 4.3). In order to test that these cell lines represented a true knockout (deletion of the gene), they were taken for sequencing. gDNA was extracted from the cells and the relevant exon was amplified and sent for sequencing. Both cell lines demonstrated sequence deletion in the sequence complimentary to the gRNA sequence (Figure 4.3).

(A)

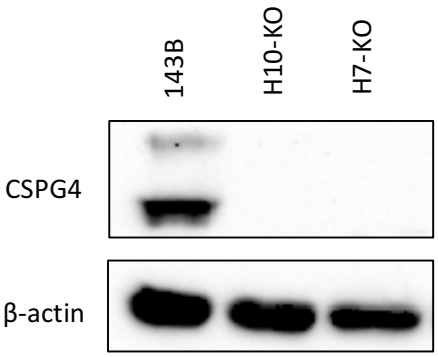

(B)

Exon 1:

CTTCCTTCTTCGGTGAGAA**CCACCTGGAGGTGCCTGTGGCCA**CGGCTCT
GACCGACATAGACCTGCAGCTGCAGTTCTCCACGTCCCAGCCCGAAGCCC
TCCTTCTCCTGGCAGCAGGCCCAGCTGACCACCTCCTGCTGCAGCTCTAC
TCTGGACGCCTGCAG

Exon 2:

GCGCCCAGGAGCAGAGCCGCGCTCGCTCCACTCAGCTCCCAGCTCCCAG
GACTCCGCTGGCTCCTCGCAAGTCCTGCCG**CCCAGCCCGCCGGGATGCA**
GTCCGGGCCGCGGCCCCCACTTCCAGCCCCCGGCCTGGCCTTGGCTTTG
ACCCTGACTATGTTGGCCAGACTTGCATCCGCGG

Figure 4.3 – **Protein and sequence analysis of CRISPR/Cas9 knock-out cell lines. (A)** Representative western blot showing negative CSPG4 expression in CRISPR/Cas9 treated cell lines. **(B)** Schematic representation of the genomic sequences represents exon 1 and exon 2 for the human CSPG4 gene. The highlighted sequences in red correspond to the deleted sequence shown through sequencing for H10-KO and H7-KO cell lines, in exon 1 and exon 2 respectively.

4.3.3 Exogenous expression of CSPG4 in knock-out cell lines

Following characterisation of CSPG4- deficient cell lines, it was important to re-introduce CSPG4 into these cells as a control of any observed phenotypic change. A CSPG4 expression plasmid was transfected in to both CRISPR/Cas9 knockout cells to re-introduce CSPG4 expression, and the parental 143B cell line to overexpress CSPG4. The experimental technique has been summarised in Figure 4.4.

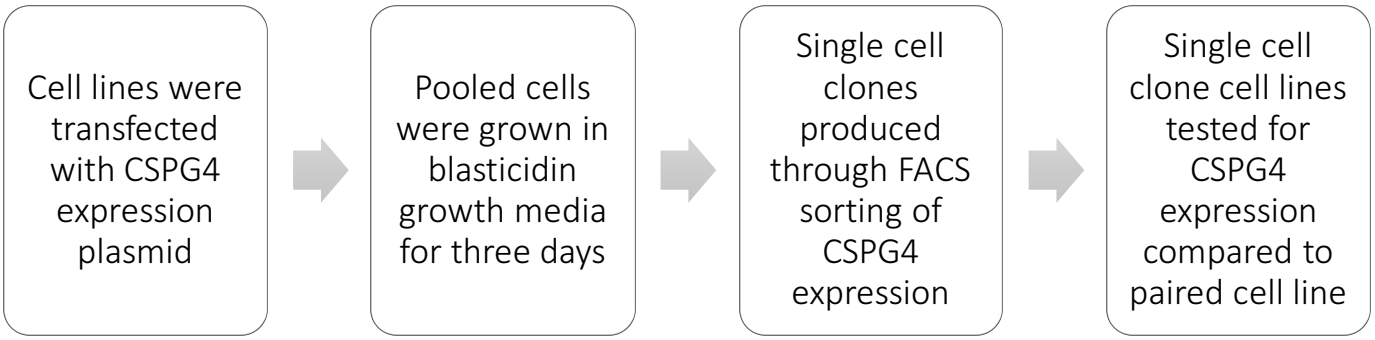

Figure 4.4 – **Experimental work flow to create exogenously expressing CSPG4 cell lines.** Schematic diagram outlining the experimental steps and protocols used to establish CSPG4 knock-out cell lines from the 143B parental cell line.

4.3.4 Characterisation of experimental cell lines

The experimental cell lines produced are detailed in Table 4.1 alongside details of how they were produced. Characterisation of these cells and their level of CSPG4 expression is detailed below.

Cell line:	Method:
143B	Parental cell line
143B-CSPG4	Single cell clone of parental cell line transfected with CSPG4 expression plasmid
H10-KO	Single cell clone of 143B cell line following CSPG4 knock-out using CRISPR #21 plasmid
H10-KO-CSPG4	Single cell clone of H10-KO cell line following transfection with CSPG4 expression plasmid
H7-KO	Single cell clone of 143B cell line following CSPG4 knock-out using CRISPR #23 plasmid
H7-KO-CSPG4	Single cell clone of H7-KO cell line following transfection with CSPG4 expression plasmid

Table 4.1 – **Panel of experimental cell lines produced with CSPG4 expression.** Details of cell lines produced from the 143B cell line containing modulated expression of the CSPG4 protein.

4.3.4.1 Western blot analysis of cell lines

Cell lines including 143B parental, CRISPR/Cas9 and CSPG4 exogenous expression cells were tested through western blotting and flow cytometry for CSPG4 expression. Western blot analysis demonstrates successful overexpression of CSPG4 in the 143B cell line, this new cell lines is classified as 143B-CSPG4 (Figure 4.5a). CSPG4 had also been successfully expressed in H10-KO and H7-KO CSPG4 –deficient cell lines, producing two new experimental cell lines, classified as H10-KO-CSPG4 and H7-KO-CSPG4 respectively (Figure 4.6a).

Using densitometry analysis of the core protein bands, expression of CSPG4 was quantified in each of the cell lines using the Bio-Rad image analysis software. CSPG4 expression in the 143B-CSPG4 cell line compared to the 143B parental cell line. Both H10-KO-CSPG4 and H7-KO-CSPG4 cell lines demonstrated expression higher than the 143B parental cell line (Figure 4.5b).

4.3.4.2 Flow cytometry analysis of cell lines

In order to confirm the expression seen in western blotting, flow cytometry was used to demonstrate CSPG4 cell surface expression on the cell lines. Cell lines were divided into three conditions, unstained condition (to show background fluorescence endogenously shown by cells), isotype condition (to show effect of non-specific binding of antibodies) and CSPG4-PE antibody condition (to show CSPG4 expression on the cell surface). In all conditions, the unstained condition (green) and the isotype

control (yellow) show overlapping fluorescence profiles showing that there is no off-target binding of the antibody type and fluorescence is no higher than background fluorescence (Figure 4.6b).

Expression of CSPG4 (red peak) is demonstrated as a rightward shift. 143B demonstrates CSPG4 expression with a single peak (Figure 4.6b). 143B-CSPG4 also demonstrates CSPG4 positivity, however the shift is further to the right and broader, suggesting a broader range of expression that is higher than the parental 143B cell line. Both H10-KO and H7-KO exhibit complete overlap with background staining which is indicative of no CSPG4 expression (Figure 3.6b).

H10-KO-CSPG4 and H7-KO-CSPG4 both exhibit two separate peaks indicative of two cell populations with differing expression of CSPG4 (Figure 4.4c). The H10-KO-CSPG4 expression pattern contains one large peak, which largely overlaps with unstained cells suggesting negative CSPG4 expression and one smaller peak, shifted to the right. H7-KO-CSPG4 cells display two peaks shifted rightwards suggesting two populations of positive cells exist (Figure 4.4c).

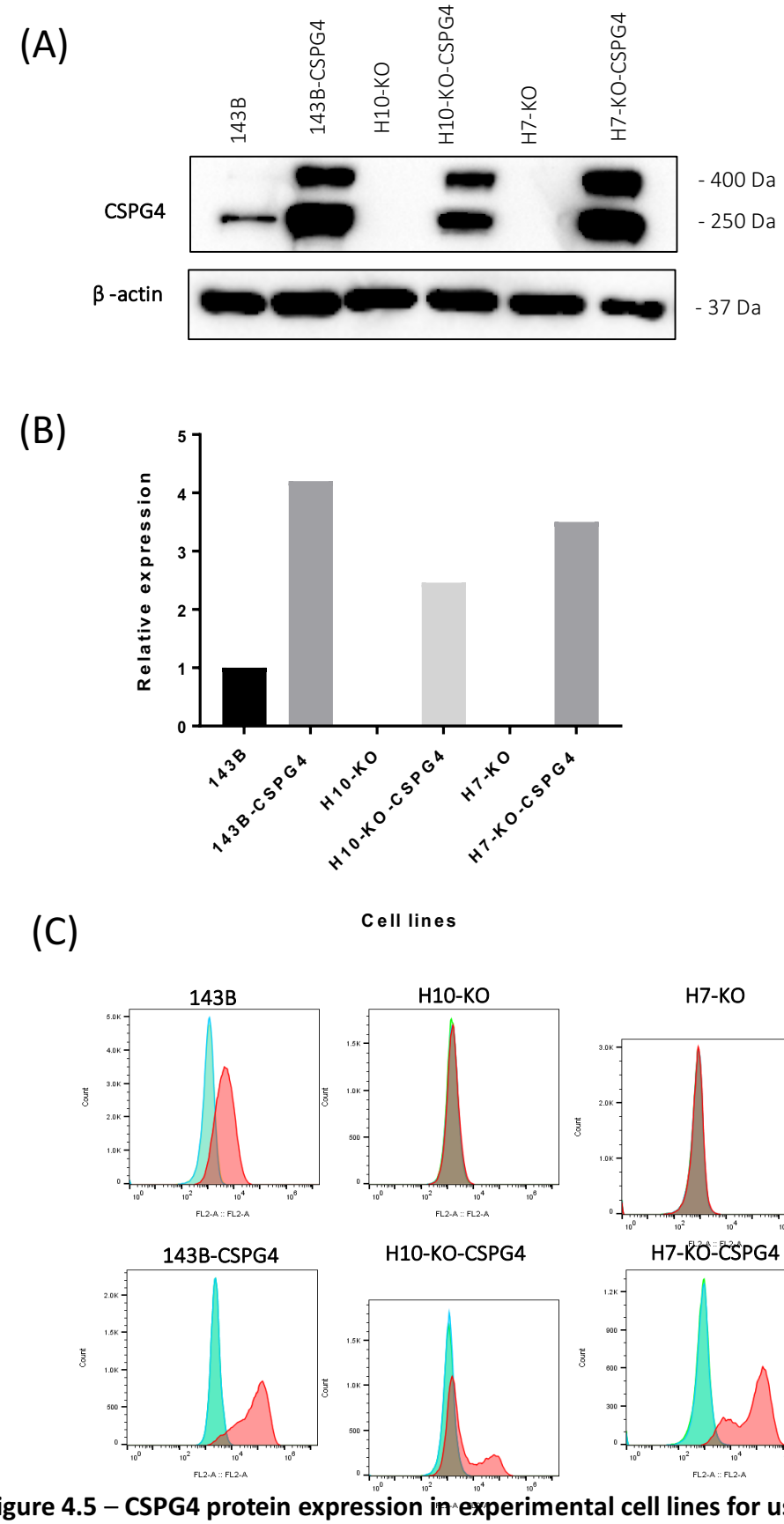

Figure 4.5 – CSPG4 protein expression in experimental cell lines for use in in vitro experiments. (A) Representative western blot image showing CSPG4 expression across the panel of experimental cell lines. B-actin was used as a loading control. **(B)** Quantification of CSPG4 expression of experimental cell lines as compared to the parental 143B line. The core protein band (~250kDa) compared between cell lines only. **(C)** Flow cytometry data showing CSG4 surface expression in experimental cell lines. Different cell populations were either unstained (blue), stained with an isotype control antibody (green) or stained with an anti-CSPG4-PE antibody (red).

4.3.4.2 Immunofluorescence analysis of CSPG4-positive cell lines

In order to investigate the difference between cell populations within single cell lines displayed by flow cytometry analysis (Figure 4.4c), immunofluorescence analysis was used. This could help define whether negative cell lines exist or whether CSPG4 protein expression was localised intracellularly rather than on the cell membrane.

143B-CSPG4, H10-KO-CSPG4 and H7-KO-CSPG4 cell lines were stained with DAPI, anti-His-Tag and anti-CSPG4 antibodies (Figure 4.5). All cell lines displayed CSPG4 expression and this co-localised with His-tag expression, as expected. 143B-CSPG4 and H7-KO-CSPG4 both displayed CSPG4 expression predominantly at the cell membrane (Figure 4.5). H10-KO-CSPG4 cell lines displayed a more disparate staining pattern of CSPG4 expression (Figure 4.5). Staining is demonstrated throughout the intracellular compartment of the cell as well as at the cell membrane.

All cell lines demonstrated that 95-100% of cells displayed positive staining of CSPG4 expression. This suggests that CSPG4 localisation explains the distinct peaks shown by flow cytometry analysis, rather than a sub-population of CSPG4-negative cells.

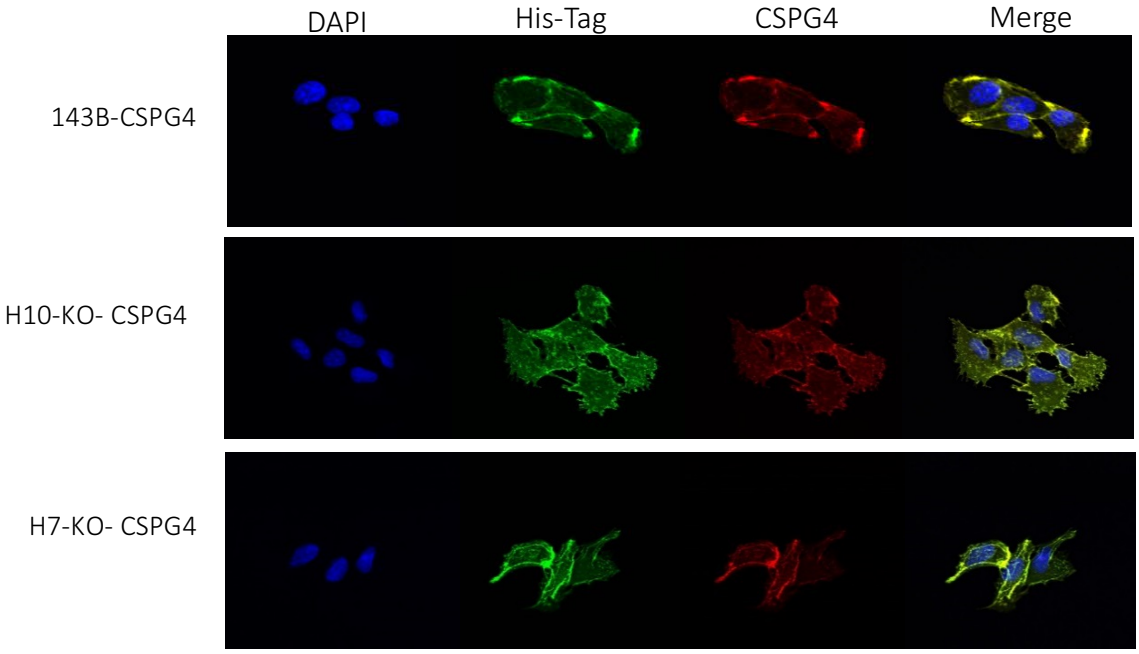

Figure 4.6 - Cellular location of exogenously expressed CSPG4 protein. Immunofluorescence data showing cell lines transfected with the CSPG4 expression plasmid. Cell nuclei is shown in blue (DAPI), his-tag positivity is shown in green and CSPG4 positivity is shown in red. Single colour images were combined to create the merge photo.

4.3.4.3 Morphology of experimental cell lines

The morphology of the experimental cell lines was investigated to assess whether CSPG4 expression altered cell shape in vitro. Light-phase images were taken of cell lines growing in culture.

Whilst CRISPR knock-out cell lines, H10-KO and H7-KO, appear to have a different morphology from parental cells, 143B is a heterogeneous cell line and could result from single cell cloning as opposed to a CSPG4-dependent change (Figure 4.7). This is underlined by the fact cell lines exogenously expressing CSPG4 do not differ from their paired cell line morphologically (Figure 4.7).

Cells in 143B and 143B-CSPG4 feature a mix of stringy cells with long processes and have a more fibroblastic morphology. H10-KO and H10-KO-CSPG4 cells are smaller and have a more stellate morphology, few cells feature long processes. H7-KO and H7-KO-CSPG4 cell lines are a mixture of both types, cells have longer processes than H10-KO and H10-KO-CSPG4 cell lines, but not as long as 143B and 143B-CSPG4 cells.

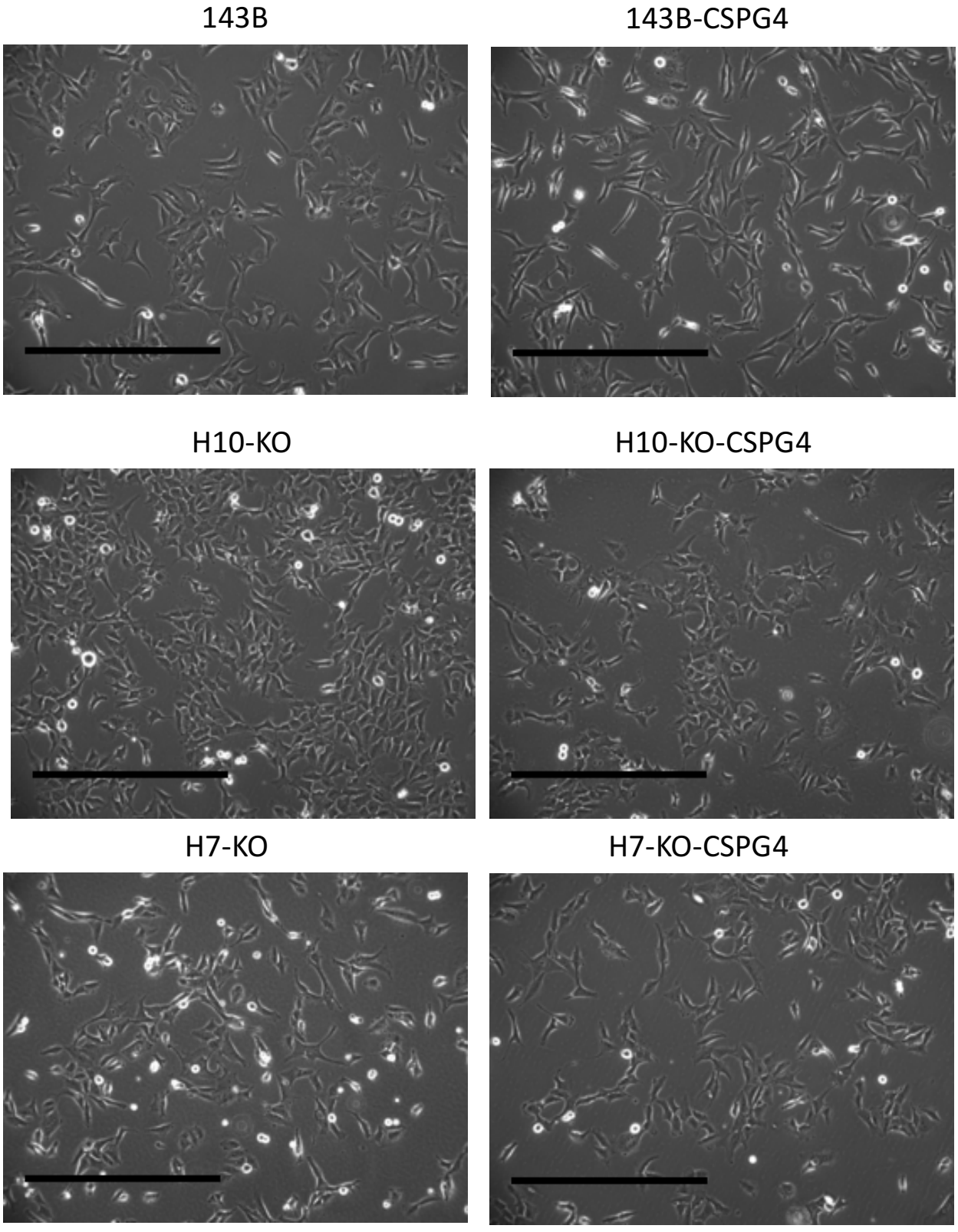

Figure 4.7 – **Morphology of CRISPR/Cas9 experimental cell lines.** Light phase images showing cell morphology in culture taken of experimental cell lines. Images taken using x20 magnification. Scale bar = 100µm.

4.4 siRNA-mediated knock-down of CSPG4 in osteosarcoma cell lines

siRNA provides an alternative mechanism to modulate CSPG4 expression. siRNA knock-down reduces protein expression rather than abolish it completely. It also represents a faster experimental technique than CRIPSR/Cas9 deletion. siRNA modulation of CSPG4 expression was used to investigate CSPG4 knock-down in a set of osteosarcoma cell lines, including U2OS, MG63 and 143B. Glioblastoma cell line, U87MG, is known to be CSPG4 positive and was used as a positive control.

4.4.1 Western blotting analysis of CSPG4 expression in osteosarcoma cell lines

Cell lines were treated for 72 hours with siRNA before being taken for protein extraction. Western blotting was used to investigate CSPG4 protein expression. β-actin was used as a loading control.

All cell lines were shown to exhibit CSPG4 protein expression, both core protein and full proteoglycan forms (Figure 4.8a). siRNA treatment over the course of 72 hours also correlated in reduced CSPG4 protein expression in all cell lines (Figure 4.6a). The relative CSPG4 expression of siRNA-treated cells compared to control cells is reduced across all cell lines (Figure 4.8b).

Therefore, siRNA-treated cells can be used for in vitro experiments investigating CSPG4 expression and osteosarcoma cell behaviour.

(A)

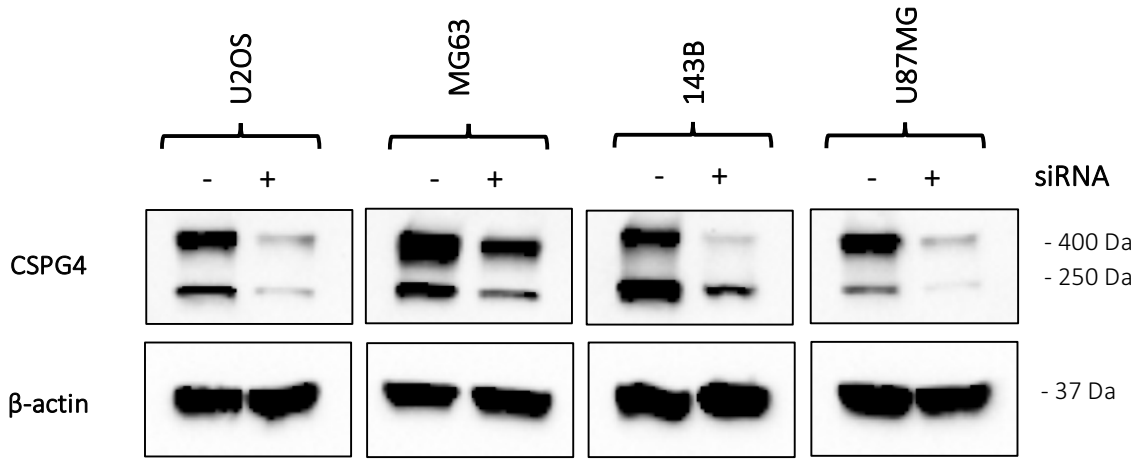

(B)

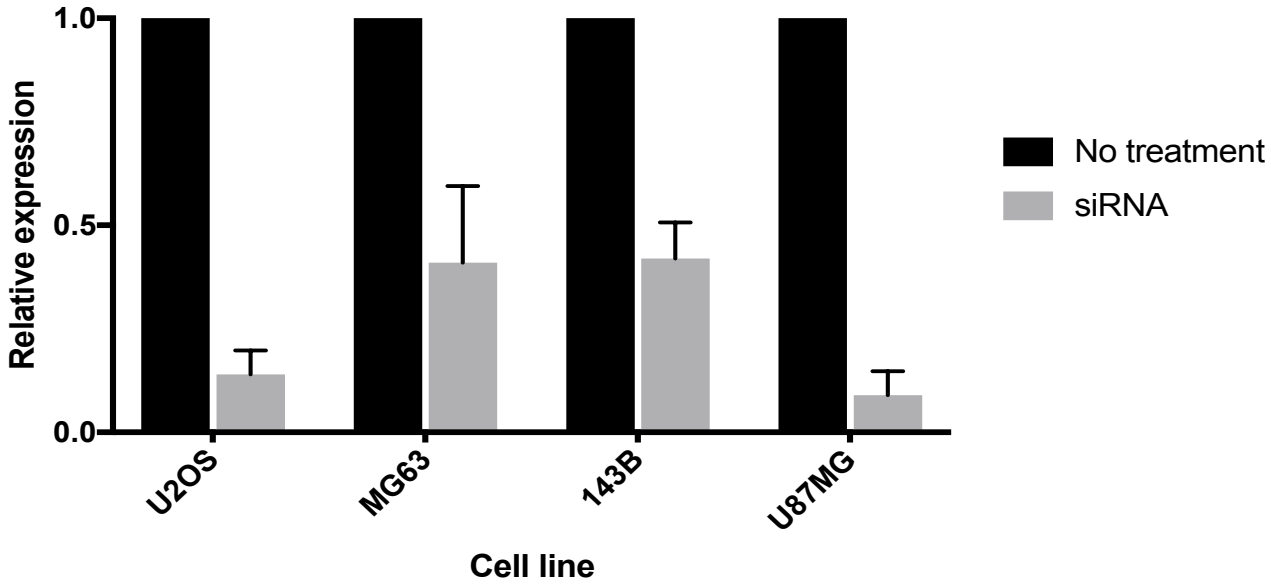

Figure 4.8 Modulation of CSPG4 expression following siRNA treatment. (A) Representative western blot image showing CSPG4 expression across the panel of cell lines, being either control (-) or siRNA treated (+). β-actin was used as a loading control. **(B)** Quantification of CSPG4 expression of non-treated cells compared to siRNA treated cells. The core protein band (~250kDa) was used for densitometry analysis.

4.4 Discussion

The aim of this chapter was to develop a human osteosarcoma cell model for use in in vitro and in vivo studies. CSPG4 protein expression was modulated through the use of CRISPR/Cas9 deletion and siRNA knock-down.

For CRISPR/Cas9, the 143B cell line was chosen due to its in vivo properties. A study by Luu et al. (2005) described that the 143B cell line was able to grow in immunocompromised mice when injected into the tibia. The 143B cell line also demonstrated the ability to metastasize readily to the lungs, the most common site for metastasis in the human disease (Luu et al. 2005). The other cell lines do not demonstrate this ability.

CRISPR/Cas9 technology was utilised to create CSPG4-deficient cells through mutation of the *CSPG4* gene. Four gRNAs produced CSPG4-deficiency, as observed through western blotting, in pooled cells (Figure 4.2). Following single cell cloning and screening for protein through western blotting, two cell lines were CSPG4-deficient. (Figure 4.3). This could be explained by deletion in the *CSPG4* gene sequence which was complimentary to the gRNA sequence. In order to observe whether any emerging phenotype was the result of CSPG4 knock-out, CSPG4 cDNA was re-introduced into cell lines in order to see if the phenotype was rescued. The western blot data demonstrating CSPG4 expression is consistent with flow cytometry data (Figure 4.5). Therefore, a panel of cell lines was produced with varying expression levels of CSPG4 (Figure 4.5).

Interestingly, the cellular localisation of CSPG4 differed between the three cell lines in which CSPG4 was overexpressed (Figure 4.6). H10-KO-CSPG4 demonstrated more intracellular CSPG4 puncta, compared to H7-KO-CSPG4 and 143B-CSPG4 (Figure 4.6). This is inconsistent with the expression of the same plasmid in a paper by Yuan et al. (2015). HeLa cells expressing CSPG4 selectively display positivity round the cellular membrane (Yuan et al. 2015). The significance of intracellular CSPG4 is unclear and is unreported in the literature. The morphologies of the different cell lines do not appear observably altered (Figure 4.7).

The use of siRNA would allow the phenotype of a less significant reduction in CSPG4 to be investigated. An issue with CRISPR/Cas9 technology is that essential genes cannot be targeted as cells will die once the gene has been deleted (Unniyampurath et al. 2016). In the case of CSPG4, if the protein was essential for cell survival or growth, endogenously CSPG4-negative 143B cells may be the only ones to survive transfection of CRISPR/Cas9 plasmid.

U2OS, MG63 and 143B were chosen on the basis of their CSPG4 expression level. U87MG, a glioblastoma cell line, was included as a positive control as it has been used to study the action of CSPG4 previously. Knock-down of CSPG4 in U87MG cells has been shown to increase chemosensitivity in vitro and slow tumour growth in vivo (Chekenya et al. 2008, Stallcup 2017).

siRNA treatment knocked-down CSPG4 expression in all cell lines (Figure 4.8).

Relative expression of the core protein band was reduced to under 50% compared to non-treated control (Figure 4.8).

This chapter demonstrates that CSPG4 expression has been modulated using both CRISPR/Cas9 and siRNA technology in two separate cell line panels. Both panels can be used for in vitro experimentation and the CRISPR/Cas9 panel can be used for in vivo investigation.

Chapter 5

Function of CSPG4 in vitro in osteosarcoma

5.1 Summary

The presence of CSPG4 on the cell membrane is associated with a number of functions. During development, CSPG4 is upregulated on progenitor cells, increasing their proliferative and migratory potential. The protein is then down-regulated as the cell progresses towards terminal differentiation. CSPG4 also influences migratory behaviour and proliferation on the small selection of adult cell lines on which it is expressed, such as pericytes.

Studies focusing on CSPG4's contribution to cancer have identified it is involved in a number of different functions. These include proliferation, migratory behaviour and chemoresistance. These functions are important for the growth and spread of osteosarcoma tumours, therefore it was important to investigate CSPG4's contribution to these functions on osteosarcoma cell lines.

Using the CRISPR/Cas9 experimental cell lines detailed in Chapter 2, CSPG4's influence on proliferation, adhesion, spreading, migration, chemoresistance and cell survival in anchorage-independent conditions was investigated. The presence of CSPG4 did not appear to influence any of the above cell behaviours.

In order to investigate whether this was a finding specific to the cell line (143B) or to the method of CSPG4 knock-out (CRISPR/Cas9), siRNA knock-down was used on further osteosarcoma cell lines. This method may elucidate an effect that would not be shown by the 143B cell line, or one that could be lost through single cell cloning.

Using siRNA treated U2OS, MG63 and 143B osteosarcoma cell lines and a CSPG4-positive glioblastoma cell line, cell proliferation and cell survival in anchorage independent conditions were investigated. Like the CRISPR/Cas9 cell lines, no effect was observed for cell proliferation or cell survival in CSPG4-deficient conditions. Therefore, these findings indicate that CSPG4 does not have any functional importance for osteosarcoma development.

Due to CSPG4's presence on osteosarcoma patient samples, it was important to investigate whether it could function as a novel therapeutic target for the treatment of osteosarcoma. On the basis that no functional role for CSPG4 could be found, an antibody-drug complex was chosen to induce cytotoxicity. The drug used was a sc-Fv antibody fragment conjugated to Pseudomonas exotoxin A. Treatment of osteosarcoma cell lines and the glioblastoma cell line U87MG resulted in reduced viability. However, the drug also reduced viability of a CSPG4-negative Ewing's sarcoma cell line. This result suggests that the drug was binding indiscriminately or the drug had become detached from the antibody fragment.

Therefore, the experiments in this chapter demonstrate that CSPG4 does not influence osteosarcoma proliferation, adhesion, spreading migration, chemoresistance and cell survival in low adhesion conditions. It also does not provide proof-of-principle that CSPG4 could be targeted for therapeutic gain.

5.2 Aims

The aim of the experiments detailed in this chapter were to:

1) Use CRISPR/Cas9 cell models to identify whether CSPG4 expression contributes to:

- Cell proliferation
- Cell migration
- Cell spreading
- Cell adhesion
- Chemoresistance
- Anoikis

2) Use siRNA treated cell models to identify whether CSPG4 expression contributes to:

- Cell proliferation
- Anoikis

3) Investigate whether CSPG4-positive osteosarcoma cell lines can be selectively targeted and killed through the use of an antibody-drug complex

5.3 CRISPR/Cas9 experimental cell line results

5.3.1 Cell proliferation

CSPG4 is implicated in the proliferation of a number of cell lines (Price et al. 2011). Initially upregulated on progenitor cell lines, its expression correlates with increased proliferative ability. Its re-expression on a number of tumour cells has also been demonstrated to increase cell proliferation (Stallcup 2008).

Whilst CSPG4 is thought to affect proliferation through increased growth factor signalling, it has also been shown to influence basal levels of proliferation (Al-Mahani et al. 2011).

The viability of each CRISPR/Cas9 cell line was measured daily for up to five days using Alamar Blue (Invitrogen). Increasing viability over time is used as an indirect measure of cellular proliferation. Due to the fact cell lines were produced by single cell cloning, only paired cell lines are compared (Figure 5.1).

The presence of CSPG4 did not appear to affect cell viability. Overexpression of CSPG4 did not alter viability between 143B and 143B-CSPG4 cell lines (Figure 5.1a). 143B cell viability was higher at the end-point than H10-KO and H7-KO cell lines (Figure 5.1). However, the re-introduction of CSPG4 did not increase the viability of either H10-KO (Figure 5.1b) or H7-KO (Figure 5.1c).

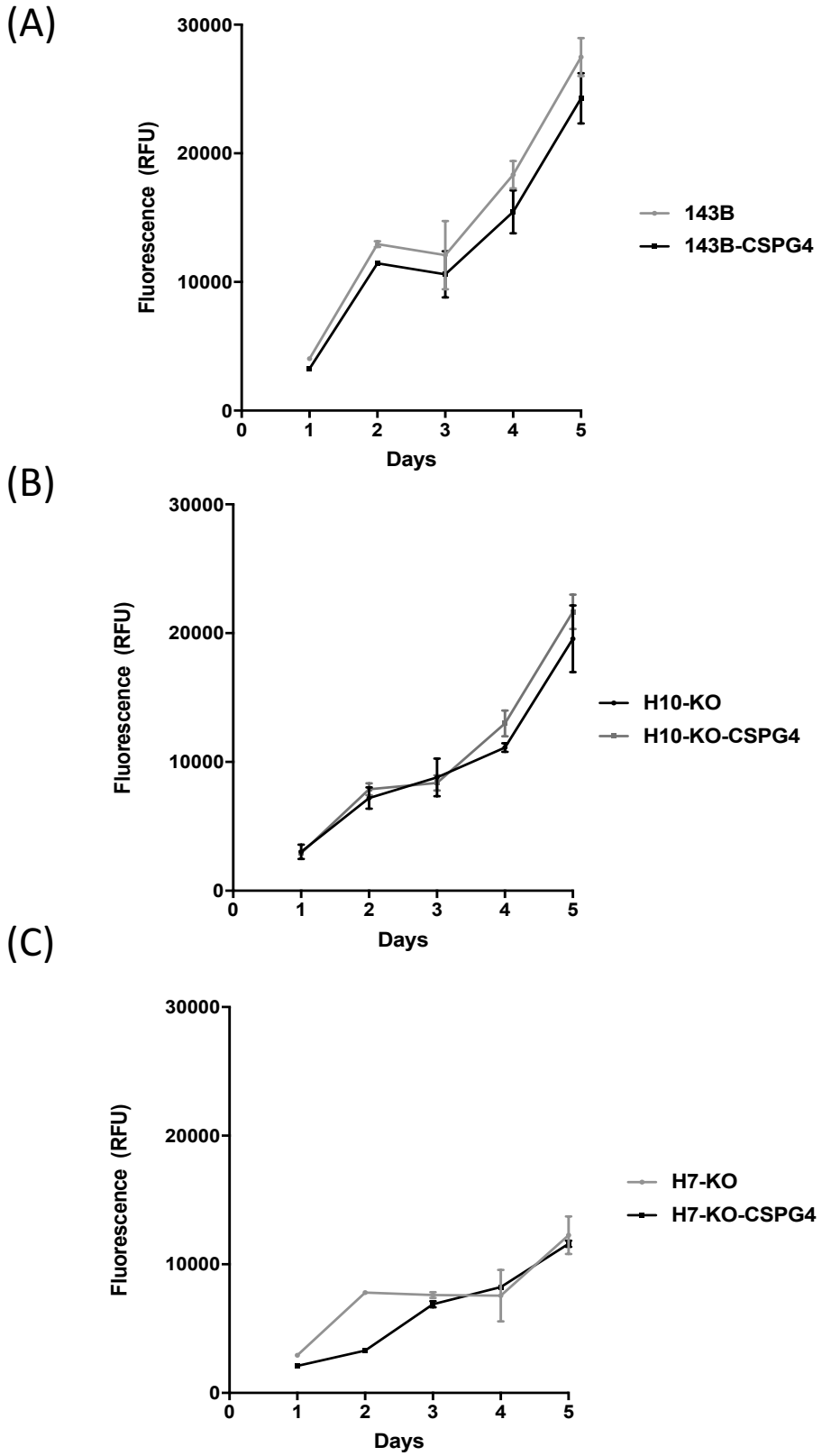

Figure 5.1 – Viability assay using Alamar Blue over five days as an indirect measurement of proliferation. (A) Viability of 143B and 143B-CSPG4. **(B)** Viability of H10-KO and H10-KO-CSPG4. **(C)** Viability of H7-KO and H7-KO-CSPG4. Values represent the mean of three separate experiments ± SEM (n=3).

5.3.2 Cell attachment, spreading and migration

The ability of cells to move is an important attribute in physiology and pathology (Makagiansar et al. 2007). This is especially true for cancer, whereby the leading cause of death is metastasis, the spread and migration of cells to different areas of the body. Metastasis depends on cell adhesion, spreading and migration (Cattruzza et al. 2013).

Attachment to the extra-cellular matrix is implicated throughout the metastatic cascade (Burg et al. 1996). CSPG4 has been shown to regulate cell attachment to a number of components of the extra-cellular matrix (Burg et al. 1996). In order to investigate whether CSPG4 regulates osteosarcoma attachment, cells were seeded on to Fibronectin and Collagen-I coated plates for up to two hours. Attachment was determined by counting the number of Hoechst-positive nuclei.

Cell attachment to collagen-I or fibronectin did not appear to be dependent on CSPG4 as cell lines with different expression levels did not demonstrate significantly different attachment (Figure 5.2). Whilst H10-KO-CSPG4 appears to exhibit higher attachment than H10-KO to fibronectin, this result is not statistically significant (Figure 5.2b).

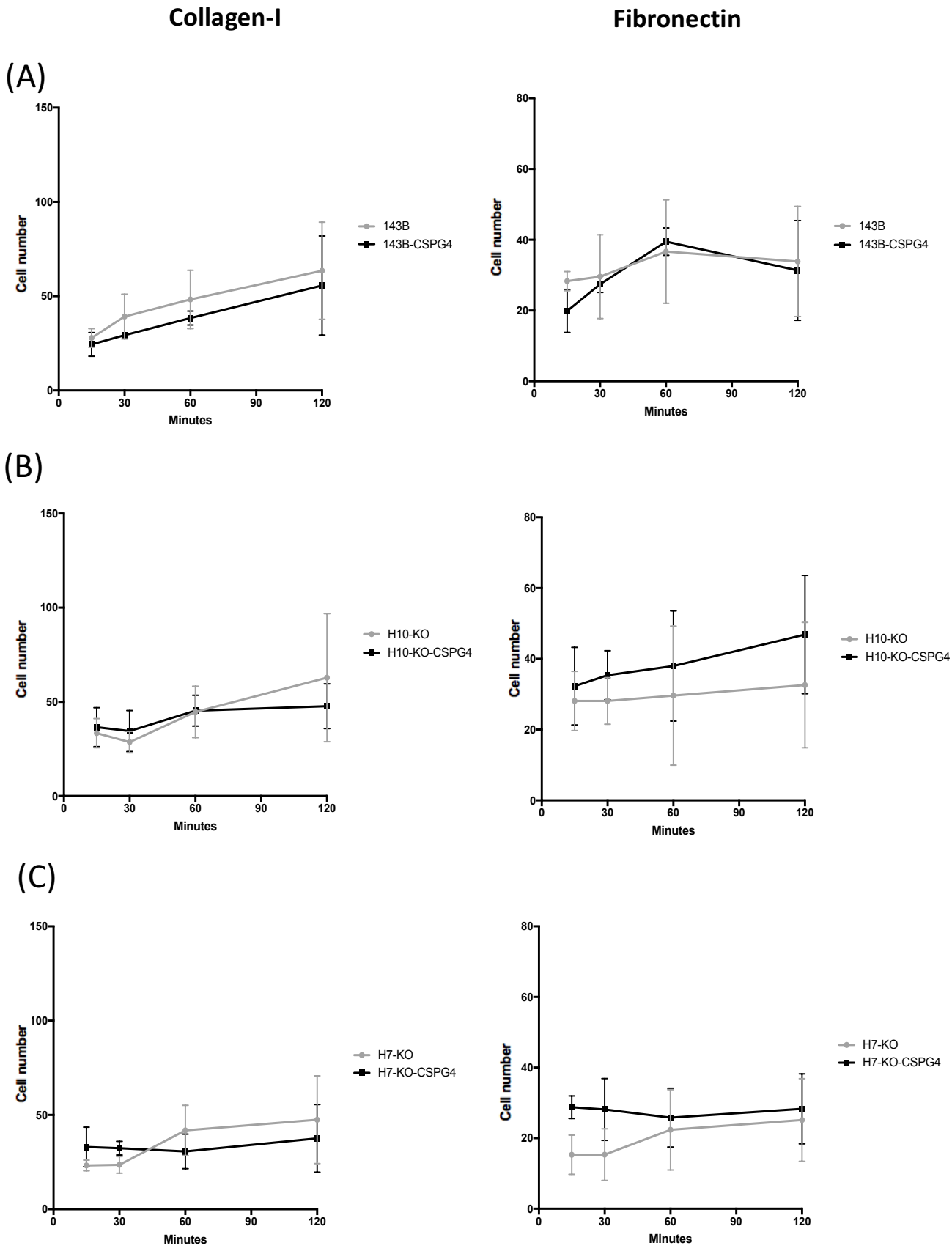

Figure 5.2 – Cellular attachment to collagen-I and fibronectin at various time points. Cell attachment to collagen-I and fibronectin after 15, 30, 60 and 120 minutes. **(A)** Cell number measurements of 143B and 143B-CSPG4 **(B)** Cell number measurements of H10-KO and H10-KO-CSPG4 **(C)** Cell number measurements of H7-KO and H7-KO-CSPG4**.** Values represent the mean of three separate experiments ± SEM (n=3).

After initial contact and attachment of cells to the extra-cellular matrix, cell spreading occurs. This process begins as a passive event but then involves actin and myosin, as the cell membrane spreads across the surface it is attached to (McGrath 2007). Cell spreading is an important step enabling cells to migrate.

Antibodies directed towards CSPG4 have resulted in reduced spreading (Price et al. 2011). CSPG4 has also been shown to enhance spreading on fibronectin when exogenously expressed on melanoma cell lines (Yang et al. 2014). The same experimental technique was used to investigate CSPG4's contribution to cell spreading as cell attachment. For this experiment, CRISPR/Cas9 panel cell lines were seeded on to fibronectin and collagen-I coated cells for up to two hours. Cell area was used as an indirect measure of cell spreading and was calculated using phalloidin staining of the cytoskeleton.

No difference was observed between 143B and 143B-CSPG4 suggesting CSPG4 overexpression does not influence spreading behaviour of this cell line on either collagen-I or fibronectin (Figure 5.3a). CSPG4-negative and CSPG4-positive cells also exhibited no difference in spreading behaviour on either collagen-I or fibronectin (Figure 5.3b/c).

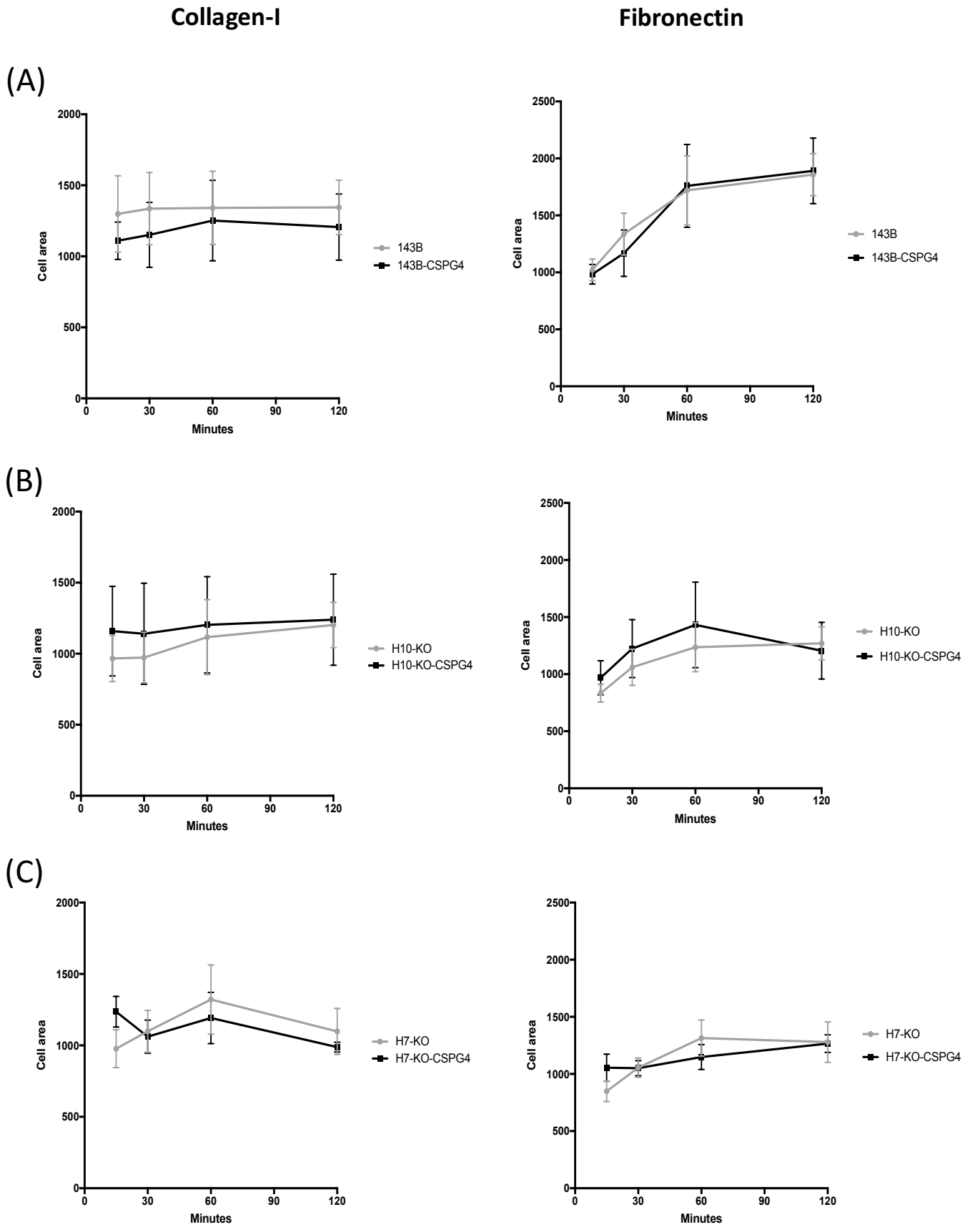

Figure 5.3 – Cellular spreading on collagen-I and fibronectin at various time points. Cell spreading was calculated using cell area of cells incubated on collagen-I and fibronectin-coated wells after 15, 30, 60 and 120 minutes. **(A)** Cell area measurements of 143B and 143B-CSPG4 **(B)** Cell area measurements of H10-KO and H10-KO-CSPG4 **(C)** Cell area measurements of H7-KO and H7-KO-CSPG4**.** Values represent the mean of three separate experiments ± SEM (n=3).

Similar to cell proliferation, cell migration was an early function of progenitor cells found to be regulated in part by CSPG4. This finding has been extended to a number of tumour cell lines. CSPG4 has been shown to modulate the cells migratory response to growth factors as well as connect the cell membrane to the cytoskeleton.

In order to investigate cell migration, a wound healing technique was used. The IncuCyte WoundMaker was used to make a scratch wound in wells containing cells. Plates were then loaded into the IncuCyte where they were imaged every 3 hours over 24 hours (Figure 5.4). The IncuCyte calculated the relative wound density (%). A relative wound density of 0% represents a fresh wound; with a relative wound density of 100% constitutes a completely closed wound. As cells migrate into the wound, relative wound density increases. Representative images of different time points are shown in Figure 5.5.

There was no CSPG4-dependent effect on wound closure (Figure 5.1). Overexpression of CSPG4 did not alter wound closure between 143B and 143B-CSPG4 cell lines (Figure 5.4). There was no difference in wound closure between CSPG4 deficient cell lines compared to the cell lines where CSPG4 expression was re-introduced (Figure 5.4).

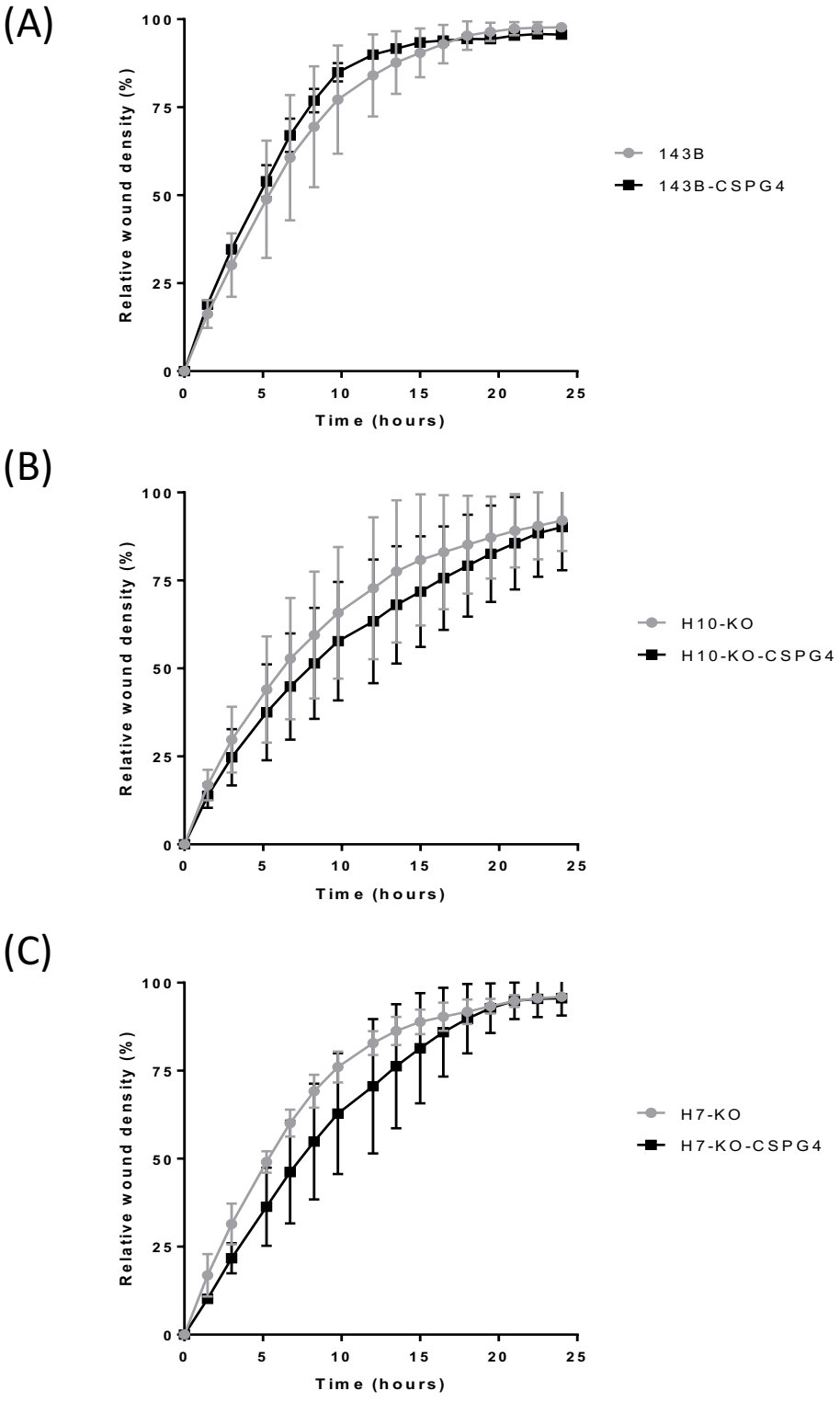

Figure 5.4 – Wound closure in a scratch wound assay as an indirect measure of migration. Relative wound density is calculated by the Incucyte using the area of the wound infiltrated by the cells over time. **(A)** Wound closure of 143B and 143B-CSPG4. **(B)** Wound closure of H10-KO and H10-KO-CSPG4. **(C)** Wound closure of H7-KO and H7-KO-CSPG4. Values represent the mean of three separate experiments ± SEM (n=3).

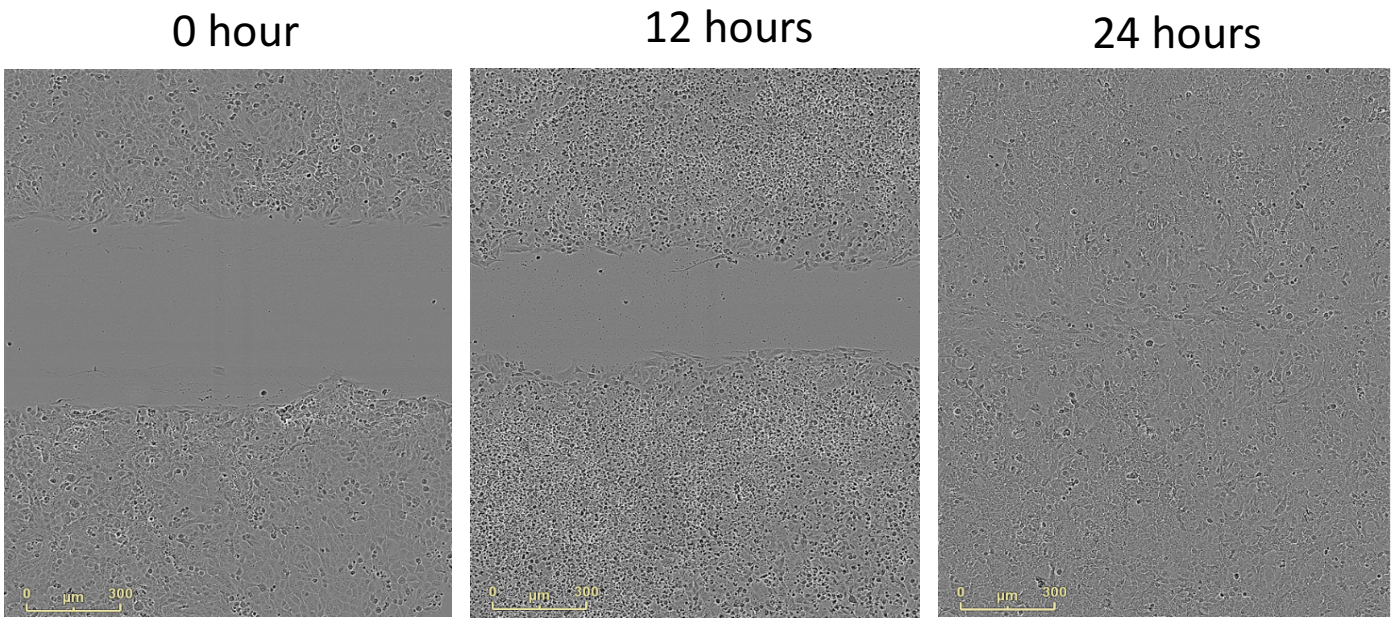

Figure 5.5 – Representative images of wound closure by cells. Photos taken from the Incucyte (Essen) showing cellular migration into the scratch wound at 0 hours, 12 hours and 24 hours. Scale bar = 300µm.

5.3.3 Resistance to chemotherapy

CSPG4 has been demonstrated to protect cell lines from chemotherapy and targeted therapy treatment (Chekenya et al. 2008). Osteosarcomas are prone to developing resistance to chemotherapy. Therefore, we hypothesised that CSPG4 may be involved in chemosensitivity of osteosarcoma cell lines.

Investigation of CSPG4's influence on the chemosensitivity of cell lines was achieved in two stages. Firstly, cells were treated with varying concentrations of doxorubicin and cisplatin for 24 hours. The viability of the cell lines was then measured to calculate cell sensitivity. Secondly, the drug was removed and replaced with growth media for 48 hours. Cell viability was then measured to calculate cell recovery. Viability was normalised to cells grown in non-treated control conditions. Doxorubicin and cisplatin were used, as these are commonly used drugs in the treatment regime of osteosarcoma.

Cells incubated with cisplatin exhibited no observable difference in viability for either cell sensitivity or recovery (Figure 5.6). This also occurred for cells treated with doxorubicin, no difference in viability was observed (Figure 5.7). Therefore, CSPG4 does not appear to influence cell sensitivity to chemotherapy, or cell recovery following treatment.

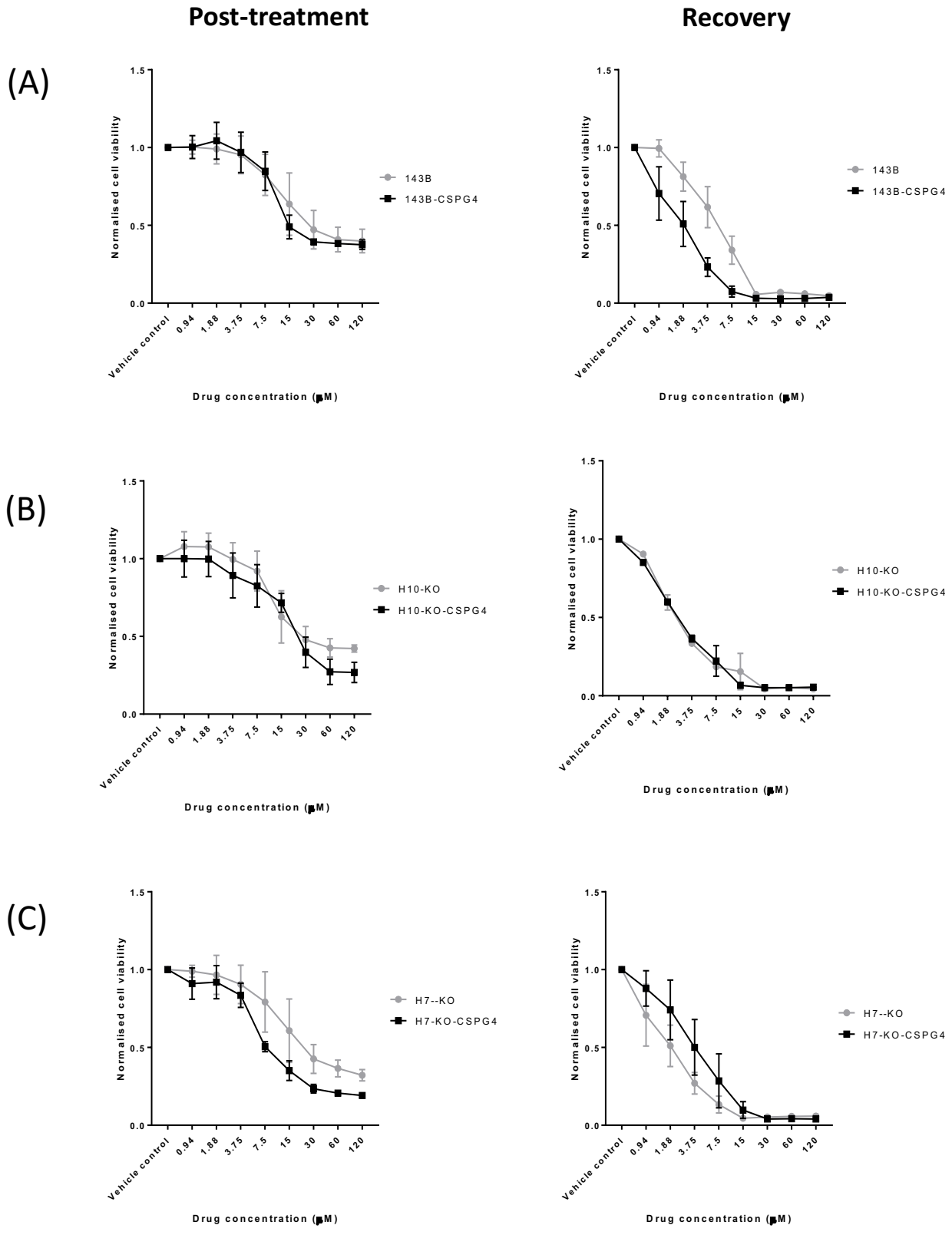

Figure 5.6 – Viability of cell lines 24 hours after cisplatin treatment and after 48 hours recovery. Cell lines were treated with cisplatin at various concentrations for 24 hours (post-treatment) and then allowed to recover for 48 hours (recovery). Alamar Blue was used to measure cell viability. **(A)** Post-treatment and recovery viability measurements of 143B and 143B-CSPG4 **(B)** Post-treatment and recovery viability measurements of H10-KO and H10-KO-CSPG4 **(C)** Post-treatment and recovery viability measurements of H7-KO and H7-KO-CSPG4**.** Values represent the mean of three separate experiments ± SEM (n=3).

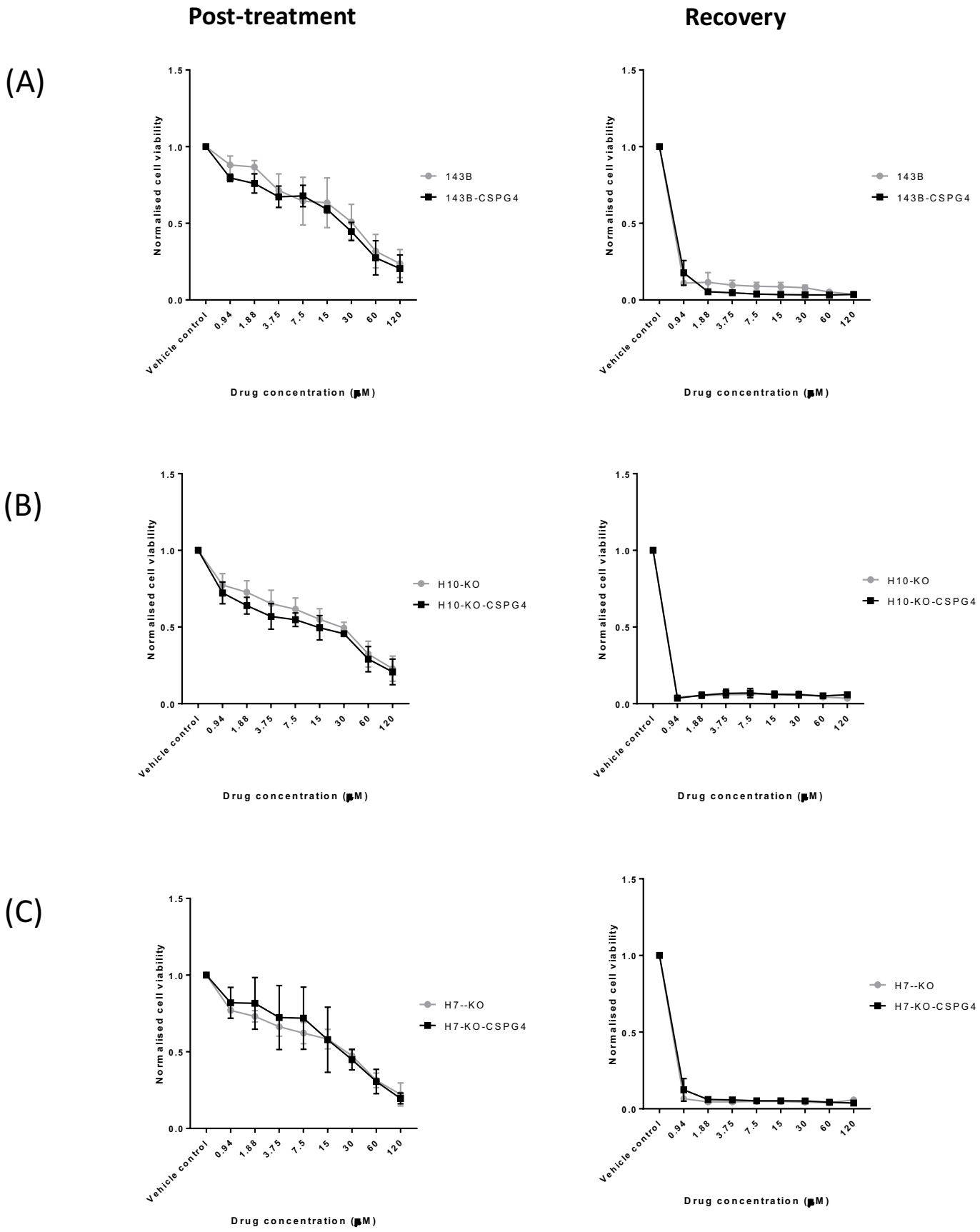

Figure 5.7 – Viability of cell lines 24 hours after doxorubicin treatment and after 48 hours recovery. Cell lines were treated with doxorubicin at various concentrations for 24 hours (post-treatment) and then allowed to recover for 48 hours (recovery). Alamar Blue was used to measure cell viability. **(A)** Post-treatment and recovery viability measurements of 143B and 143B-CSPG4 **(B)** Post-treatment and recovery viability measurements of H10-KO and H10-KO-CSPG4 **(C)** Post-treatment and recovery viability measurements of H7-KO and H7-KO-CSPG4**.** Values represent the mean of three separate experiments ± SEM (n=3).

In order to assess whether chemotherapy drug treatment results in apoptosis, cells were investigated with flow cytometry.

Cells were treated with 7.5μM of cisplatin and doxorubicin for 24 hours. A mid-range concentration was selected to ensure that enough cells survived. Cells were then treated with Annexin-V dye and PI to label early and late apoptotic cells respectively.

Cells were gated to remove doublet cells and cell debris. Cell plot data was produced for 143B/143B-CSPG4 (Figure 5.8), H10-KO/H10-KO-CSPG4 (Figure 5.9) and H7-KO/H7-KO-CSPG4 (Figure 5.10). Cells are divided into four quadrants (Q1-4). Quadrant 1 represents free floating nuclei; quadrant 2 represents cells positive for PI (late apoptotic cells); quadrant 3 represents cells negative for staining (live cells) and quadrant 4 represents cells positive for Annexin V (early apoptotic cells).

Live cells, early apoptotic and late apoptotic cells are expressed graphically in a sequenced clustered column (Figure 5.11). Cells are expressed as a percentage from a total of cells in quadrants 2-4.

As only one experiment was performed, it isn't possible to compare conditions statistically. However, there appears to be no observable difference between conditions, except for H7-KO and H7-KO-CSPG4 (Figure 5.10). H7-KO-CSPG4 exhibits greater apoptosis than H7-KO.

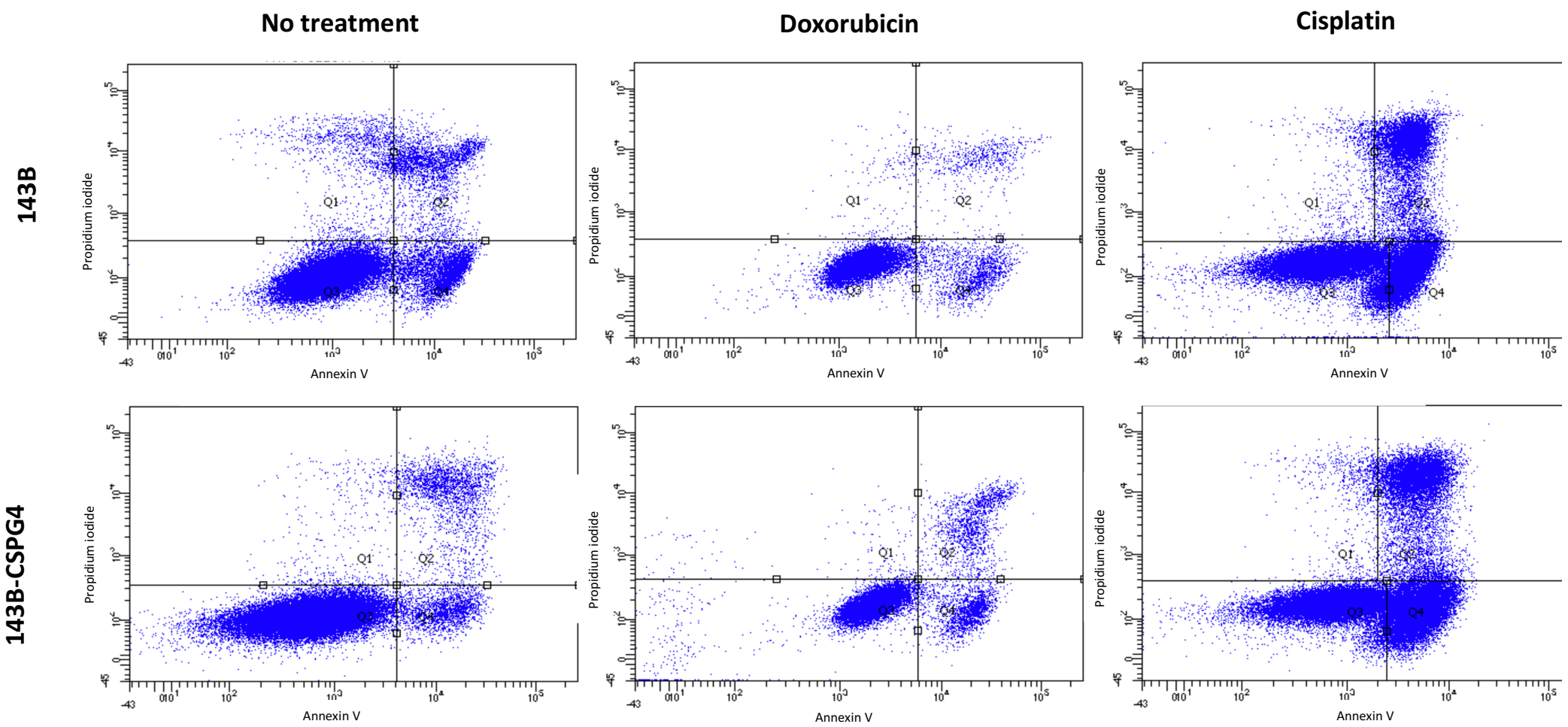

Figure 5.8 – Cell plot data for 143B and 143B-CSPG4 cell lines after cisplatin and doxorubicin treatment. Cells were either not treated, treated with 7.5µM doxorubicin or treated with 7.5µM cisplatin for 24 hours. Cells were then stained with Annexin V and PI to identify apoptotic cells. The four quadrants represent free-floating nuclei, late apoptotic cells (PI-positive), live cells (negative for staining) and early apoptotic cells (Annexin V positive) in numerical order. Plots represent the values from a single experiment.

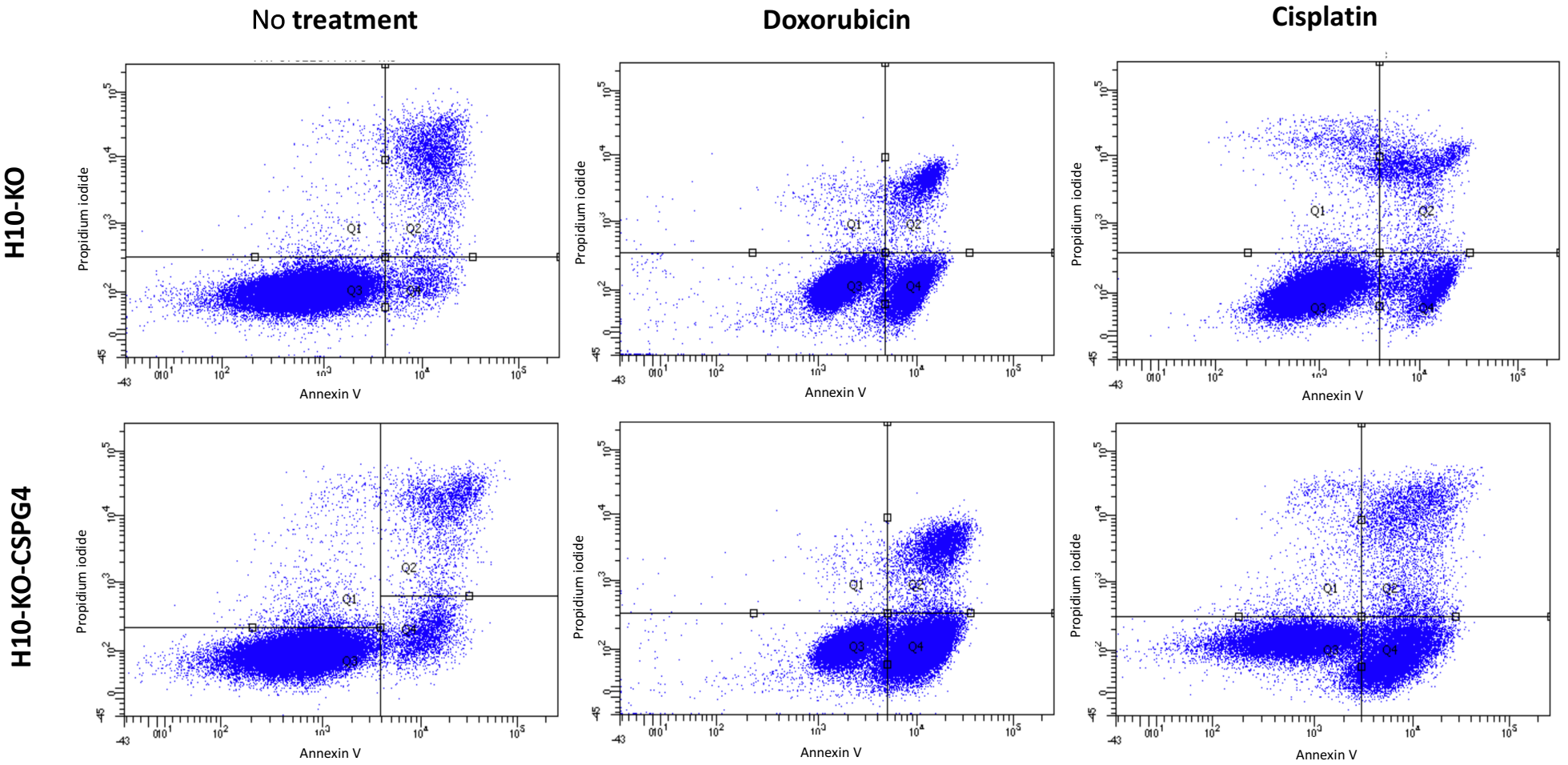

Figure 5.9 – Cell plot data for H10-KO and H10-KO- cell lines after cisplatin and doxorubicin treatment. Cells were either not treated, treated with 7.5µM doxorubicin or treated with 7.5µM cisplatin for 24 hours. Cells were then stained with Annexin V and PI to identify apoptotic cells. The four quadrants represent free floating nuclei, late apoptotic cells (PI-positive), live cells (negative for staining) and early apoptotic cells (Annexin V positive) in numerical order. Plots represent the values from a single experiment.

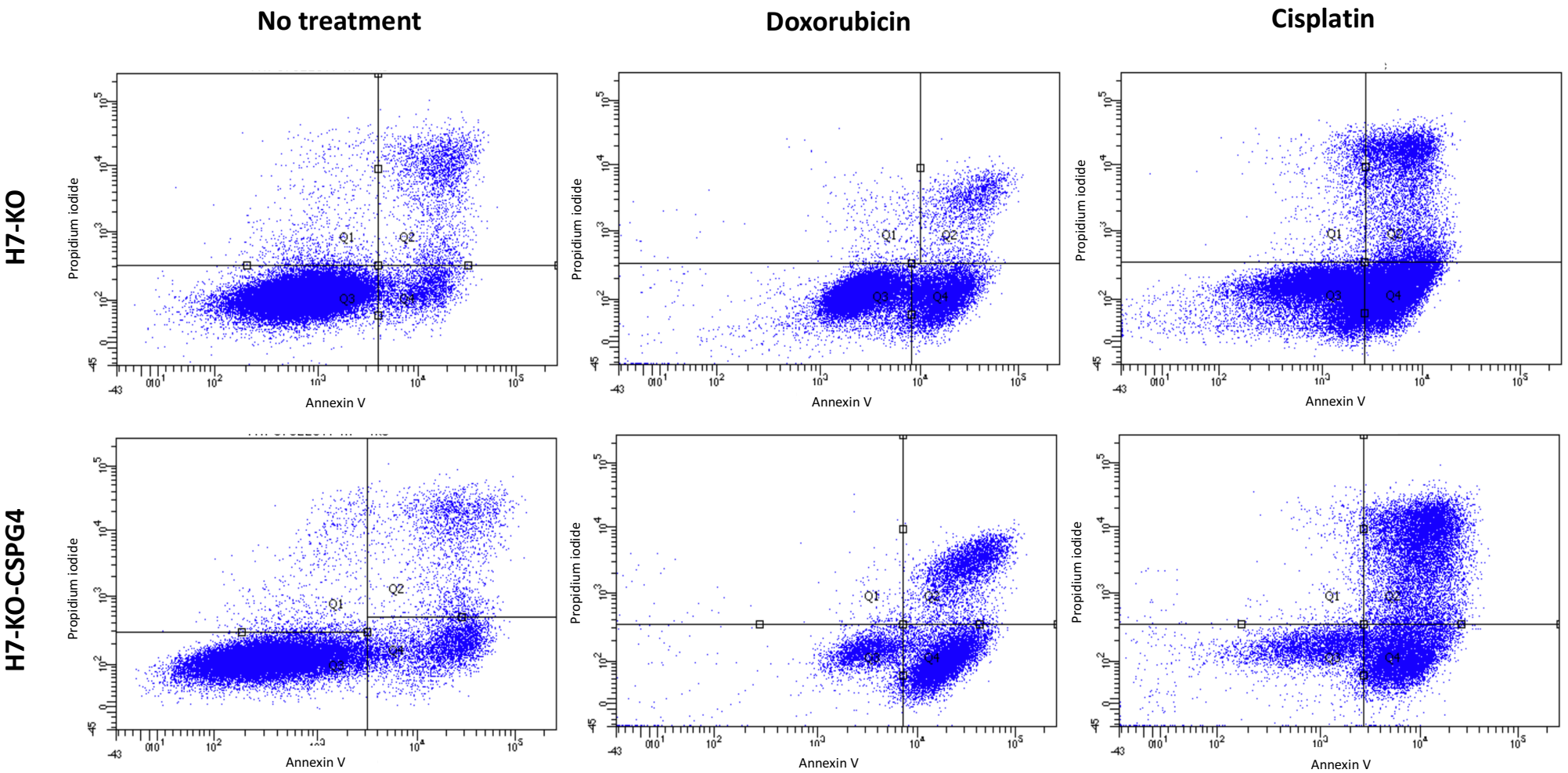

Figure 5.10 – Cell plot data for H7-KO and H7-KO-CSPG4 cell lines after cisplatin and doxorubicin treatment. Cells were either not treated, treated with 7.5µM doxorubicin or treated with 7.5µM cisplatin for 24 hours. Cells were then stained with Annexin V and PI to identify apoptotic cells. The four quadrants represent free floating nuclei, late apoptotic cells (PI-positive), live cells (negative for staining) and early apoptotic cells (Annexin V positive) in numerical order. Plots represent the values from a single experiment.

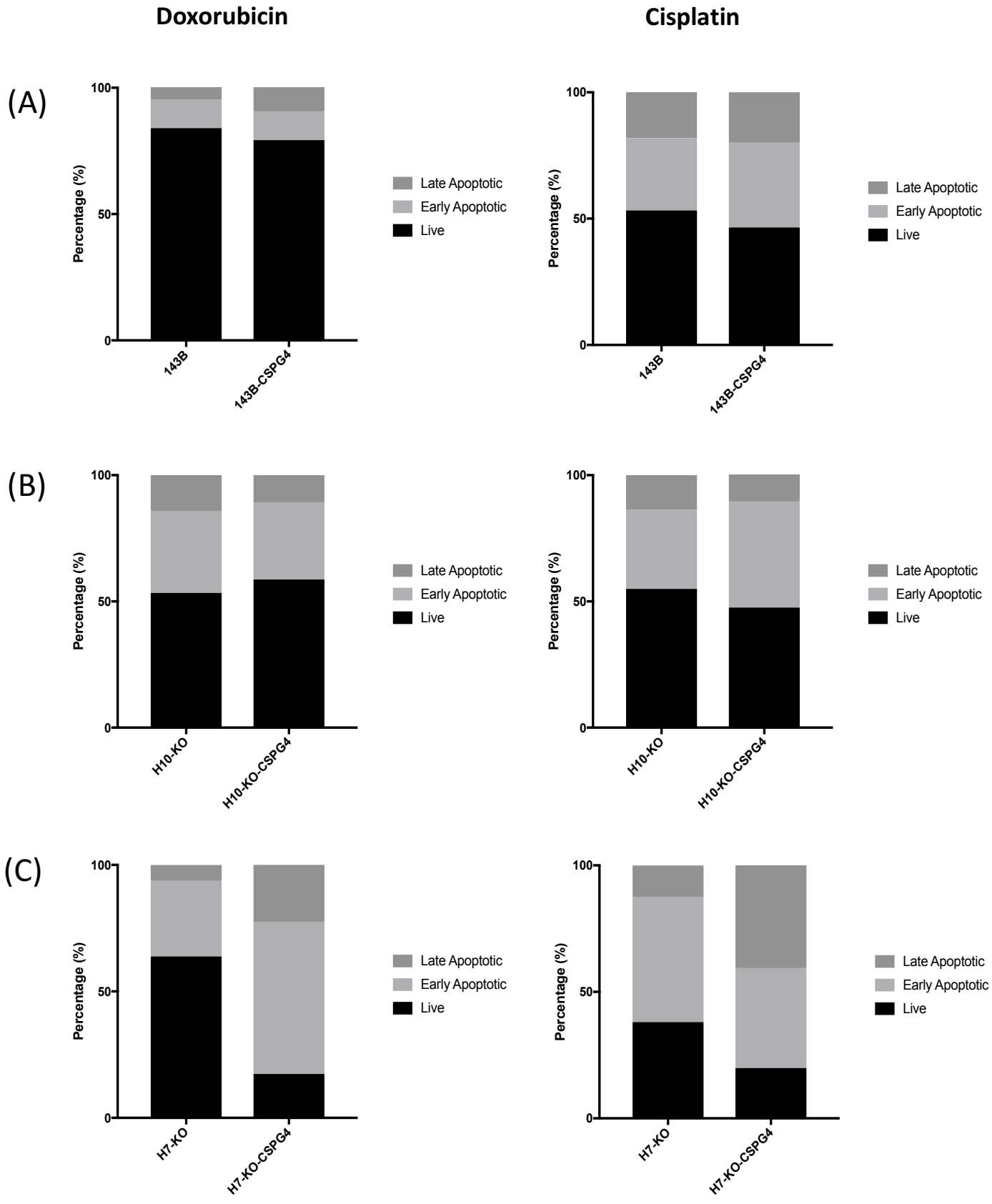

Figure 5.11 – Summary data for the detection of apoptosis by flow cytometry following cisplatin and doxorubicin treatment. Cell lines were treated with chemotherapeutic drugs for 24 hours and then stained for Annexin V and PI in order to signify early and late stage apoptosis respectively. Cell lines were treated with 7.5uM of cisplatin or doxorubicin for 24 hours. Values represent data from a single experiment. **(A)** Post-treatment viability measurements of 143B and 143B-CSPG4 **(B)** Post-treatment viability measurements of H10-KO and H10-KO-CSPG4 **(C)** Post-treatment viability measurements of H7-KO and H7-KO-CSPG4

5.3.4 Cell survival

Anchorage-independent growth is a hallmark of cancer (Paoli et al 2013). For healthy cells, the absence of correct signals from the ECM causes cell detachment induced apoptosis, known as anoikis (Paoli et al 2013, Guadamillas et al. 2011). Anoikis prevents abnormal detachment from the ECM, therefore overcoming this mechanism is essential for the development of tumours and dissemination that leads to metastasis (Paoli et al 2013).

CSPG4 has been implicated as being a novel anoikis receptor (Joo et al 2008). If CSPG4 expression was suppressed through siRNA treatment, fibroblasts were rescued from anoikis resulting from altered fibronectin (Joo et al. 2008). However, it has also been suggested that cell survival is a non-cell line specific function of the CSPG4 receptor (R. Perris, personal communication). Therefore, it was important to investigate whether CSPG4 contributed to cell survival in low attachment conditions.

Cells were grown for three days in ultra-low attachment plates which prevent cell adhesion. After three days, cell survival was investigated through flow cytometry. Cells were stained with Annexin V (early apoptotic marker) and PI (late apoptotic marker).

There is no observable difference between various cell lines. 143B-CSPG4 displays slightly lower percentage of live cells (Figure 5.11a). Whereas H10-KO and H7-KO display a slightly higher percentage of live cells and a greater percentage of cells

positive for PI, therefore, in the late stage of apoptosis. Therefore, CSPG4 does not contribute to the survival of osteosarcoma cells grown in anchorage-independent conditions.

(A)

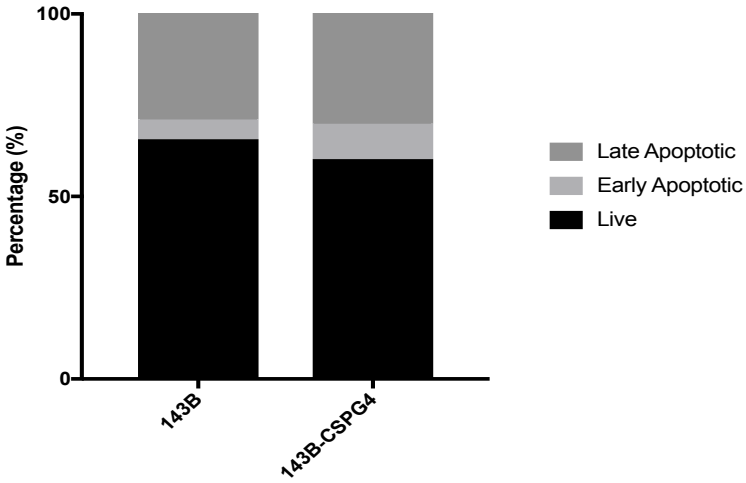

(B)

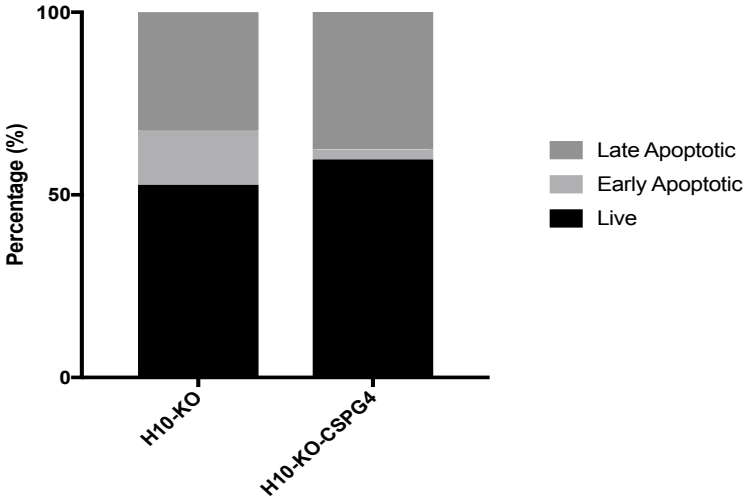

(C)

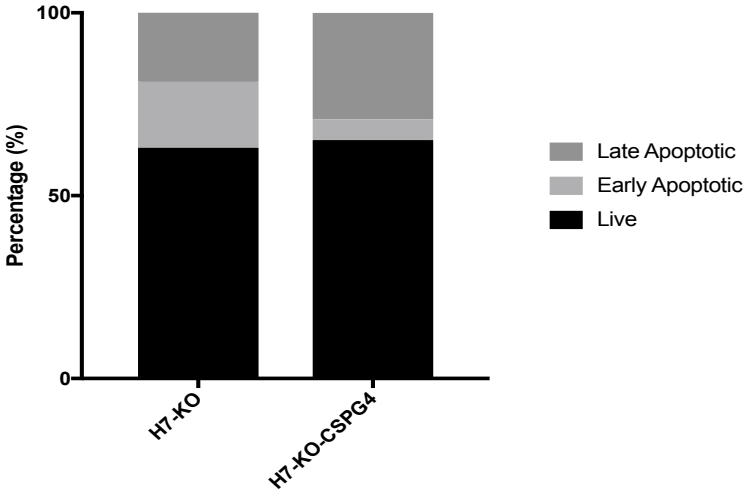

Figure 5.12 – Detection of anoikis following cell growth in low attachment conditions. CRISPR/Cas9 experimental cell lines were grown for three days in ultra-low attachment plates. Cells were then stained with Annexin V (early apoptotic marker) and PI (late apoptotic marker) to measure levels of apoptosis. **(A)** Cell survival of 143B and 143B-CSPG4. **(B)** Cell survival of H10-KO and H10-KO-CSPG4. **(C)** Cell survival of H7-KO and H7-KO-CSPG4. Values are derived from a single experiment (n=1).

5.4 siRNA-mediated knock-down results

Following on from the negative results of experiments using of CRISPR/Cas9-mediate knock-out, it was essential to investigate whether use of another method to modulate CSPG4 expression or another cell line would produce different results. Therefore, siRNA was used to knock-down CSPG4 expression, rather than knock it out completely. siRNA also provides a quicker method to achieve knock-down in a number of cell lines.

In order to assess whether CSPG4 knock-down impacted on osteosarcoma cell behaviour, cell proliferation and cell survival were investigated using osteosarcoma cell lines U2OS, MG63 and 143B. In addition to osteosarcoma cells, U87MG, a glioblastoma cell line, shown to be CSPG4-positive was included as a positive-control for CSPG4 expression.

5.4.1 Cell proliferation

To investigate cell proliferation, cells were plated and left to grow for up to 72 hours. At 24, 48 and 72 hours, cells were incubated with Alamar Blue and their viability was measured. Increased numbers of viable cells were used as an indirect measure of proliferation. No significant variation in proliferation was observed between any cell type, including the glioblastoma positive control (Figure 5.12).

(A)

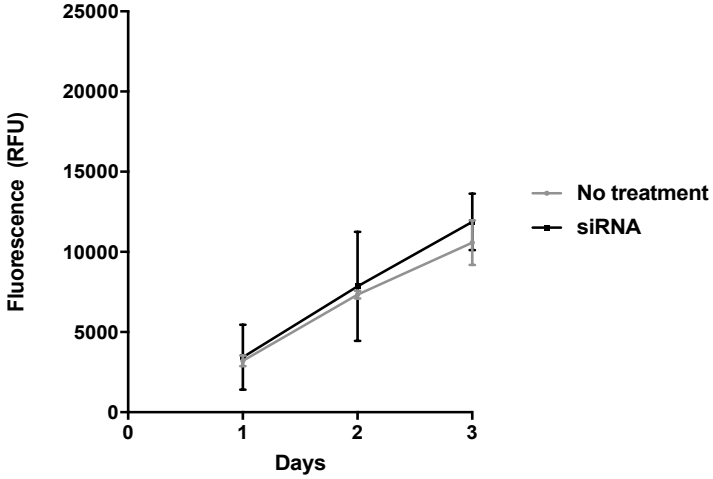

(B)

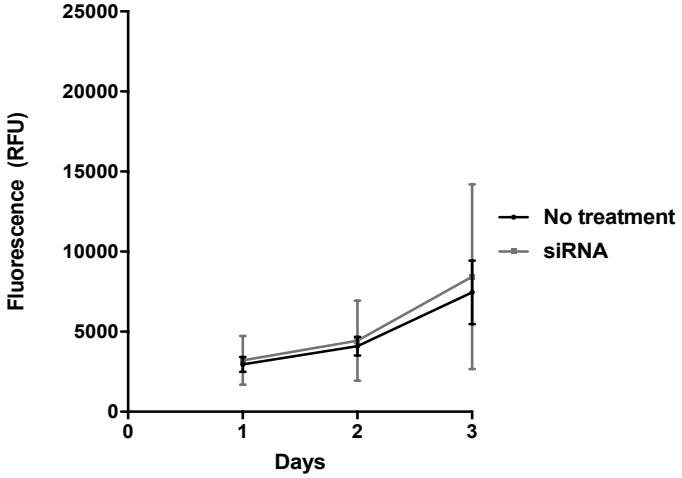

(C)

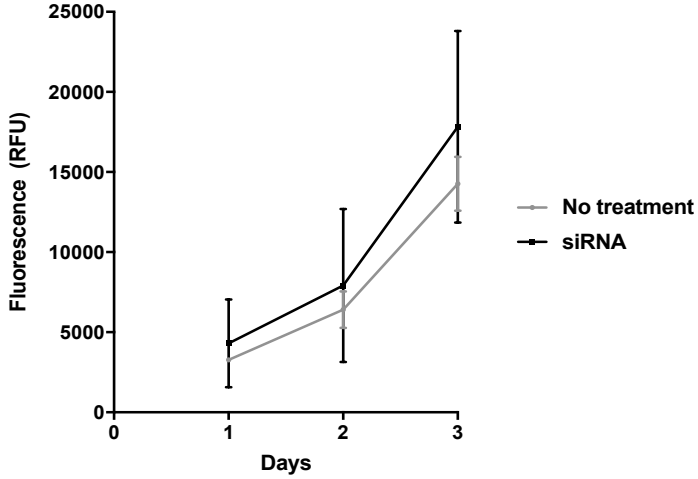

(D)

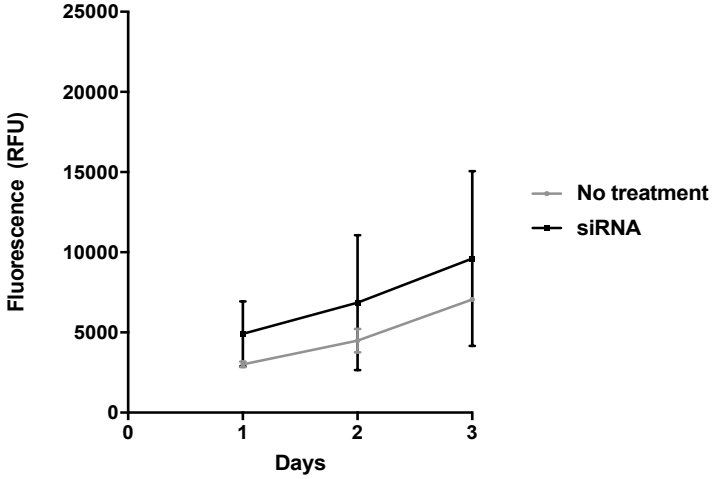

Figure 5.13 – Viability assay of siRNA treated cells using Alamar Blue over three days as an indirect measure of proliferation. Cell lines, either non-treated and treated with siRNA against CSPG4 were grown over three days. **(A)**Viability of U2OS control (no treatment) and CSPG4 knock-down cell lines (siRNA). **(B)** Viability of MG63 control (no treatment) and CSPG4 knock-down cell lines (siRNA). **(C)** Viability of 143B control (no treatment) and CSPG4 knock-down cell lines (siRNA). **(D)** Viability of U87MG control (no treatment) and CSPG4 knock-down cell lines (siRNA). Values represent the mean of three separate experiments ± SEM (n=3).

5.4.2 Cell survival

In order to investigate whether siRNA-mediated knock-down of CSPG4 impacted on cell survival, cells were grown in anchorage-independent conditions. Following 72-hour treatment with siRNA, cells were seeded into ultra-low attachment plates and left to grow for 72 hours. Cells were stained with Annexin V (early apoptotic marker) and PI (late apoptotic marker) and analysed with flow cytometry.

The three osteosarcoma cell lines do not display difference cell survival percentages when treated with siRNA (Figure 5.13). U2OS CSPG4 knock-down condition features slightly more live cells and less cells in the late stage of apoptosis (Figure 5.13a). MG63 cell line did not display much change when treated with siRNA (Figure 5.13b). 143B CSPG4 knock-down cells feature less live cells and have a greater proportion in the early stages of apoptosis. The positive control cell line, U87MG, displayed no difference in percentage of cells (Figure 5.13d).

As these results are based on one experiment, it is not possible to compare the conditions statistically.

(A)

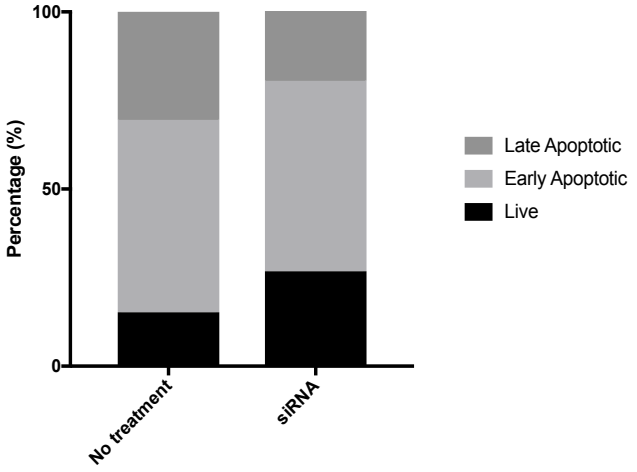

(B)

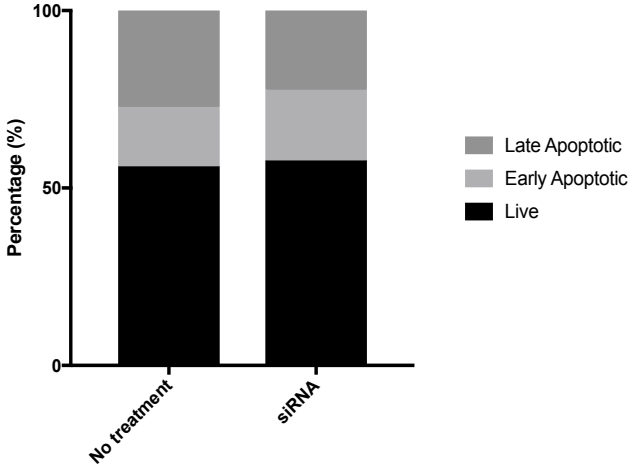

(C)

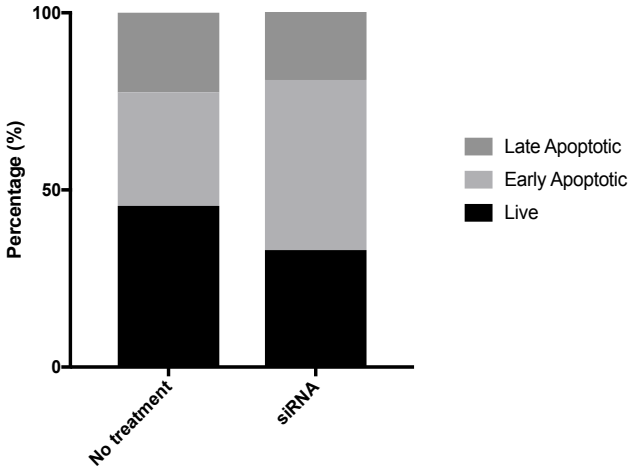

(D)

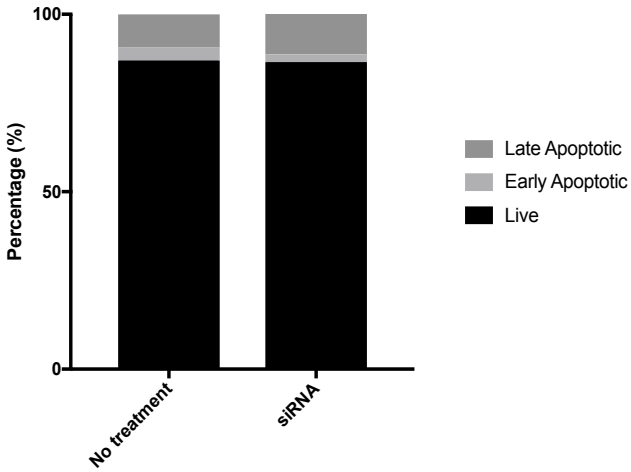

Figure 5.14 – Detection of anoikis following cell growth of siRNA-treated cells in low attachment conditions. Cell lines, either non-treated and treated with siRNA against CSPG4 were grown for three days in ultra-low attachment plates. Cells were then stained with Annexin V (early apoptotic marker) and PI (late apoptotic marker) to measure levels of apoptosis. **(A)** Cell survival of U2OS control (no treatment) and CSPG4 knock-down cell lines (siRNA). **(B)** Cell survival of MG63 control (no treatment) and CSPG4 knock-down cell lines (siRNA). **(C)** Cell survival of 143B control (no treatment) and CSPG4 knock-down cell lines (siRNA). **(D)** Cell survival of U87MG control (no treatment) and CSPG4 knock-down cell lines (siRNA). Values are derived from a single experiment (n=1).

5.5 Treatment of osteosarcoma cell lines with an anti-CSPG4 sc-Fv antibody

As CSPG4 was found to be present on osteosarcoma tumours from patient samples, it was important to see if it could be targeted therapeutically. As results have so far suggested that CSPG4 plays no role in osteosarcoma behaviour, a function-blocking antibody may have no impact on cell death. Therefore, a drug-conjugated antibody complex was selected to target osteosarcoma cells.

An antibody fragment conjugated to Pseudomonas exotoxin A (sc-Fv-PE) was chosen to treat osteosarcoma cells. U2OS, MG63, and 143B osteosarcoma cell lines were treated. The U87MG glioblastoma cell line was used as a positive control. TC71, an Ewing's sarcoma cell line, shown to be negative for CSPG4 was used as a negative control. Cells were treated with eight concentrations of the drug for 72 hours in normal cell growth media. Cell viability was then measured using Alamar Blue. Cell death per concentration was normalised to cell viability of vehicle control cells.

Increasing drug concentrations reduced the viability of all cell lines (Figure 5.14). The pattern of decreasing cell viability followed a similar pattern for all cell lines. This suggests the drug may have targeted the cell indirectly, or the sc-Fv fragment and drug become decoupled. Therefore, the sc-Fv-PE drug has not provided a proof-of-principle approach for selectively targeting CSPG4 in osteosarcoma for therapeutic gain.

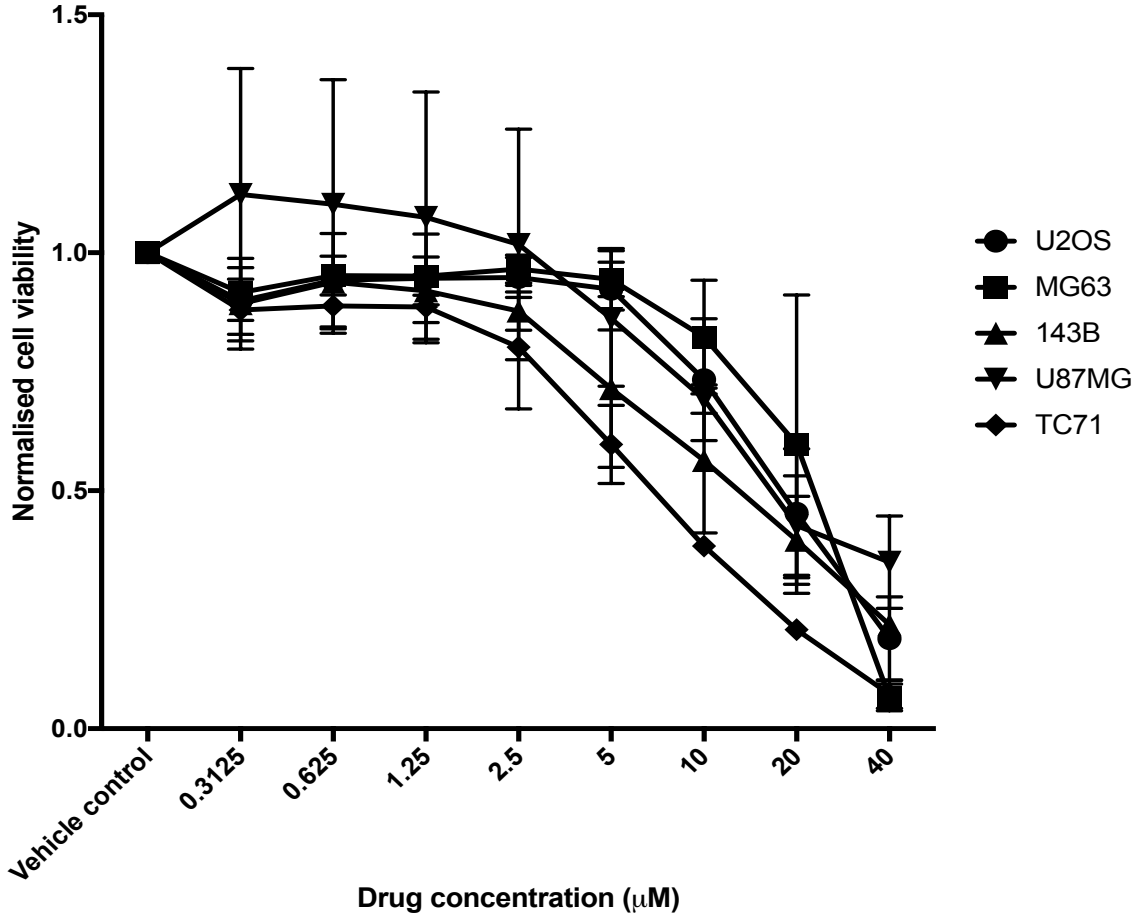

Figure 5.15 – Viability of cell lines treated with a CSPG4-specific sc-Fv-PE antibody for 72 hours. Cell lines were treated with sc-Fv at various concentrations for 72 hours. Alamar Blue was used to measure cell viability. Osteosarcoma cells include U2OS, MG63 and 143B cell lines. U87MG and TC71 were included as positive and negative controls respectively. Values represent the mean of three separate experiments ± SEM (n=3).

5.6 Discussion

The purpose of this chapter was to use the two cell line panels to investigate the role CSPG4 plays in osteosarcoma tumorigenesis. Both panels were used for in vitro experiments. The CRISPR/Cas9 panel was be used to investigate cell proliferation, adhesion, spreading, migration, chemoresistance and survival. The siRNA panel was used to investigate cell proliferation and survival. Another aim of this chapter was to provide proof-of-principle evidence that CSPG4 could be utilised for therapeutic gain in osteosarcoma through the use of a cytotoxic antibody.

The chapter has failed to demonstrate that CSPG4 plays any role in osteosarcoma proliferation, spreading, adhesion, migration, chemoresistance or cell survival. This was consistent for both CRISPR/Cas9 and siRNA treated cell line panels.

CSPG4 has been associated with cell proliferation on a number of cell types, during development and during tumorigenesis (Stallcup 2008). In this study, no impact on osteosarcoma proliferation was observed following CSPG4 modulation (Figure 5.1, Figure 5.12). In experiments with both CRISPR/Cas9 and siRNA cell panels, viability over time was used as a metric of proliferation. Whilst CSPG4's contribution to proliferation has been related to growth factor signalling, studies have demonstrated that it can influence basal proliferation rates. U251 cells exogenously expressing CSPG4 proliferate more than wild-type U251 cells (Makagiansar et al. 2007). Proliferation of glioblastoma cells taken from patient samples and cultured was higher in those expressing CSPG4 (Al-Mayhani et al. 2011). This was found to be cell autonomous and did not depend on extracellular cues (Al-

Mayhani et al. 2011). Both of these studies used glioblastoma cell lines and CSPG4 could act to increase proliferation independently in a tumour-specific manner.

More evidence is provided in the literature for CSPG4's role as a co-receptor for growth factor signalling pathways. CSPG4 co-localises with PDGFR, forming a molecular complex in vivo and potentiates proliferation in response to PDGF-aa (Nishiyama et al. 1996b, Grako et al. 1995). CSPG4 also interacts with FGF-2, increasing its availability for its receptor and can compensate for low FGFR expression (Cattaruzza et al. 2013). Through interacting with the growth factor ligand or the growth factor receptor CSPG4 activates signalling downstream (Price et al. 2007).

Future work on CSPG4's influence on osteosarcoma cell proliferation should focus on the contribution of growth factors. PDGFR-β has been demonstrated within osteosarcoma samples, but its expression is variable (Hassan et al. 2012). Another study found that the mean expression of PDGF-aa and PDGFR was 33.97% and 27.13% respectively (Sulzbacher et al. 2000). In addition, PDGF-inhibition halted growth and induced osteosarcoma cell apoptosis (McGary et al 2002). Similarly, FGF signalling pathway components are found within osteosarcoma. FGFR1 gene has been reported as being overexpressed in 18.5% of patients (Fernanda Amary et al. 2014). FGFR1 can promote osteosarcoma cell proliferation as well as colony formation within the lungs (Zhou et al. 2016). Therefore, both the PDGF and FGF signalling pathways are active within osteosarcoma tumorigenesis. Future experiments should investigate whether the addition of PDGF and FGF ligands increases the proliferation of CSPG4-positive cells over CSPG4-negative osteosarcoma cells.

The relationship between CSPG4 and growth factor signalling also extends to cellular migration. PDGF-BB activates PKCα which in turn phosphorylates the intracellular tail of CSPG4 at Thr^{2256}. This causes a re-location of CSPG4 and interaction with integrin sub-unit β1 (Makagiansar et al. 2007). In this study, cell migration was assessed through wound closure after 24 hours using a scratch-wound assay. The CRISPR/Cas9 cell panel was used but no difference in wound closure was observable (Figure 5.4). Future experiments should investigate whether the addition of growth factors, such as PDGF-BB, contributes to a CSPG4-dependent change in migration.

Other reports have indicated that CSPG4-mediated motility does not depend on growth factor signalling. Trophoblast motility is reduced following treatment of anti-CSPG4 siRNA (van Sinderen et al. 2013). Glioblastoma cell lines which exogenously expressed CSPG4 exhibit higher migratory behaviour than wild-type cells (Fang et al. 1999). Therefore, the lack of migratory response observed using the 143B cell line may be a cell-type specific effect. It would be interesting for future experiments to investigate CSPG4's contribution to osteosarcoma migration using different osteosarcoma cell line models. CSPG4's influence on migration is regulated by integrins (Price et al. 2011). The integrin repertoire featured on osteosarcoma model cell lines may also influence whether CSPG4 exacts any migratory advantage. This would be an important consideration for future experiments.

CSPG4 has been widely reported to have a role in cellular adhesion and attachment. CSPG4 is able to interact with the extra-cellular matrix through its extra-cellular component (Stallcup 2008). CSPG4 has the ability to influence cell behaviours, such as cell spreading, through its intracellular tail which is activated by the extracellular tails attachment to

different components of the ECM (Stallcup 2008).

In this study, no observable difference was seen in cell adhesion or cell spreading between any of the CRISPR/Cas9 cell lines (Figure 5.2, Figure 5.3). Therefore, CSPG4 has not been found to influence spreading or adhesion in osteosarcoma. The CRISPR/Cas9 cell lines were grown on collagen-I and fibronectin for 15, 30, 60 and 90 minutes. The number of cells attached, as well as the extent of spreading was measured.

Collagen-I was chosen as it is the most predominant component of the extra-cellular matrix in bone and therefore must interact with tumour cells to some extent (Luu et al. 2005). It has also been reported in osteosarcoma tumours. 9 tumour samples were analysed for their collagen content, collagen-I represented 65% (Shapiro and Eyre 1982). In addition, in vitro analysis has described that osteosarcoma cell lines deposit collagen-I as well as adhering and migrating on it (Fernandes et al. 2007, Vihinen et al. 1996). HOS cell adhesion and migration only occurred in cell lines expressing alpha 2 beta 1 integrin (Vihinen et al. 1996). Interaction between collagen-I and HOS cell line causes the synthesis and activation of MMP-2, potentially potentiating invasion through the ECM (Vihinen et al. 1996). CSPG4 has been shown to mediate invasion through collagen-I through activation of MMP2 (Iida et al. 2001). In this study, CSPG4 expression did not influence the ability of osteosarcoma cells to adhere to spread on collagen-I.

Fibronectin was chosen due to its association with CSPG4 and osteosarcoma. CSPG4 regulates adhesion to fibronectin in melanoma in conjunction with integrins (Iida et al. 1992). Melanoma only achieve a fully spread out morphology on substrate chimera

consisting of CSPG4 antibodies and fibronectin (Iida et al. 1995). While not as researched as collagen-I, fibronectin has been researched in osteosarcoma. In one study, fibronectin was expressed in 69% of samples, of which 64% featured high expression (Na et al. 2012). Fibronectin expression was increased in higher grade tumours and was associated with metastasis and shorter overall survival (Na et al. 2012). Furthermore, the MG63 cell line has been shown to deposit fibronectin in vitro (Vial et al. 2006). Addition of PAI-1 to MG63 cells increases fibronectin deposition through cross-talk between $\alpha v\beta 5$ and $\alpha v\beta 1$ integrins (Vial and McKeown-Longo 2008). In this study, CSPG4 expression did not influence the ability of osteosarcoma cells to adhere to spread on fibronectin.

Given the influence of integrins that has been reported for osteosarcoma attachment to collagen-I and fibronectin, future studies should focus on cell lines with integrin expression patterns proven to interact with CSPG4. For example, would the HOS cell line with exogenously expressed CSPG4 increase adhesion to collagen I. Future experiments may also focus on other collagen types, such as collagen V and collagen III. These types have been demonstrated within osteosarcoma tumours, as well as bone (Niyibizi and Eyre 1989a, Niyibizi and Eyre 1989b, Shapiro and Eyre 1982). In order to identify other components of the ECM, deposits created by specific cell lines grown in vivo could be discovered through IHC staining. The ability for CSPG4 to adhere to and spread on these matrices could then be assessed.

This chapter also assessed the contribution CPSG4 made to chemosensitivity for the CSPG4/Cas9 cell panel. CSPG4's role in multi-drug chemoresistance has been demonstrated by a seminal study by Chekenya et al. (2008). High expression of CSPG4 protects

glioblastoma cell lines and biopsy spheroids derived from brain tumour patient samples from drug-induced apoptosis (Chekenya et al. 2008). A number of drugs were examined including doxorubicin and cisplatin (Chekenya et al. 2008). CSPG4 interacts with alpha 3 beta 1 integrin in order to resist apoptosis. The interaction of these two protein serves to increase PI3K/Akt signalling, a widely reported cell survival signalling pathway (Chekenya et al. 2008).

Osteosarcoma is usually treated with a combination of surgery and chemotherapy, with the most common drugs being doxorubicin, cisplatin and methotrexate (He et al. 2014). Osteosarcoma tumours commonly develop resistance to chemotherapy which limits the effectiveness of cytotoxic drugs (He et al. 2014). Therefore, there is a clear clinical need to develop drugs that undermine osteosarcoma chemoresistance pathways. Given CSPG4's role in chemoresistance, it was hypothesised that CSPG4 may play a similar role in osteosarcomas.

In this study, CSPG4 expression did not demonstrate any protective effect from either doxorubicin or cisplatin (Figure 5.6). Eight concentrations were used and cells were treated for 24 hours before their viability was measured. Cell recovery following drug treatment was also investigated. Cells were grown for 48 hours following drug incubation, in fresh growth media. No difference was found for CSPG4-positive cell lines to CSPG4-negative cell lines (Figure 5.7). The decrease in viability was shown to be through apoptosis, demonstrated through the increase in Annexin-V and PI staining (Figure 5.10). Therefore, it can be concluded that CSPG4 offers osteosarcoma cells no protection from drug-induced apoptosis.

Due to the involvement of integrins and PI3K/Akt signalling in the protection conferred to CSPG4-positive cells, future experiments should be altered. Firstly, the cell line(s) of choice should be assessed for integrin expression. The 143B cell line may lack the appropriate protein partners for CSPG4 leading to any protective effect from apoptosis in osteosarcoma being missed. Furthermore, the drug incubation time of 24 hours may be too short for any PI3K/Akt signalling increase to occur. The study by Chekenya et al. (2008) used longer incubation times (96-120 hours) combined with lower concentrations of drug. This may allow any PI3K-Akt signalling dependent effect the time to alter the phenotype.

Anchorage-independent growth is an important component of tumorigenesis and can help in facilitating metastatic spread (Mori et al. 2009). CSPG4 has been found to promote the anchorage-independent growth of RGB melanoma cells (Price et al. 2011). CSPG4 is thought to achieve this through phosphorylation of $p130^{CAS}$, a known promotor of anchorage-independent growth (Eisennmann et al. 1999, Wei et al. 2002). Treatment with anti-CSPG4 antibodies reduces anchorage-independent growth (Harper and Reisfeld 1983). Anchorage-independence growth was reduced by 50% when treated with CSPG4 antibody fragments bound to human soluble TRAIL. This was seen alongside a rapid dephosphorylation of FAK, an anti-anoikis protein (de Bruyn et al. 2010, Buchheit et al. 2014). CSPG4 impacts on cell survival across a number of different tumour types (Personal communication, R. Perris).

If a cell is unable to achieve anchorage-independent growth, it undergoes anoikis, a form of programmed cell death. Paradoxically, CSPG4 has been shown to act as a pro-anoikis mediator following a loss of matrix contacts. Altered fibronectin caused an increase in CSPG4 and downregulation of integrin $\alpha 4$ in fibroblasts, which in turn increased anoikis (Joo

et al. 2008). Targeting CSPG4 with siRNA reduced anoikis (Joo et al. 2008). MMP-13 acts to reduce anoikis by shedding CSPG4 from the surface of fibroblast cells (Joo et al. 2014). Therefore, CSPG4's involvement in cell survival following a loss of contact with the extra-cellular matrix, could be cell type specific.

In this study, both CRISPR/Cas9 and siRNA cell panels were grown in ultra-low attachment conditions and then assessed for apoptotic markers. For both the CRISPR/Cas9 and siRNA cell line panels, no difference in anoikis was seen between the CSPG4-negative and CSPG4-positive cell lines (Figure 5.11, Figure 5.13). Therefore, it does not appear that CSPG4 plays a role in anchorage-independent growth in osteosarcoma, either as a pro- or anti-anoikis factor.

The final aim of this chapter was to provide proof-of-principle evidence that CSPG4 could be used as a target for therapeutic gain in osteosarcoma. As described in chapter one, CSPG4 is widely expressed across a number of osteosarcoma samples, shown through PCR and IHC analysis. It is therefore a viable option for treatment. Cell surface markers can be successfully targeted through antibody-based treatments and have led to therapeutic success (Adams and Weiner 2005). Due to the earlier results revealing no functional role for CSPG4 in osteosarcoma, there is no rationale behind using function-blocking or 'naked' antibodies. Therefore, an antibody-drug complex was chosen. The drug consisted of a CSPG4 antibody fragment covalently linked to *Pseudomonas* exotoxin A (PE).

PE is a toxic virulence from the pathogenic bacterium *Pseudomonas aeruginosa* (Michalska and Wolf 2015). PE is a NAD+-diphthamide-ADP-ribosyltransferase and is through to halt

protein synthesis through ADP-ribosylation of eEF-2 (Michalska and Wolf 2015). This inactivates eEF-2 and blocks mRNA translocation from the A-site to the P-site on the ribosome (Michalska and Wolf 2015). ETA bound to CSPG4 antibodies and antibody fragments has demonstrated effective killing of CSPG4-positive cells in vitro and in vivo across a number of tumour types.

A number of cell lines, such as rhabdomyosarcoma, melanoma, glioblastoma and breast cancer, undergo cytotoxicity when treated with PE conjugated to CSPG4 antibodies (Brehm et al 2014, Schwenkert et al. 2008, Hjortland et al. 2004, Amoury et al. 2014). PE conjugated to anti-CSPG4 antibody 9.2.27 causes cytotoxicity of glioblastoma cell lines when used in vitro and prolongs survival of mice by 43% compared to controls, when used in vivo (Hjortland et al. 2004). sc-Fv antibody fragments conjugated to ETA can also produce apoptosis. When used in melanoma cell lines, it has an EC50 of 1nm and kills 80% of cells within 72 hours. sc-Fv-PE also targets primary melanoma cell lines (Schwenkert et al. 2008). An sc-Fv-PE drug can also kill breast cancer cell lines in vitro and reduces in vivo growth (Amoury et al. 2016).

PE conjugated to anti-CSPG4 antibody 9.2.27 killed melanoma cell lines through reduction in protein synthesis (Risberg et al. 2009). Cells demonstrated elements of apoptotic death, but not others, such as Bcl-2 reduction (Risbergh et al. 2009). This apoptosis-independent mode of cell death is helpful for apoptosis-resistance cell lines. Melanoma cell lines that have developed a resistance to dacarbazine can be targeted effectively with the 9.2.27PE drug (Risberg et al. 2010). In addition, CSPG4-PE antibodies bind to rhabdomyosarcoma patient samples (Brehm et al. 2014). Therefore, CSPG4 antibodies conjugated to PE have shown

effectiveness in vitro (including for primary cell lines and drug resistant cell lines), in vivo and can recognise patient samples.

In addition to effectiveness against CSPG4-positive tumours, ETA has been reported to kill osteosarcoma cell lines when conjugated to other antibodies directed to a range of antigens. ETA conjugated to HER-2 antibody causes cytotoxicity of osteosarcoma cells in vitro and limits tumour growth and metastasis in vivo. It also extends animal survival (Shan et al. 2008). PE conjugated to 8H9 monoclonal antibody was tested in a number of tumours, including osteosarcoma. Treatment produced cell death in vitro (Onda et al. 2004). OHS-M1 injected in SCID mice treated with the drug produced a dose-dependent anti-tumour effect (Onda et al. 2004). It also demonstrated good tolerance in monkeys suggesting ETA-conjugated antibodies may provide a good therapeutic (Onda et al. 2004).

In this study, a CSPG4 sc-Fv antibody fragment bound to ETA, failed to produce selective cell death of CSPG4-positive cell lines. Three osteosarcoma cell lines were used, U2OS, MG63 and 143B. The glioblastoma cell line, U87MG, was used as a positive control as Hjortland et al. (2004) demonstrated the cell line was sensitive to treatment with 9.2.27 ETA. TC71, an Ewing's sarcoma cell line, shown to be negative for CSPG4 was used as a negative control. The drug produced reduced cell viability in all cell lines. Therefore, the antibody was not selectively targeting CSPG4-positive cells. This could have occurred through two mechanisms. Firstly, the sc-Fv could have been internalised into the cell through non-selective binding. Secondly, the PE molecule could have become decoupled from the sc-Fv and was therefore was acting as a soluble agent.

In conclusion, this chapter has failed to demonstrate that CSPG4 is involved in cell proliferation or cell survival, as shown through CSPG4/Cas9 knock-out and siRNA knock-down of the protein. In addition, CRISPR/Cas9 with varying levels of CSPG4 failed to demonstrate that CSPG4 was involved in cell adhesion, spreading, migration and chemoresistance. It has also failed to produce proof-of-principle evidence that CSPG4 can be used as a target for therapeutic outcomes in osteosarcoma. However, given the expression pattern of CSPG4 in osteosarcoma demonstrated earlier, it is still a viable therapeutic option.

Chapter 6

Function of CSPG4 in vivo in osteosarcoma

6.1 Summary

CSPG4 contribution to tumour growth and metastasis in vivo has been documented in a number of studies, focusing on different tumour types. In order to investigate CSPG4's contribution to osteosarcoma, it was essential to optimise an in vivo model.

The CRISPR/Cas9 cell panel was used for observing tumour growth in vivo. Experiments were based on a study by Luu et al. (2009). The authors described an orthotopic model using 143B cells demonstrating that the cell line grew in vivo and metastasised to the lung.

It was observed that 143B cells could grow in vivo when injected subcutaneously and intratibially. Intratibial injected cells were able to spread to the lungs for both $1x10^6$ and $2x10^6$ cell conditions. Both primary and secondary tumours retained CSPG4 protein expression as shown through IHC. As tumours with $1x10^6$ exhibited more consistent growth kinetics, this number was selected for further experiments.

CSPG4-positive and CSPG4 negative cell lines injected in vivo did not observably differ in terms of tumour growth, metastatic spread or mouse survival. Tumours within groups did not appear to grow in a consistent manner, this is also reflected in terms of mouse survival.

Intratibial injections of the 143B and 143B-CSPG4 cell lines was repeated with the animals being scanned at the experimental end-point with a microCT scanner. This allowed the measurement of bone volume, cortical thickness, medullary cavity diameter and cortical diameter. The growth of tumours was not significantly different between groups; however,

the 143B-CSPG4 group's growth was slower. Bone characteristics did not differ between groups, nor did they differ when compared to control mice who received a sham injection of PBS.

In conclusion, this chapter fails to demonstrate that CSPG4 contributes to osteosarcoma tumour growth or metastatic spread. However, the model used appears to provide inconsistent results and would have to be altered in future experiments.

6.2 Aims

The aim of the experiments detailed in this chapter were to:

1) Optimise an in vivo model of osteosarcoma growth and spread using the 143B cell line.

2) Utilise the model to test CRISPR/Cas9 experimental cell lines and assess influence of CSPG4 expression on osteosarcoma growth and spread.

3) Investigate the effect of CSPG4 on osteolytic damage arising from tumour growth using microCT technology

6.3 Optimisation of in vivo growth

In order to study CSPG4's contribution to tumourigenesis in vivo, it was critical to develop an in vivo model. An in vivo model would also allow investigation of metastatic spread. Metastasis is important clinically for osteosarcoma, as 80% of patients are believed to have undetectable metastatic disease (Luu et al. 2005).

The model described below is based on the model described by Luu et al. (2005). They found that the 143B cell line has good orthotopic tumour formation when injected into the tibia. (Luu et al. 2005). The study found 143B cells spontaneously metastasised to the lungs (Luu et al. 2005). Therefore, the 143B cell line could provide a clinically relevant model cell line for xenograft studies.

6.3.1 Subcutaneous growth

Firstly, subcutaneous injections were used to assess in vivo growth of the 143B cell line. Four athymic female nude mice were injected with 1 million cells into each flank. The growth was measured twice weekly until growth exceeded a humane end-point.

By 20 days the tumours had started to reach maximum growth and mice were sacrificed (Figure 6.1). Therefore, 143B cells could grow and form tumours in vivo in athymic nude mice. As expected from previous results in the literature, necropsied lung samples did not display any metastatic spread (data not shown).

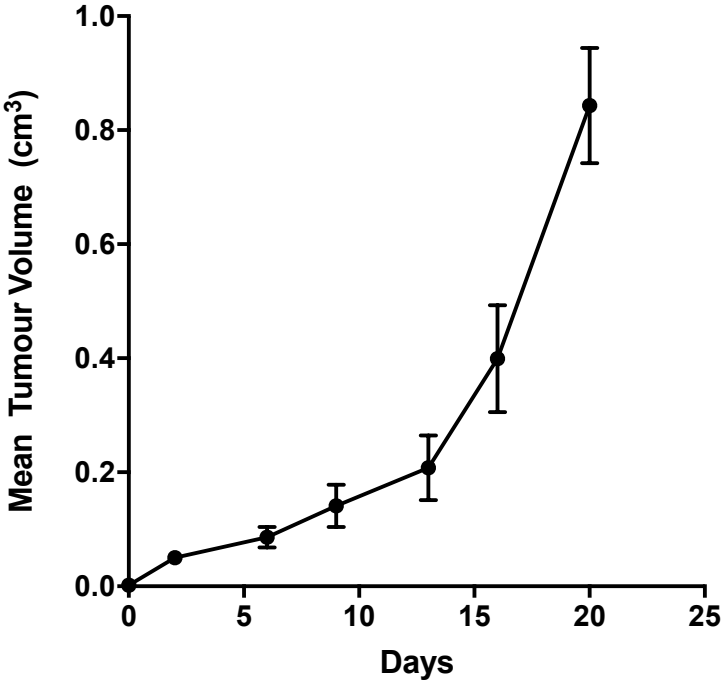

Figure 6.1 – Subcutaneous growth of 143B cells in athymic nude mice. $1x10^6$ 143B cells were injected subcutaneously into athymic nude mice. Two injections were performed on the right and left flank of the mouse. Tumour values were averaged across the two flanks. Values represent average tumour volumes from four athymic nude mice ± SEM (n=4).

6.3.2 Intratibial growth

An orthotopic model using intratibial cell injections presents a more clinically relevant model for osteosarcoma. Intratibial xenografts have been found to give rise to spontaneous metastasis (Luu et al. 2005).

Four athymic nude mice were split into two groups, one group had $1x10^6$ 143B cells injected and the other had $2x10^6$ 143B cells injected into the tibia of the mice after the bone marrow had been flushed out. Resulting tumours were measured with callipers once they were observable beneath the skin. Tumours were allowed to grow until they reached maximum size or the mice became lame. At this point mice were culled and the afflicted leg and lungs

were taken.

143B cells were able to grow and form tumours intratibially in athymic nude mice (Figure 6.2a). Mice injected with $1x10^6$ cells had a steeper growth curve than those injected with $2x10^6$ cells (Figure 6.2a). The two mice injected with $1x10^6$ also demonstrated similar growth pattern whereas the two mice injected with $2x10^6$ did not (Figure 6.2a). This tumour growth was seen alongside a destruction of the bone architecture compared to a control non-surgery leg (Figure 6.2b).

Metastatic spread to the lungs was observed with intratibial growth (Figure 6.2c). Both the primary tumour and pulmonary metastasis were positive for CSPG4 as shown through immunohistochemistry (Figure 6.2c).

In order to assess the tumour burden of pulmonary metastasis on the lungs, a series of non-sequential sections were taken of the lungs. Using the Nanozoom, the area of tumour lesions was calculated as a percentage of the area of the lung tissue. Evidence of metastasis was seen in the lungs of each mouse (Figure 6.2d). However, the extent of the tumour burden was not consistent across groups.

Due to the inconsistency in the growth pattern of mice injected with $2x10^6$ cells, $1x10^6$ cells were used for further experiments.

(A)

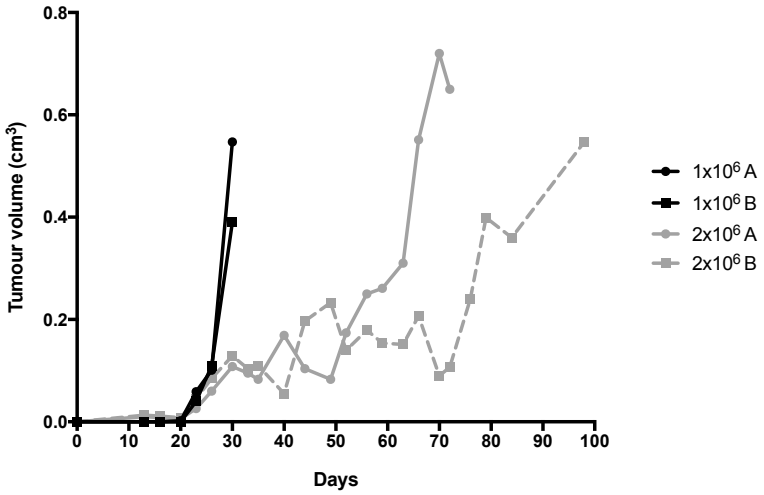

(B)

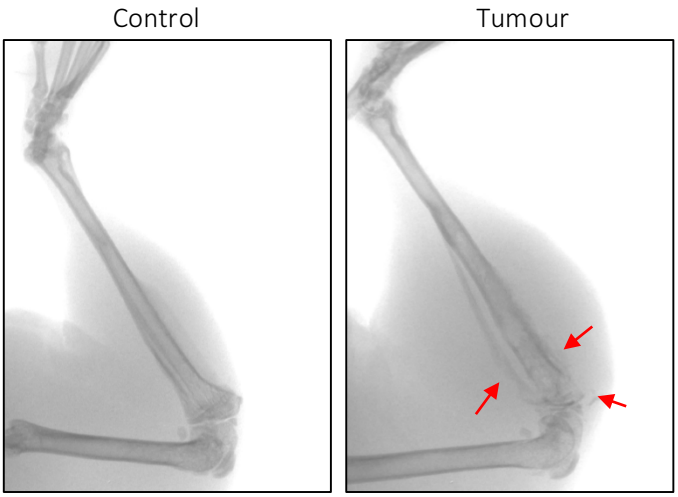

(C)

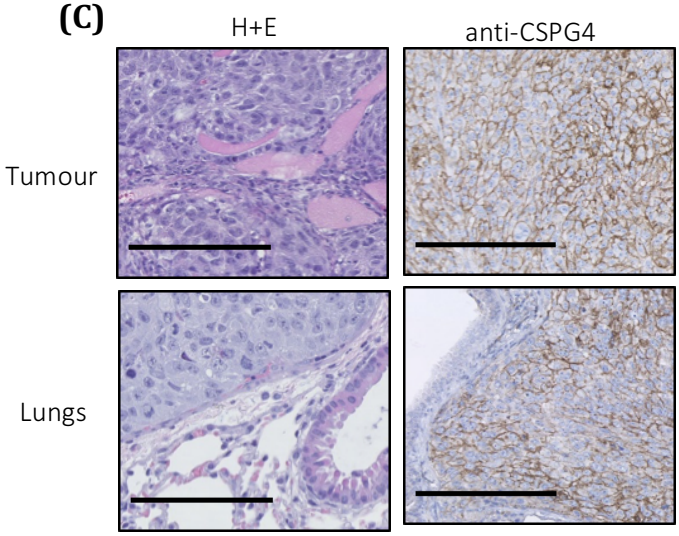

(D)

Cell line	Mouse ID	Tumour burden (%)
1 x 10^6	A	0.29
	B	0.98
2 x 10^6	A	6.01
	B	0.93

Figure 6.2 – Development of an orthotopic model using intratibial injections of 143B cells in athymic nude mice. 143B cell lines were injected in athymic nude mice to establish its in vivo growth kinetics. **(A)** Comparison of 1x10^6 and 2x10^6 cells injected intratibially into athymic nude mice. **(B)** microCT images from one mouse. Control leg received PBS injection into the tibia whereas tumour condition had 1x10^6 cells injected. Red arrows refer to areas of osteolytic damage. **(C)** Immunohistological images of both tumour and lung tissues stained with H+E and anti-CSPG4 antibody. Scale bar = 100µm. **(D)** Table detailing the pulmonary tumour burden per mouse.

6.4 Intratibial injection of CRISPR/Cas9 cell lines

6.4.1 Investigation of tumour growth, metastasis and mouse survival

Using the orthotopic intratibial model, the CRISPR/Cas9 cells would be used to investigate CSPG4's contribution to osteosarcoma growth and metastasis in vivo. Mice were culled once they reached a humane end-point, this would allow the comparison of survival between groups.

Five athymic nude mice were injected with $1x10^6$ cells from the cell lines 143B, 143B-CSPG4, H10-KO and H10-KO-CSPG4. H10-KO and H10-KO-CSPG4 cells were chosen as their in vitro proliferation rate was closer to 143B and 143B-CSPG4 than H7-KO and H7-KO-CSPG4 (Figure 5.1).

Tumour growth showed no discernible link to CSPG4 expression (Figure 7.3a). Tumours from all cell lines appeared to grow, however tumours from each mouse did not, with some tumours from across the different cell lines exhibiting flat line growth (Figure 7.3a). This inconsistency is reflected in Kaplan-Meier survival curves of each group (Figure 7.3b). There was also no evidence of pulmonary metastasis from any mouse (Data not shown).

Therefore, tumour growth in vivo, mouse survival and metastatic spread does not appear to correlate with CSPG4 function.

(A)

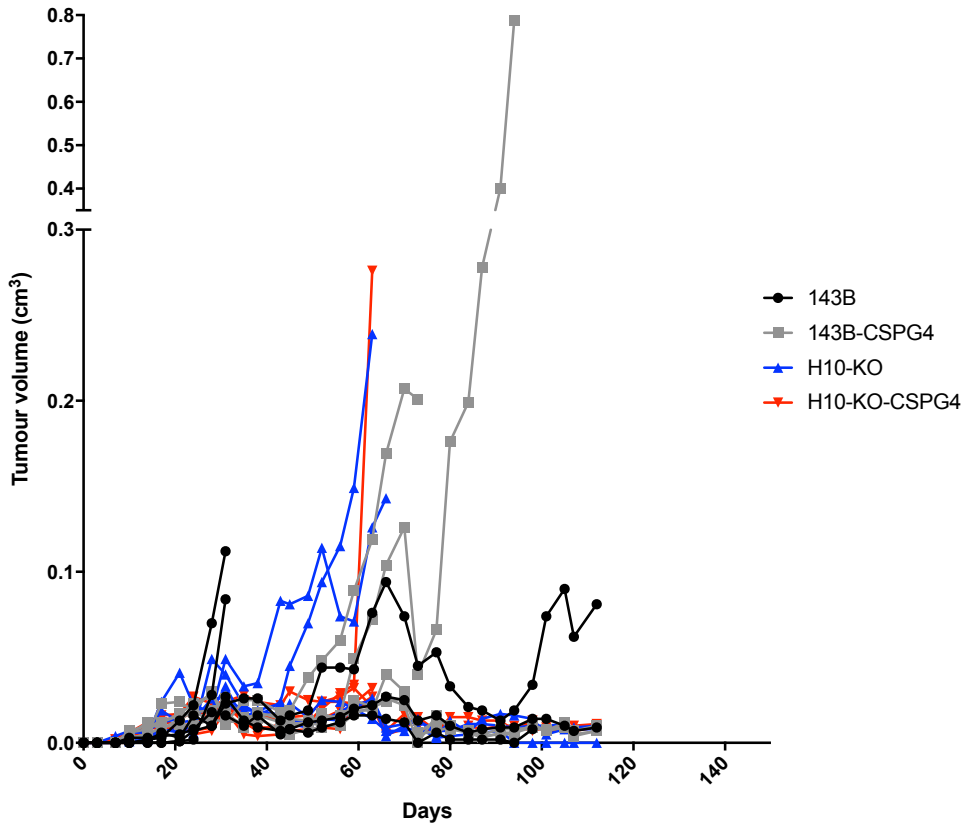

(B)

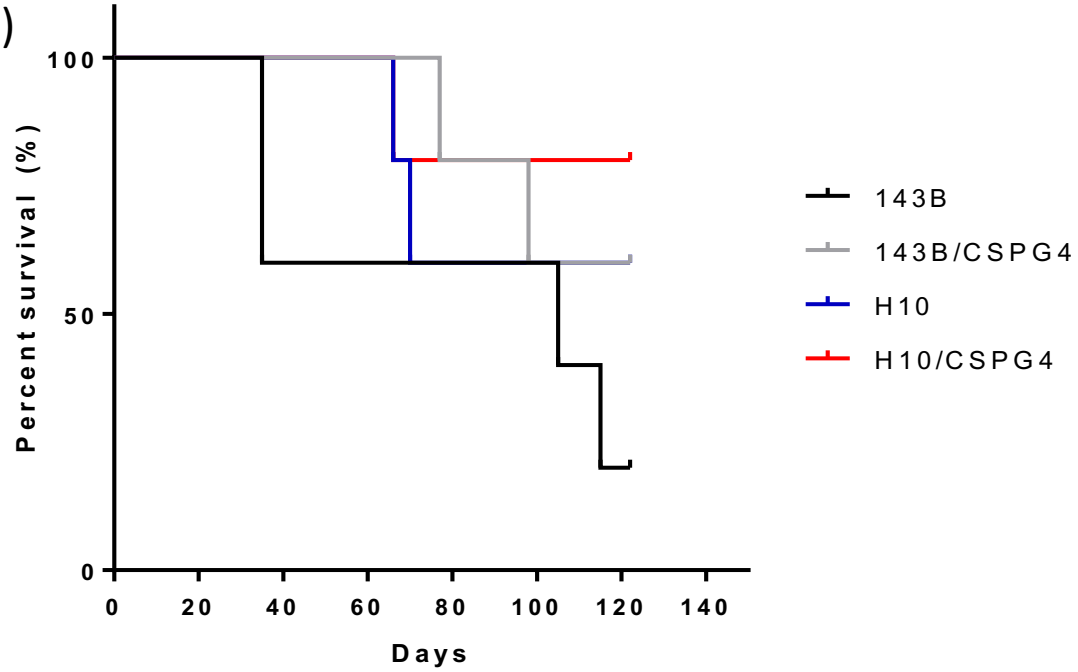

Figure 6.3 – Tumour growth and mouse survival following intratibial injections of CSPG4-negative and CSPG4-positive cell lines in athymic nude mice. (A) Five mice, per group, were injected with $1x10^6$ cells. Mice were measured twice weekly until they reached a human end-point. Lines represent individual mice, colour coded by cell line. **(B)** Kaplan-Meier graph detailing the survival of mice per experimental group.

6.4.2 microCT analysis of bone after intratibial injection

Given the inconsistency in tumour growth and mouse survival, both between and within groups, it was important to investigate effect of osteosarcoma growth on the bone.

Cell lines 143B and 143B-CSPG4 were used as the experimental cell lines. $1x10^6$ cells were injected into the tibia of five mice for both of these cell lines. In addition, one mouse per group underwent a sham injection of PBS-only. This would allow observation of the impact surgery alone had on bone structure. Mice were culled 35 days after surgery. Observable tumours were measured on the leg surface using callipers.

In contrast to the previous experiment, mice from both groups demonstrated tumour growth that increased throughout the incubation time (Figure 6.4a). However, tumour growth did not appear to relate to CSPG4 expression, indeed the 143B-CSPG4 cell line exhibiting overexpressed CSPG4, appears to grow slightly slower than the parental cell line (Figure 6.4a). No metastatic spread was observed from either group.

The two sham mice also exhibited palpable lumps, usually interpreted as tumours. This suggests that injection also causes an inflammatory reaction resulting in observable protrusions.

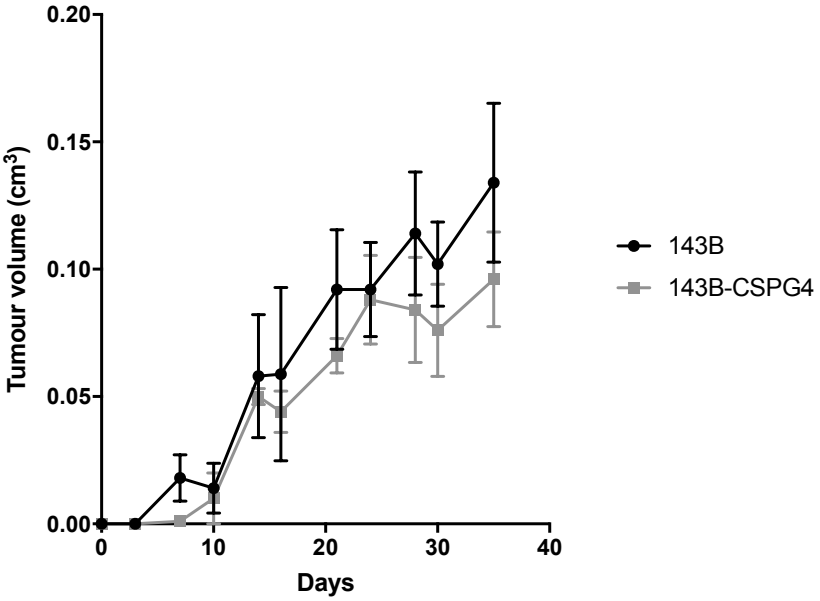

Figure 6.4 – Repeat experiment of intratibial growth of 143B and 143B-CSPG4 cell lines in athymic nude mice. Four mice, per group, were injected with $1x10^6$ cells. Mice were measured twice weekly for 35 days. Values represent average tumour volumes from four athymic nude mice ± SEM (n=4).

Mice were also scanned at the experiment end-point using a microCT scanner. Using reconstruction software, bone volume, cortical thickness, medullary cavity diameter and cortical diameter were calculated. 3D bone reconstruction models were also produced. Mice were scanned and images were analysed following guidelines set out by Campbell and Sophocleous (2014).

The microCT scans show that there is no significant difference between 143B and 143B-CSPG4 group for any of the bone measurements (Figure 6.5). Interestingly, the two sham mice demonstrated bone characteristics at the experiment end-point that were very similar to the experimental groups. 3D images demonstrate tibia from (Figure 6.5). The tumour leg from the 143B group (Figure 6.5e, lower left panel) represents the most extreme sample. This was not representative of other legs, where little osteolytic damage was seen, as

demonstrated by the tumour sample from group 143B-CSPG4 (Figure 6.53, lower right panel). Therefore, CSPG4 overexpression does not appear to influence tumour growth in vivo, metastatic spread or alter bone characteristics.

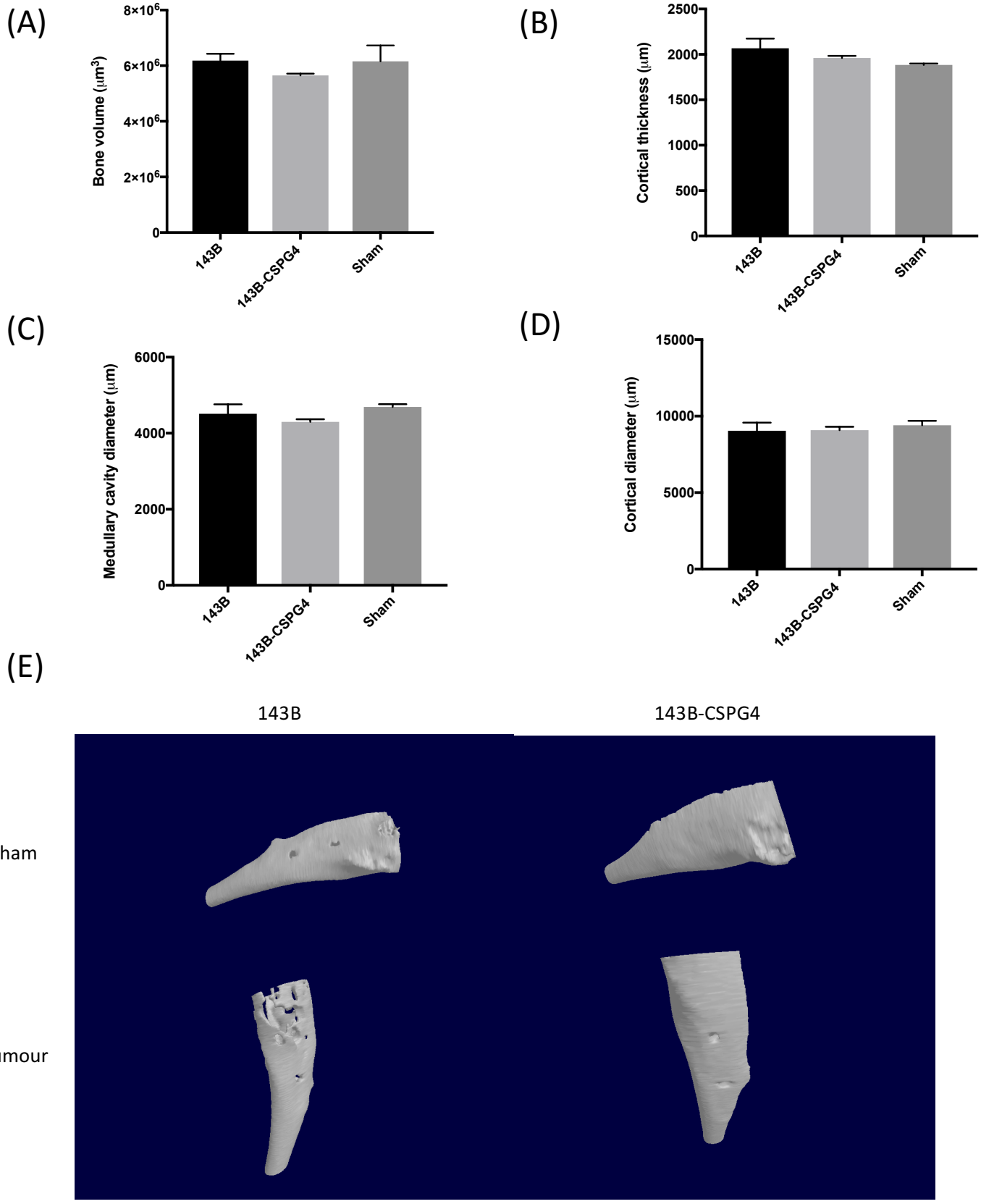

Figure 6.5 – microCT analysis of bone characteristics between 143B and 143B-CSPG4 orthotopic tumours. Five mice per group were injected with tumour cells for 35 days. Mice were then scanned at the experiment end-point. One mouse per group had a sham injection of PBS. **(A)** Value for bone volume **(B)** Volume for cortical thickness **(C)** Volume for medullary cavity diameter **(D)** Volume for cortical diameter **(E)** 3D tibia reconstruction images demonstrating the extent of bone destruction for sham-injections and injections of tumour cells, both 143B and 143B-CSPG4. Experimental group values are the average of five mice and the sham.

6.5 Discussion

The aim of this chapter was to optimise an in vivo model using athymic nude mice and use it to assess CSPG4 mediation of tumour growth and metastatic spread. Firstly, the 143B cell line would be grown through subcutaneous injections with mice investigated for tumour growth. Secondly, 143B cells would be injected intratibially and investigated for tumour growth and metastatic growth.

143B cells successfully grew in vivo when injected subcutaneously (Figure 6.1). This is consistent with other reports that have demonstrated this finding (Sun et al. 2015). Orthotopic models provide a more relevant way to model osteosarcoma growth. A study by Luu et al. (2005) provided evidence that 143B cells could be injected intratibially where they grew and gave rise to spontaneous pulmonary metastasis. $1x10^6$ cells were injected in to male athymic nude mice ages four to six weeks (Luu et al. 2005). In this study, two xell numbers, $1x10^6$ and $2x10^6$, were injected into separate mice. 143B cell numbers were able to grow following intratibial injection (Figure 6.2). $1x10^6$ mice displayed more consistent growth between the two mice, whereas the $2x10^6$ mice were less consistent (Figure 6.2a). Metastatic spread was seen with all four mice (Figure 6.2d). Therefore, $1x10^6$ cells was the injection number taken forward.

Using intratibial injections of $1x10^6$ cells, the 143B, 143B-CSPG4, H10-KO and H10-KO-CSPG4. H10-KO and H10-KO-CSPG4 were chosen for in vivo study as they demonstrated similar in vitro growth rates to the parental 143B cell line. Expression of CSPG4 did not appear to influence tumour growth, metastatic spread or mouse survival. Growth and

survival differed both within groups and between groups with no obvious pattern. Metastatic spread to the lungs was not observed in any of the mice studied.

The lack of consistency within experimental groups and lack of metastatic spread is not consistent with published reports. Luu et al. (2005) found that the 143B cell line demonstrated observable tumours by 5 days and tumours continued to grow until mice were culled. In addition, 143B cells readily metastasised to the lungs. These findings could not have been related to CSPG4 expression as growth was inconsistent for all experimental groups.

In order to explain this result, the experiment was repeated with the 143B and 143B-CSPG4 cell lines. In addition, mice were scanned at the experimental end-point to observe bone destruction. As a control, one mouse per group received a sham injection of PBS in order to discount bone remodelling or destruction as a result of surgery. Both cell lines exhibited tumour growth in this experiment (Figure 6.4). However, CSPG4 did not appear to influence growth, as the 143B cell line exhibited a faster growth rate. Metastasis was not observed in any of the mice injected.

microCT allows investigation of bone characteristics. Mice were scanned at the experimental end-point. Both the 143B, 143B-CSPG4 and the sham mice did not statistically differ in any of the metrics investigated, such as bone volume, cortical thickness, medullary cavity diameter or cortical diameter (Figure 6.5). Therefore, tumour growth over 35 days did not appear to cause more bone destruction than a sham injection. This varied within the mice as one mouse (displayed in Figure 6.5e lower left panel).

These results raise questions about the reproducibility and therefore, the validity of using the tibia for injection of tumour cells. The lack of consistency of results (displayed in Figure 6.3) undermines the model's ability to produce reliable data. A number of technical issues could contribute to this. Firstly, injection of the tumour cells is not precise as the volume injected depends on intramedullary space. Cells are injected into the hole made in the proximal tibia until cells leak from the distal hole. Therefore, the amount injected depends on the individual mouse and on speed of injection. $1x10^6$ cells in 100uL means that even slight variation in volume can mean a large change in tumour cells. The leakiness of an intratibial injection is increased by the lack of space offered by the tibia. Volume injected into the intramedullary space increases pressure which increases leaks (Sasaki et al. 2015). A high intramedullary space can also cause venous emboli, causing tumour cells to enter the bloodstream directly. This could be a possible cause for the high tumour burden observed in mouse $2x10^6$ A (Figure 6.2d). A second issue arises from tumour cells leaking into the surrounding soft tissue, whilst effort is made to remove these with PBS, some could remain. Tumour cells implanting and growing in soft tissue could appear earlier, distorting growth occurring within the bone.

The limitations of space and leakiness has been addressed by Sasaki et al. (2015). They propose using intrafemoral injections. The femur is larger and is less bowed, offering more intramedullary space. The use of one injection site which is then covered by bone wax acts to reduce leakiness (Sasaki et al. 2015). Using this model, metastasis was observed to the liver and to the lungs (Sasaki et al. 2015).

Another issue could have been length of surgery. Five mice operated on by one technician means cells can sit on ice for considerable time. If left on ice for too long or if using the same needle on more than ~3 mice, cell sedimentation can occur which could lead to unequal distribution within the liquid (Sasaki et al. 2015). This could then lead to different cell numbers being injected.

Another technical issue with the injections directly into the bone cavity, be that of the tibia or the femur, is accurate measurement. Palpable tumour growth may differ between mice and depends on observer measurement. Cells expressing a fluorescent marker detectable by imaging could represent a quantifiable way to measure tumour growth in vivo.

Therefore, future experiments should focus on using the intrafemoral injection with cell lines transfected with a fluorescence marker. Future studies, should investigate the tumour potential of 143B cell lines that have been immunosorted for CSPG4 expression. This would avoid single cell clones being used with the inherent clonal variation. This would allow a quick and straight forward mechanism of clarifying CSPG4's contribution to tumour growth and metastasis in vivo unhindered by clonal variation.

Chapter 7

Discussion

7.1 Discussion

Osteosarcoma is the most common malignancy of bone, which is common in children and adolescence. Since the advent of neoadjuvant chemotherapy four decades ago, no new treatments have emerged. Osteosarcoma tumours are aggressive and prone to developing resistance to chemotherapy and undergo distal metastasis. CSPG4 is a transmembrane proteoglycan molecule involved in progenitor cell proliferation and migration (Stallcup and Huang 2008). It has been identified on a number of tumour types and associated with proliferation, migration, chemoresistance, invasion and metastasis. Preliminary experiments revealed CSPG4 expression on osteosarcoma cell lines and patient samples. The main aim of this study was to investigate the role CSPG4 plays in osteosarcoma tumorigenesis and whether it represented a novel therapeutic target.

In chapter 3, it was demonstrated that CSPG4 expression was found on patient samples and model cell lines. Both mRNA and protein expression was found. mRNA expression was overexpressed compared to healthy mature osteoblast cells. As discussed, the relevance of this finding depends on whether mature osteoblasts represent the cell of origin. Further experiments should investigate whether transcript level can predict clinicopathological features, based on a study by Benassi et al. (2009) who investigated CSPG4 in soft tissue sarcomas. This may identify CSPG4 as a biomarker for osteosarcoma.

Furthermore, 86% of samples from a TMA were positive for CSPG4 protein

expression. This is an important finding for a disease that exhibits vast tumour heterogeneity (Poos et al. 2015). It was also demonstrated that CSPG4 featured on a number of osteosarcoma sub-types. More samples would be needed to definitively answer if CSPG4 is expressed widely on all osteosarcoma subtypes. Due to its wide expression pattern, CSPG4 represents a novel therapeutic target.

In chapter 4, CSPG4 expression was modulated in osteosarcoma cell lines using CRISPR/Cas9 and siRNA technology. CRISPR/Cas9 treatment of the 143B cell line deleted CSPG4 protein expression through selective sequence deletion within the *CSPG4* gene. Protein expression was unidentifiable through western blotting and flow cytometry analysis. CSPG4 cDNA was introduced into knock-out cell lines and CSPG4 was successfully re-expressed. This was found predominantly around the cell membrane in 2 out of 3 cell lines. Localisation of exogenously expressed CSPG4 should be compared to localisation in the parental cell, especially in terms of co-localisation with known protein interactors. Furthermore, siRNA treatment was utilised to downregulate CSPG4 expression. CSPG4 protein expressed was reduced in U2OS, MG63 and143B osteosarcoma cell lines, as well as the U87MG glioblastoma cell line.

In chapter 5, no difference was found between CSPG4-positive and CSPG4-negative or CSPG4-reduced cell lines for cell proliferation, adhesion, spreading, migration, chemoresistance or anchorage-independent growth. Future experiments should investigate the growth factor dependent influence on proliferation and migration for CSPG4-positive and CSPG4-negative cells, given CSPG4's role as a co-receptor for FGF

and PDGF signalling pathways. Indeed, cells may have been able to proliferate at the same rate using growth factors in the growth medium unrelated to CSPG4 expression. siRNA treatment of the U87MG cell line also failed to alter viability. Targeting of CPSG4 in an U87MG allograft in vivo led to attenuated tumour cell proliferation (Poli et al. 2013). This demonstrates that in the right environment CSPG4 does contribute to U87MG proliferation. This may also depend on the influence of relevant growth factors, such as PDGF.

It may also be the case that the role CSPG4 plays in osteosarcoma is missed due to CRISPR/Cas9 editing producing unrepresentative cell lines. The single cell cloning aspect of CRIPR/Cas9 deletion mean clonal variation can limit the usefulness of cells produced (Veres et al. 2015). It could also produce cell lines that did not depend on CSPG4 to survive, whilst those that did, are unable to grow and die. Given the extent to which osteosarcoma cells undergo mutations in culture, variations within a heterogeneous cell line could potentially be large. It could also be possible that the negative results seen are a specific result relating to the 143B cell line. Future experiments should focus on using siRNA treated cell lines to investigate functions not investigated in this study such as adhesion, spreading, migration and chemoresistance.

As previously mentioned, the localisation of CSPG4 in exogenously expressing cell lines may not be in the correct proximity to other proteins it interacts with. For example, many of the functions that CSPG4 mediates, rely on other proteins such as integrins and growth factor receptors. The 143B cell line should be investigated for

whether it contains complementary integrins or growth factor receptors.

In chapter 5, it was investigated whether proof-of-principle evidence could be provided for therapeutic targeting of CSPG4 on osteosarcoma cells, using an sc-Fv antibody fragment linked to *Pseudomonas exotoxin A* (ETA). Reduced viability of the CSPG4-negative TC71 cell line was observed following treatment of the drug. This suggests that an indirect mechanism is causing toxicity, not specific binding of the antibody fragment to CSPG4 and subsequent internalisation of ETA.

Given the expression pattern observed of CSPG4 on osteosarcoma patient samples, it remains a viable therapeutic target. Indeed, CSPG4 has been utilised for targeting of osteosarcoma. Treatment of MG63 and U2OS cells with the anti-CSPG4 225.28 antibody inhibits cell growth by ~60%, significantly higher than treatment with a control mAb (Campoli et al. 2010, Wang et al. 2013). Treatment of MG63 cells was associated with the downregulation of several proteins, such as pFAK, pAkt, pPDK1 and PKCr (Wang et al. 2013) Furthermore, treatment of U2OS with 225.28 was found to reduce migration by 55% (Wang et al. 2013). Targeting of 143B cells with a CSPG4-directed CAR and T-cells resulted in 40% cell lysis (Tschernia et al. 2014). This demonstrates that CSPG4 expression can be exploited for therapeutic gain in osteosarcoma.

Recent work by Salanti et al. (2015) has demonstrated that CSPG4 can be targeted using rVAR2 recombinant protein. rVAR2 is a recombinant version of the VAR2CSA protein which binds to placental chondroitin sulphate chains (CS A). CS A is present

on a number of tumour types, whilst not being present on healthy tissues. The study demonstrated that CSPG4, as well as other proteins, are modified with CS A and CSPG4 can be pulled-down using the rVAR2 protein. Therefore, a conjugated version of rVAR2, bound to hemiasterlin was used to kill U2OS, MG63 and HOS-MNNG cell lines (Salanti et al. 2015). Further work has demonstrated that rVAR2 treatment of U2OS and MG63 cells reduces their attachment to fibronectin, collagen-I and collagen-V (Clausen et al. 2016). Treatment of MG63 cells with rVAR2 also reduces migration, invasion and anchorage-independent growth (Clausen et al. 2016). Further work, not on osteosarcoma, demonstrated that metastatic lesions, which display CS A (or oncofetal CS) can be targeted with rVAR2 (Clausen et al. 2016). Therefore, targeting post-translational modifications (such as CS chains) shared by a number of proteins on tumour cells could represent a more efficacious way to kill tumour cells. Future experiments should focus on investigating whether the rVAR2 protein can be used to target osteosarcoma cell lines, in vitro and in vivo.

In chapter 6, an in vivo model was optimised for 143B cell implantation into athymic nude mice. 143B cells were shown to grow when injected subcutaneously and into the tibia. Evidence of metastasis was also observed. However, results from intratibial injections of 143B, 143B-CSPG4, H10-KO and H10-KO-CSPG4 were inconclusive. Large variation existed between and within groups. This could have been due to limitations of the intratibial injection model, discussed earlier. A repeat experiment with intratibial injections of 143B and 143B-CSPG4 produced more consistent growth within groups. However, the 143B-CSPG4 tumours grew slower and were smaller at the experimental end-point suggesting that CSPG4 does not influence osteosarcoma

tumour growth in vivo. Metastatic spread was not seen in any mouse for either group. Bone characteristics measured through microCT scanning did not reveal any difference between the two groups. Future work should focus on using intrafemoral injections which have fewer drawbacks (Sasaki et al. 2015). Given the clonal variation and/or mutation that may occur to single cell clones in culture, the focus for future experiments should focus on 143B cells immunosorted for CSPG4 in the first instance. This should ensure that the only difference between groups is level of CSPG4 protein expression. Furthermore, if metastatic spread could not be replicated in future studies, the tail injection method should be utilised to observe whether CSPG4 expression enhances colonisation.

In conclusion, this study has failed to identify any functional roles for CSPG4 in osteosarcoma both in vitro and in vivo. However, CSPG4 has a wide expression across osteosarcoma samples and therefore remains a viable therapeutic target in osteosarcoma.

Chapter 8

Bibliography

8.1 References

Abarrategi, A., Tornin, J., Martinez-Cruzado, L., Hamilton, A., Martinez-Campos, E., Rodrigo, J. P., González, M. V., Baldini, N., Garcia-Castro, J. & Rodriguez, R. 2016. Osteosarcoma: Cells-of-Origin, Cancer Stem Cells, and Targeted Therapies. *Stem Cells Int,* 2016

Adams, G. P. & Weiner, L. M. 2005. Monoclonal antibody therapy of cancer. *Nat Biotechnol,* 23(9)**,** pp 1147-57.

Al-Mayhani, M. T. F., Grenfell, R., Narita, M., Piccirillo, S., Kenney-Herbert, E., Fawcett, J. W., Collins, V. P., Ichimura, K. & Watts, C. 2011. NG2 expression in glioblastoma identifies an actively proliferating population with an aggressive molecular signature. *Neuro-Oncology,* 13(8)**,** pp 830-845.

Allison, D. C., Carney, S. C., Ahlmann, E. R., Hendifar, A., Chawla, S., Fedenko, A., Angeles, C. & Menendez, L. R. 2012. A meta-analysis of osteosarcoma outcomes in the modern medical era. *Sarcoma,* 2012(704872.

Amoury, M., Mladenov, R., Nachreiner, T., Pham, A. T., Hristodorov, D., Di Fiore, S., Helfrich, W., Pardo, A., Fey, G., Schwenkert, M., Thepen, T., Kiessling, F., Hussain, A. F., Fischer, R., Kolberg, K. & Barth, S. 2016. A novel approach for targeted elimination of CSPG4-positive triple-negative breast cancer cells using a MAP tau-based fusion protein. *Int J Cancer,* 139(4)**,** pp 916-27.

Asher, R. A., Morgenstern, D. A., Properzi, F., Nishiyama, A., Levine, J. M. & Fawcett, J. W. 2005. Two separate metalloproteinase activities are responsible for the shedding and processing of the NG2 proteoglycan in vitro. *Mol Cell Neurosci,* 29(1)**,** pp 82-96.

Beard, R. E., Zheng, Z., Lagisetty, K. H., Burns, W. R., Tran, E., Hewitt, S. M., Abate-Daga, D., Rosati, S. F., Fine, H. A., Ferrone, S., Rosenberg, S. A. & Morgan, R. A. 2014. Multiple chimeric antigen receptors successfully target chondroitin sulfate proteoglycan 4 in several different cancer histologies and cancer stem cells. *J Immunother Cancer,* 2(25.

Behjati, S., Tarpey, P. S., Haase, K., Ye, H., Young, M. D., Alexandrov, L. B., Farndon, S. J., Collord, G., Wedge, D. C., Martincorena, I., Cooke, S. L., Davies, H., Mifsud, W., Lidgren, M., Martin, S., Latimer, C., Maddison, M., Butler, A. P., Teague, J. W., Pillay, N., Shlien, A., McDermott, U., Futreal, P. A., Baumhoer, D., Zaikova, O., Bjerkehagen, B., Myklebost, O., Amary, M. F., Tirabosco, R., Van Loo, P., Stratton, M. R., Flanagan, A. M. & Campbell, P. J. 2017. Recurrent mutation of IGF signalling genes and distinct patterns of genomic rearrangement in osteosarcoma. *Nat Commun,* 8(15936.

Behm, F. G., Smith, F. O., Raimondi, S. C., Pui, C. H. & Bernstein, I. D. 1996. Human homologue of the rat chondroitin sulfate proteoglycan, NG2, detected by monoclonal antibody 7.1, identifies childhood acute lymphoblastic leukemias with t(4;11)(q21;q23) or t(11;19)(q23;p13) and MLL gene rearrangements. *Blood,* 87(3)**,** pp 1134-1139.

Belachew, S., Chittajallu, R., Aguirre, A. A., Yuan, X., Kirby, M., Anderson, S. & Gallo, V. 2003. Postnatal NG2 proteoglycan-expressing progenitor cells are intrinsically multipotent and generate functional neurons. *J Cell Biol,* 161(1)**,** pp 169-86.

Benassi, M. S., Pazzaglia, L., Chiechi, A., Alberghini, M., Conti, A., Cattaruzza, S., Wassermann, B., Picci, P. & Perris, R. 2009. NG2 Expression Predicts the Metastasis Formation in Soft-Tissue Sarcoma Patients. *Journal of Orthopaedic Research,* 27(1)**,** pp 135-140.

Bertoni, F., Bacchini, P., Fabbri, N., Mercuri, M., Picci, P., Ruggieri, P. & Campanacci, M. 1993. Osteosarcoma. Low-grade intraosseous-type osteosarcoma, histologically resembling parosteal osteosarcoma, fibrous dysplasia, and desmoplastic fibroma. *Cancer,* 71(2)**,** pp 338-45.

Bougeard, G., Renaux-Petel, M., Flaman, J. M., Charbonnier, C., Fermey, P., Belotti, M., Gauthier-Villars, M., Stoppa-Lyonnet, D., Consolino, E., Brugieres, L., Caron, O., Benusiglio, P. R., Bressac-de Paillerets, B., Bonadona, V., Bonaiti-Pellie, C., Tinat, J., Baert-Desurmont, S. & Frebourg, T. 2015. Revisiting Li-Fraumeni Syndrome From TP53 Mutation Carriers. *J Clin Oncol,* 33(21)**,** pp 2345-52.

Brehm, H., Niesen, J., Mladenov, R., Stein, C., Pardo, A., Fey, G., Helfrich, W., Fischer, R., Gattenloehner, S. & Barth, S. 2014. A CSPG4-specific immunotoxin kills rhabdomyosarcoma cells and binds to primary tumor tissues. *Cancer Letters,* 352(2)**,** pp 228-235.

Buchheit, C. L., Weigel, K. J. & Schafer, Z. T. 2014. Cancer cell survival during detachment from the ECM: multiple barriers to tumour progression. *Nat Rev Cancer,* 14(9)**,** pp 632-41.

Bumol, T. F., Walker, L. E. & Reisfeld, R. A. 1984. Biosynthetic studies of proteoglycans in human melanoma cells with a monoclonal antibody to a core glycoprotein of chondroitin sulfate proteoglycans. *J Biol Chem,* 259(20)**,** pp 12733-41.

Burg, M. A., Nishiyama, A. & Stallcup, W. B. 1997. A central segment of the NG2 proteoglycan is critical for the ability of glioma cells to bind and migrate toward type VI collagen. *Experimental Cell Research,* 235(1)**,** pp 254-264.

Burg, M. A., Tillet, E., Timpl, R. & Stallcup, W. B. 1996. Binding of the NG2 proteoglycan to type VI collagen and other extracellular matrix molecules. *J Biol Chem,* 271(42)**,** pp 26110-6.

Cai, Y., Cai, T. & Chen, Y. 2014. Wnt pathway in osteosarcoma, from oncogenic to therapeutic. *J Cell Biochem,* 115(4)**,** pp 625-31.

Cai, Y., Mohseny, A. B., Karperien, M., Hogendoorn, P. C., Zhou, G. & Cleton-Jansen, A. M. 2010. Inactive Wnt/beta-catenin pathway in conventional high-grade osteosarcoma. *J Pathol,* 220(1)**,** pp 24-33.

Campbell, G. M. & Sophocleous, A. 2014. Quantitative analysis of bone and soft tissue by micro-computed tomography: applications to ex vivo and in vivo studies. *Bonekey Rep.*

Campoli, M., Ferrone, S. & Wang, X. 2010. Functional and clinical relevance of chondroitin sulfate proteoglycan 4. *Adv Cancer Res,* 109(73-121.

Cattaruzza, S., Nicolosi, P. A., Braghetta, P., Pazzaglia, L., Benassi, M. S., Picci, P., Lacrima, K., Zanocco, D., Rizzo, E., Stallcup, W. B., Colombatti, A. & Perris, R. 2013. NG2/CSPG4collagen type VI interplays putatively involved in the microenvironmental control of tumour engraftment and local expansion. *Journal of Molecular Cell Biology,* 5(3)**,** pp 176-193.

Cattaruzza, S., Ragni, M., Russo, S., Wasserman, B., Colombatti, A. & Perris, R. 2003. NG2 proteoglycan modulates the convergence of ECM and growth factor-induced cell signalling in soft tissue sarcomas. *International Journal of Molecular Medicine,* 12(Supplement 1)**,** pp S51-S51.

Cattaruzza, S., Tommasetti, G., Bertani, N., Pala, S., Montanini, L., Stallcup, W. B., Colombatti, A. & Perris, R. 2006. Drug resistance in highly aggressive acute leukemias is controlled by de novo, expressed NG2 proteoglycan acting via modulation of selected transporters. *Ejc Supplements,* 4(12)**,** pp 55-55.

Chekenya, M., Hjelstuen, M., Enger, P. O., Thorsen, F., Jacob, A. L., Probst, B., Haraldseth, O., Pilkington, G., Butt, A., Levine, J. M. & Bjerkvig, R. 2002. NG2 proteoglycan promotes angiogenesis-dependent tumor growth in the central nervous system by sequestering angiostatin. *Faseb Journal,* 16(2)**,** pp 586-+.

Chekenya, M., Krakstad, C., Svendsen, A., Netland, I. A., Staalesen, V., Tysnes, B. B., Selheim, F., Wang, J., Sakariassen, P. O., Sandal, T., Lonning, P. E., Flatmark, T., Enger, P. O., Bjerkvig, R., Sioud, M. & Stallcup, W. B. 2008. The progenitor cell marker NG2/MPG promotes chemoresistance by activation of integrin-dependent PI3K/Akt signaling. *Oncogene,* 27(39)**,** pp 5182-5194.

Chen, X., Bahrami, A., Pappo, A., Easton, J., Dalton, J., Hedlund, E., Ellison, D., Shurtleff, S., Wu, G., Wei, L., Parker, M., Rusch, M., Nagahawatte, P., Wu, J., Mao, S., Boggs, K., Mulder, H., Yergeau, D., Lu, C., Ding, L., Edmonson, M., Qu, C., Wang, J., Li, Y., Navid, F., Daw, N. C., Mardis, E. R., Wilson, R. K., Downing, J. R., Zhang, J. & Dyer, M. A. 2014. Recurrent somatic structural variations contribute to tumorigenesis in pediatric osteosarcoma. *Cell Rep,* 7(1)**,** pp 104-12.

Chung, E. B. & Enzinger, F. M. 1987. Extraskeletal osteosarcoma. *Cancer,* 60(5)**,** pp 1132-42.

Clausen, T. M., Pereira, M. A., Al Nakouzi, N., Oo, H. Z., Agerbaek, M. O., Lee, S., Orum-Madsen, M. S., Kristensen, A. R., El-Naggar, A., Grandgenett, P. M., Grem, J. L., Hollingsworth, M. A., Holst, P. J., Theander, T., Sorensen, P. H., Daugaard, M. & Salanti, A. 2016. Oncofetal Chondroitin Sulfate Glycosaminoglycans Are Key Players in Integrin Signaling and Tumor Cell Motility. *Mol Cancer Res,* 14(12)**,** pp 1288-1299.

Cooney, C. A., Jousheghany, F., Yao-Borengasser, A., Phanavanh, B., Gomes, T., Kieber-Emmons, A. M., Siegel, E. R., Suva, L. J., Ferrone, S., Kieber-Emmons, T. & Monzavi-Karbassi, B. 2011. Chondroitin sulfates play a major role in breast cancer metastasis: a role for CSPG4 and CHST11 gene expression in forming surface P-selectin ligands in aggressive breast cancer cells. *Breast Cancer Res,* 13(3)**,** pp R58.

Dallatomasina A. 2017. Structural and Functional Traits of NG2/CSPG4 Proteoglycan in Relation to its Role in Tumours. Masters thesis. University of Parma (2017)

de Bruyn, M., Rybczynska, A. A., Wei, Y., Schwenkert, M., Fey, G. H., Dierckx, R. A., van Waarde, A., Helfrich, W. & Bremer, E. 2010. Melanoma-associated Chondroitin Sulfate Proteoglycan (MCSP)-targeted delivery of soluble TRAIL potently inhibits melanoma outgrowth in vitro and in vivo. *Mol Cancer,* 9(301.

de Castro, R., Jr., Tajrishi, R., Claros, J. & Stallcup, W. B. 2005. Differential responses of spinal axons to transection: influence of the NG2 proteoglycan. *Exp Neurol,* 192(2)**,** pp 299-309.

de Souza, L. E., Malta, T. M., Kashima Haddad, S. & Covas, D. T. 2016. Mesenchymal Stem Cells and Pericytes: To What Extent Are They Related? *Stem Cells Dev,* 25(24)**,** pp 1843-1852.

Diamantis, N. & Banerji, U. 2016. Antibody-drug conjugates--an emerging class of cancer treatment. *Br J Cancer,* 114(4)**,** pp 362-7.

Dorfman, H. D. & Czerniak, B. 1995. Bone cancers. *Cancer,* 75(1 Suppl)**,** pp 203-10.

Durfee, R. A., Mohammed, M. & Luu, H. H. 2016. Review of Osteosarcoma and Current Management. *Rheumatol Ther.*

Eisenmann, K. M., McCarthy, J. B., Simpson, M. A., Keely, P. J., Guan, J. L., Tachibana, K., Lim, L., Manser, E., Furcht, L. T. & Iida, J. 1999. Melanoma chondroitin sulphate proteoglycan regulates cell spreading through Cdc42, Ack-1 and p130cas. *Nat Cell Biol,* 1(8)**,** pp 507-13.

Elenjord, R., Allen, J. B., Johansen, H. T., Kildalsen, H., Svineng, G., Maelandsmo, G. M., Loennechen, T. & Winberg, J. O. 2009. Collagen I regulates matrix metalloproteinase-2 activation in osteosarcoma cells independent of S100A4. *Febs j,* 276(18)**,** pp 5275-86.

Engin, F., Bertin, T., Ma, O., Jiang, M. M., Wang, L., Sutton, R. E., Donehower, L. A. & Lee, B. 2009. Notch signaling contributes to the pathogenesis of human osteosarcomas. *Hum Mol Genet,* 18(8)**,** pp 1464-70.

Fang, X., Burg, M. A., Barritt, D., Dahlin-Huppe, K., Nishiyama, A. & Stallcup, W. B. 1999. Cytoskeletal reorganization induced by engagement of the NG2 proteoglycan leads to cell spreading and migration. *Mol Biol Cell,* 10(10)**,** pp 3373-87.

Fernanda Amary, M., Ye, H., Berisha, F., Khatri, B., Forbes, G., Lehovsky, K., Frezza, A. M., Behjati, S., Tarpey, P., Pillay, N., Campbell, P. J., Tirabosco, R., Presneau, N., Strauss, S. J. & Flanagan, A. M. 2014. Fibroblastic growth factor receptor 1 amplification in osteosarcoma is associated with poor response to neo-adjuvant chemotherapy. *Cancer Med,* 3(4)**,** pp 980-7.

Fernandes, R. J., Harkey, M. A., Weis, M., Askew, J. W. & Eyre, D. R. 2007. The Post-Translational Phenotype of Collagen Synthesized by Saos-2 Osteosarcoma Cells. *Bone,* 40(5)**,** pp 1343-51.

Fukushi, J., Inatani, M., Yamaguchi, Y. & Stallcup, W. B. 2003. Expression of NG2 proteoglycan during endochondral and intramembranous ossification. *Dev Dyn,* 228(1)**,** pp 143-8.

Fukushi, J., Makagiansar, I. T. & Stallcup, W. B. 2004. NG2 proteoglycan promotes endothelial cell motility and angiogenesis via engagement of galectin-3 and alpha3beta1 integrin. *Mol Biol Cell,* 15(8)**,** pp 3580-90.

Geldres, C., Savoldo, B., Hoyos, V., Caruana, I., Zhang, M., Yvon, E., Del Vecchio, M., Creighton, C. J., Ittmann, M., Ferrone, S. & Dotti, G. 2014. T lymphocytes redirected against the chondroitin sulfate proteoglycan-4 control the growth of multiple solid tumors both in vitro and in vivo. *Clin Cancer Res,* 20(4)**,** pp 962-71.

Ghali, L., Wong, S. T., Tidman, N., Quinn, A., Philpott, M. P. & Leigh, I. M. 2004. Epidermal and hair follicle progenitor cells express melanoma-associated chondroitin sulfate proteoglycan core protein. *Journal of Investigative Dermatology,* 122(2)**,** pp 433-442.

Ghose, T., Ferrone, S., Blair, A. H., Kralovec, Y., Temponi, M., Singh, M. & Mammen, M. 1991. Regression of human melanoma xenografts in nude mice injected with methotrexate linked to monoclonal antibody 225.28 to human high molecular weight-melanoma associated antigen. *Cancer Immunol Immunother,* 34(2)**,** pp 90-6.

Gianferante, D. M., Mirabello, L. & Savage, S. A. 2017. Germline and somatic genetics of osteosarcoma - connecting aetiology, biology and therapy. *Nat Rev Endocrinol,* 13(8)**,** pp 480-491.

Girolamo, F., Dallatomasina, A., Rizzi, M., Errede, M., Walchli, T., Mucignat, M. T., Frei, K., Roncali, L., Perris, R. & Virgintino, D. 2013. Diversified expression of NG2/CSPG4 isoforms in glioblastoma and human foetal brain identifies pericyte subsets. *PLoS One,* 8(12)**,** pp e84883.

Goretzki, L., Burg, M. A., Grako, K. A. & Stallcup, W. B. 1999. High-affinity binding of basic fibroblast growth factor and platelet-derived growth factor-AA to the core protein of the NG2 proteoglycan. *J Biol Chem,* 274(24)**,** pp 16831-7.

Goretzki, L., Lombardo, C. R. & Stallcup, W. B. 2000. Binding of the NG2 proteoglycan to kringle domains modulates the functional properties of angiostatin and plasmin(ogen). *J Biol Chem,* 275(37)**,** pp 28625-33.

Gorlick, R. 2009. Current concepts on the molecular biology of osteosarcoma. *Cancer Treat Res,* 152(467-78.

Goto, M., Miller, R. W., Ishikawa, Y. & Sugano, H. 1996. Excess of rare cancers in Werner syndrome (adult progeria). *Cancer Epidemiol Biomarkers Prev,* 5(4)**,** pp 239-46.

Grako, K. A., Ochiya, T., Barritt, D., Nishiyama, A. & Stallcup, W. B. 1999. PDGF (alpha)-receptor is unresponsive to PDGF-AA in aortic smooth muscle cells from the NG2 knockout mouse. *J Cell Sci,* 112 (Pt 6)(905-15.

Grako, K. A. & Stallcup, W. B. 1995. Participation of the NG2 proteoglycan in rat aortic smooth muscle cell responses to platelet-derived growth factor. *Exp Cell Res,* 221(1)**,** pp 231-40.

Guadamillas, M. C., Cerezo, A. & Del Pozo, M. A. 2011. Overcoming anoikis--pathways to anchorage-independent growth in cancer. *J Cell Sci,* 124(Pt 19)**,** pp 3189-97.

Guan, Y. Y., Luan, X., Xu, J. R., Liu, Y. R., Lu, Q., Wang, C., Liu, H. J., Gao, Y. G., Chen, H. Z. & Fang, C. 2014. Selective eradication of tumor vascular pericytes by peptide-conjugated nanoparticles for antiangiogenic therapy of melanoma lung metastasis. *Biomaterials,* 35(9)**,** pp 3060-70.

Guimaraes-Camboa, N., Cattaneo, P., Sun, Y., Moore-Morris, T., Gu, Y., Dalton, N. D., Rockenstein, E., Masliah, E., Peterson, K. L., Stallcup, W. B., Chen, J. & Evans, S. M. 2017. Pericytes of Multiple Organs Do Not Behave as Mesenchymal Stem Cells In Vivo. *Cell Stem Cell,* 20(3)**,** pp 345-359.e5.

Harbour, J. W. & Dean, D. C. 2000. Rb function in cell-cycle regulation and apoptosis. *Nat Cell Biol,* 2(4)**,** pp E65-7.

Harper, J. R. & Reisfeld, R. A. 1983. Inhibition of anchorage-independent growth of human melanoma cells by a monoclonal antibody to a chondroitin sulfate proteoglycan. *J Natl Cancer Inst,* 71(2)**,** pp 259-63.

Hassan, S. E., Bekarev, M., Kim, M. Y., Lin, J., Piperdi, S., Gorlick, R. & Geller, D. S. 2012. Cell surface receptor expression patterns in osteosarcoma. *Cancer,* 118(3)**,** pp 740-9.

Hattinger, C. M., Fanelli, M., Tavanti, E., Vella, S., Ferrari, S., Picci, P. & Serra, M. 2015. Advances in emerging drugs for osteosarcoma. *Expert Opin Emerg Drugs,* 20(3)**,** pp 495-514.

He, H., Ni, J. & Huang, J. 2014. Molecular mechanisms of chemoresistance in osteosarcoma (Review). *Oncol Lett.*

He, M. L., Wu, Y., Zhao, J. M., Wang, Z. & Chen, Y. B. 2013. PIK3CA and AKT gene polymorphisms in susceptibility to osteosarcoma in a Chinese population. *Asian Pac J Cancer Prev,* 14(9)**,** pp 5117-22.

Henderson, T. O., Whitton, J., Stovall, M., Mertens, A. C., Mitby, P., Friedman, D., Strong, L. C., Hammond, S., Neglia, J. P., Meadows, A. T., Robison, L. & Diller, L. 2007. Secondary sarcomas in childhood cancer survivors: a report from the Childhood Cancer Survivor Study. *J Natl Cancer Inst,* 99(4)**,** pp 300-8.

Hjortland, G. O., Garman-Vik, S. S., Juell, S., Olsen, O. E., Hirschberg, H., Fodstad, O. & Engebraaten, O. 2004. Immunotoxin treatment targeted to the high-molecular-weight melanoma-associated antigen prolonging the survival of immunodeficient rats with invasive intracranial human glioblastoma multiforme. *J Neurosurg,* 100(2)**,** pp 320-7.

Hsu S.H.C, Nadesan P, Puviindran V, Stallcup W.B., Kirsch D.G. & Alman B.A. 2018. Effects of chondroitin sulfate proteoglycan 4 (NG2/CSPG4) on soft-tissue sarcoma growth depend on tumor developmental stage. J. Biol. Chem. 2018 293: 2466-. doi:10.1074/jbc.M117.805051

Iida, J., Pei, D., Kang, T., Simpson, M. A., Herlyn, M., Furcht, L. T. & McCarthy, J. B. 2001. Melanoma chondroitin sulfate proteoglycan regulates matrix metalloproteinase-dependent human melanoma invasion into type I collagen. *J Biol Chem,* 276(22)**,** pp 18786-94.

Iida, J., Skubitz, A. P., Furcht, L. T., Wayner, E. A. & McCarthy, J. B. 1992. Coordinate role for cell surface chondroitin sulfate proteoglycan and alpha 4 beta 1 integrin in mediating melanoma cell adhesion to fibronectin. *J Cell Biol,* 118(2)**,** pp 431-44.

Iida, J., Wilhelmson, K. L., Ng, J., Lee, P., Morrison, C., Tam, E., Overall, C. M. & McCarthy, J. B. 2007. Cell surface chondroitin sulfate glycosaminoglycan in melanoma: role in the activation of pro-MMP-2 (pro-gelatinase A). *Biochem J,* 403(3)**,** pp 553-63.

Jamil, N. S., Azfer, A., Worrell, H. & Salter, D. M. 2016. Functional roles of CSPG4/NG2 in chondrosarcoma. *Int J Exp Pathol,* 97(2)**,** pp 178-86.

Javaid, S., Terai, K. & Dudek, A. Z. 2015. Chondroitin sulfate proteoglycan-4 does not protect melanoma cells during inhibition of PI3K and mTOR pathways. *Anticancer Res,* 35(3)**,** pp 1279-84.

Jones, L. L., Yamaguchi, Y., Stallcup, W. B. & Tuszynski, M. H. 2002. NG2 is a major chondroitin sulfate proteoglycan produced after spinal cord injury and is expressed by macrophages and oligodendrocyte progenitors. *J Neurosci,* 22(7)**,** pp 2792-803.

Joo, N. E., Watanabe, T., Chen, C., Chekenya, M., Stallcup, W. B. & Kapila, Y. L. 2008. NG2, a novel proapoptotic receptor, opposes integrin alpha4 to mediate anoikis through PKCalpha-dependent suppression of FAK phosphorylation. *Cell Death Differ,* 15(5)**,** pp 899-907.

Kadoya, K., Fukushi, J., Matsumoto, Y., Yamaguchi, Y. & Stallcup, W. B. 2008. NG2 Proteoglycan Expression in Mouse Skin: Altered Postnatal Skin Development in the NG2 Null Mouse. *J Histochem Cytochem.*

Keleg, S., Titov, A., Heller, A., Giese, T., Tjaden, C., Ahmad, S. S., Gaida, M. M., Bauer, A. S., Werner, J. & Giese, N. A. 2014. Chondroitin sulfate proteoglycan CSPG4 as a novel hypoxia-sensitive marker in pancreatic tumors. *PLoS One,* 9(6)**,** pp e100178.

Kelly-Goss, M. R., Sweat, R. S., Stapor, P. C., Peirce, S. M. & Murfee, W. L. 2014. Targeting pericytes for angiogenic therapies. *Microcirculation,* 21(4)**,** pp 345-57.

Keskin, D., Kim, J., Cooke, V. G., Wu, C. C., Sugimoto, H., Gu, C., De Palma, M., Kalluri, R. & LeBleu, V. S. 2015. Targeting vascular pericytes in hypoxic tumors increases lung metastasis via angiopoietin-2. *Cell Rep,* 10(7)**,** pp 1066-81.

Khanna, C., Wan, X., Bose, S., Cassaday, R., Olomu, O., Mendoza, A., Yeung, C., Gorlick, R., Hewitt, S. M. & Helman, L. J. 2004. The membrane-cytoskeleton linker ezrin is necessary for osteosarcoma metastasis. *Nat Med,* 10(2)**,** pp 182-6.

Klein, M. J. & Siegal, G. P. 2006. Osteosarcoma: anatomic and histologic variants. *Am J Clin Pathol,* 125(4)**,** pp 555-81.

Kleinerman, R. A., Schonfeld, S. J. & Tucker, M. A. 2012. Sarcomas in hereditary retinoblastoma. *Clin Sarcoma Res.*

Kohara, Y., Soeta, S., Izu, Y., Arai, K. & Amasaki, H. 2016. Distribution of type VI collagen in association with osteoblast lineages in the groove of Ranvier during rat postnatal development. *Ann Anat,* 208(58-68.

Kubo, T., Piperdi, S., Rosenblum, J., Antonescu, C. R., Chen, W., Kim, H. S., Huvos, A. G., Sowers, R., Meyers, P. A., Healey, J. H. & Gorlick, R. 2008. Platelet-derived growth

factor receptor as a prognostic marker and a therapeutic target for imatinib mesylate therapy in osteosarcoma. *Cancer,* 112(10)**,** pp 2119-29.

Kundu, Z. S. 2014. Classification, imaging, biopsy and staging of osteosarcoma. *Indian J Orthop,* 48(3)**,** pp 238-46.

Laplante, M. & Sabatini, D. M. 2012. mTOR signaling in growth control and disease. *Cell,* 149(2)**,** pp 274-93.

Le Vu, B., de Vathaire, F., Shamsaldin, A., Hawkins, M. M., Grimaud, E., Hardiman, C., Diallo, I., Vassal, G., Bessa, E., Campbell, S., Panis, X., Daly-Schveitzer, N., Lagrange, J. L., Zucker, J. M., Eschwege, F., Chavaudra, J. & Lemerle, J. 1998. Radiation dose, chemotherapy and risk of osteosarcoma after solid tumours during childhood. *Int J Cancer,* 77(3)**,** pp 370-7.

Legg, J., Jensen, U. B., Broad, S., Leigh, I. & Watt, F. M. 2003. Role of melanoma chondroitin sulphate proteoglycan in patterning stem cells in human interfollicular epidermis. *Development,* 130(24)**,** pp 6049-63.

Li, H., Min, D., Zhao, H., Wang, Z., Qi, W., Zheng, S., Tang, L., He, A., Sun, Y., Yao, Y. & Shen, Z. 2013. The Prognostic Role of Ezrin Immunoexpression in Osteosarcoma: A Meta-Analysis of Published Data. *PLoS One.*

Lin, C. H., Guo, Y., Ghaffar, S., McQueen, P., Pourmorady, J., Christ, A., Rooney, K., Ji, T., Eskander, R., Zi, X. & Hoang, B. H. 2013. Dkk-3, a secreted wnt antagonist, suppresses tumorigenic potential and pulmonary metastasis in osteosarcoma. *Sarcoma,* 2013(147541.

Lin, X. H., Dahlin-Huppe, K. & Stallcup, W. B. 1996a. Interaction of the NG2 proteoglycan with the actin cytoskeleton. *J Cell Biochem,* 63(4)**,** pp 463-77.

Lin, X. H., Grako, K. A., Burg, M. A. & Stallcup, W. B. 1996b. NG2 proteoglycan and the actin-binding protein fascin define separate populations of actin-containing filopodia and lamellipodia during cell spreading and migration. *Mol Biol Cell,* 7(12)**,** pp 1977-93.

Liu, A., Han, Y. R., Li, J., Sun, D., Ouyang, M., Plummer, M. R. & Casaccia-Bonnefil, P. 2007. The Glial or Neuronal Fate Choice of Oligodendrocyte Progenitors Is Modulated by Their Ability to Acquire an Epigenetic Memory. *J Neurosci,* 27(27)**,** pp 7339-43.

Liu, J. J., Liu, S., Wang, J. G., Zhu, W., Hua, Y. Q., Sun, W. & Cai, Z. D. 2013. Telangiectatic osteosarcoma: a review of literature. *Onco Targets Ther,* 6(593-602.

Lohmann, D. 2010. Retinoblastoma. *Adv Exp Med Biol,* 685(220-7.

Longhi, A., Barbieri, E., Fabbri, N., Macchiagodena, M., Favale, L., Lippo, C., Salducca, N. & Bacci, G. 2003. Radiation-induced osteosarcoma arising 20 years after the treatment of Ewing's sarcoma. *Tumori,* 89(5)**,** pp 569-72.

Longhi, A., Pasini, A., Cicognani, A., Baronio, F., Pellacani, A., Baldini, N. & Bacci, G. 2005. Height as a risk factor for osteosarcoma. *J Pediatr Hematol Oncol,* 27(6)**,** pp 314-8.

Lu, L. L., Sun, J., Lai, J. J., Jiang, Y., Bai, L. H. & Zhang, L. D. 2015. Neuron-glial antigen 2 overexpression in hepatocellular carcinoma predicts poor prognosis. *World J Gastroenterol,* 21(21)**,** pp 6649-59.

Luetke, A., Meyers, P. A., Lewis, I. & Juergens, H. 2014. Osteosarcoma treatment - where do we stand? A state of the art review. *Cancer Treat Rev,* 40(4)**,** pp 523-32.

Lugowska, I., Mierzejewska, E., Lenarcik, M., Klepacka, T., Koch, I., Michalak, E. & Szamotulska, K. 2016. The clinical significance of changes in ezrin expression in osteosarcoma of children and young adults. *Tumour Biol,* 37(9)**,** pp 12071-12078.

Lun, D. X., Hu, Y. C., Xu, Z. W., Xu, L. N. & Wang, B. W. 2014. The prognostic value of elevated ezrin in patients with osteosarcoma. *Tumour Biol,* 35(2)**,** pp 1263-6.

Luu, H. H., Kang, Q., Park, J. K., Si, W., Luo, Q., Jiang, W., Yin, H., Montag, A. G., Simon, M. A., Peabody, T. D., Haydon, R. C., Rinker-Schaeffer, C. W. & He, T. C. 2005. An orthotopic model of human osteosarcoma growth and spontaneous pulmonary metastasis. *Clin Exp Metastasis,* 22(4)**,** pp 319-29.

Ma, Y., Ren, Y., Han, E. Q., Li, H., Chen, D., Jacobs, J. J., Gitelis, S., O'Keefe, R. J., Konttinen, Y. T., Yin, G. & Li, T. F. 2013. Inhibition of the Wnt-beta-catenin and Notch signaling pathways sensitizes osteosarcoma cells to chemotherapy. *Biochem Biophys Res Commun,* 431(2)**,** pp 274-9.

Maciag, P. C., Seavey, M., Pan, Z. K., Ferrone, S. & Paterson, Y. 2008. Cancer immunotherapy targeting the HMW-MAA protein results in a broad antitumor response and reduction of pericytes in the tumor vasculature. *Cancer Res,* 68(19)**,** pp 8066-75.

Majumdar, M., Vuori, K. & Stallcup, W. B. 2003. Engagement of the NG2 proteoglycan triggers cell spreading via rac and p130cas. *Cell Signal,* 15(1)**,** pp 79-84.

Makagiansar, I. T., Williams, S., Mustelin, T. & Stallcup, W. B. 2007. Differential phosphorylation of NG2 proteoglycan by ERK and PKCalpha helps balance cell proliferation and migration. *J Cell Biol,* 178(1)**,** pp 155-65.

Martin, J. W., Squire, J. A. & Zielenska, M. 2012. The genetics of osteosarcoma. *Sarcoma,* 2012(627254.

Matsuno, T., Unni, K. K., McLeod, R. A. & Dahlin, D. C. 1976. Telangiectatic osteogenic sarcoma. *Cancer,* 38(6)**,** pp 2538-47.

Maus, F., Sakry, D., Biname, F., Karram, K., Rajalingam, K., Watts, C., Heywood, R., Kruger, R., Stegmuller, J., Werner, H. B., Nave, K. A., Kramer-Albers, E. M. & Trotter, J. 2015. The NG2 Proteoglycan Protects Oligodendrocyte Precursor Cells against Oxidative Stress via Interaction with OMI/HtrA2. *PLoS One,* 10(9)**,** pp e0137311.

Mauvieux, L., Delabesse, E., Bourquelot, P., Radford-Weiss, I., Bennaceur, A., Flandrin, G., Valensi, F. & MacIntyre, E. A. 1999. NG2 expression in MLL rearranged acute myeloid leukaemia is restricted to monoblastic cases. *Br J Haematol,* 107(3)**,** pp 674-6.

McGary, E. C., Weber, K., Mills, L., Doucet, M., Lewis, V., Lev, D. C., Fidler, I. J. & Bar-Eli, M. 2002. Inhibition of platelet-derived growth factor-mediated proliferation of osteosarcoma cells by the novel tyrosine kinase inhibitor STI571. *Clin Cancer Res,* 8(11)**,** pp 3584-91.

McGrath, J. L. 2007. Cell spreading: the power to simplify. *Curr Biol,* 17(10)**,** pp R357-8.

McManus, M. M., Weiss, K. R. & Hughes, D. P. 2014. Understanding the role of Notch in osteosarcoma. *Adv Exp Med Biol,* 804(67-92.

Michalska, M. & Wolf, P. 2015. Pseudomonas Exotoxin A: optimized by evolution for effective killing. *Front Microbiol,* 6(

Midwood, K. S. & Salter, D. M. 1998. Expression of NG2/human melanoma proteoglycan in human adult articular chondrocytes. *Osteoarthritis and Cartilage,* 6(5)**,** pp 297-305.

Midwood, K. S. & Salter, D. M. 2001. NG2/HMPG modulation of human articular chondrocyte adhesion to type VI collagen is lost in osteoarthritis. *J Pathol,* 195(5)**,** pp 631-5.

Miller, B. J., Cram, P., Lynch, C. F. & Buckwalter, J. A. 2013. Risk factors for metastatic disease at presentation with osteosarcoma: an analysis of the SEER database. *J Bone Joint Surg Am,* 95(13)**,** pp e89.

Miller, R. H. & Raff, M. C. 1984. Fibrous and protoplasmic astrocytes are biochemically and developmentally distinct. *J Neurosci,* 4(2)**,** pp 585-92.

Miller, R. W. 1981. Contrasting epidemiology of childhood osteosarcoma, Ewing's tumor, and rhabdomyosarcoma. *Natl Cancer Inst Monogr,* 56)**,** pp 9-15.

Mirabello, L., Troisi, R. J. & Savage, S. A. 2009. Osteosarcoma incidence and survival rates from 1973 to 2004: data from the Surveillance, Epidemiology, and End Results Program. *Cancer,* 115(7)**,** pp 1531-43.

Mittelman, A., Chen, G. Z., Wong, G. Y., Liu, C., Hirai, S. & Ferrone, S. 1995. Human high molecular weight-melanoma associated antigen mimicry by mouse anti-idiotypic monoclonal antibody MK2-23: modulation of the immunogenicity in patients with malignant melanoma. *Clin Cancer Res,* 1(7)**,** pp 705-13.

Mittelman, A., Chen, Z. J., Liu, C. C., Hirai, S. & Ferrone, S. 1994. Kinetics of the immune response and regression of metastatic lesions following development of humoral anti-high molecular weight-melanoma associated antigen immunity in three patients with advanced malignant melanoma immunized with mouse antiidiotypic monoclonal antibody MK2-23. *Cancer Res,* 54(2)**,** pp 415-21.

Mittelman, A., Chen, Z. J., Yang, H., Wong, G. Y. & Ferrone, S. 1992. Human high molecular weight melanoma-associated antigen (HMW-MAA) mimicry by mouse anti-idiotypic monoclonal antibody MK2-23: induction of humoral anti-HMW-MAA immunity and prolongation of survival in patients with stage IV melanoma. *Proc Natl Acad Sci U S A,* 89(2)**,** pp 466-70.

Mori, S., Chang, J. T., Andrechek, E. R., Matsumura, N., Baba, T., Yao, G., Kim, J. W., Gatza, M., Murphy, S. & Nevins, J. R. 2009. An Anchorage-Independent Cell Growth Signature Identifies Tumors with Metastatic Potential. *Oncogene,* 28(31)**,** pp 2796-805.

Mu, X., Isaac, C., Greco, N., Huard, J. & Weiss, K. 2013. Notch Signaling is Associated with ALDH Activity and an Aggressive Metastatic Phenotype in Murine Osteosarcoma Cells. *Front Oncol,* 3(143.

Muff, R., Rath, P., Ram Kumar, R. M., Husmann, K., Born, W., Baudis, M. & Fuchs, B. 2015. Genomic instability of osteosarcoma cell lines in culture: impact on the prediction of metastasis relevant genes. *PLoS One,* 10(5)**,** pp e0125611.

Mutsaers, A. J. & Walkley, C. R. 2014. Cells of origin in osteosarcoma: mesenchymal stem cells or osteoblast committed cells? *Bone,* 62(56-63.

Mödder, U. I., Oursler, M. J., Khosla, S. & Monroe, D. G. 2011. Wnt10b Activates the Wnt, Notch and NFκB Pathways in U2OS Osteosarcoma Cells. *J Cell Biochem,* 112(5)**,** pp 1392-402.

Na, K. Y., Bacchini, P., Bertoni, F., Kim, Y. W. & Park, Y. K. 2012. Syndecan-4 and fibronectin in osteosarcoma. *Pathology,* 44(4)**,** pp 325-30.

Nakajima, H., Sim, F. H., Bond, J. R. & Unni, K. K. 1997. Small cell osteosarcoma of bone. Review of 72 cases. *Cancer,* 79(11)**,** pp 2095-106.

Newton, W. A., Jr., Meadows, A. T., Shimada, H., Bunin, G. R. & Vawter, G. F. 1991. Bone sarcomas as second malignant neoplasms following childhood cancer. *Cancer,* 67(1)**,** pp 193-201.

Nicolosi, P. A., Dallatomasina, A. & Perris, R. 2015. Theranostic Impact of NG2/CSPG4 Proteoglycan in Cancer. *Theranostics.*

Nishiyama, A., Dahlin, K. J., Prince, J. T., Johnstone, S. R. & Stallcup, W. B. 1991a. The primary structure of NG2, a novel membrane-spanning proteoglycan. *J Cell Biol,* 114(2)**,** pp 359-71.

Nishiyama, A., Dahlin, K. J. & Stallcup, W. B. 1991b. The expression of NG2 proteoglycan in the developing rat limb. *Development,* 111(4)**,** pp 933-44.

Nishiyama, A., Komitova, M., Suzuki, R. & Zhu, X. 2009. Polydendrocytes (NG2 cells): multifunctional cells with lineage plasticity. *Nat Rev Neurosci,* 10(1)**,** pp 9-22.

Nishiyama, A., Lin, X. H., Giese, N., Heldin, C. H. & Stallcup, W. B. 1996. Interaction between NG2 proteoglycan and PDGF alpha-receptor on O2A progenitor cells is required for optimal response to PDGF. *J Neurosci Res,* 43(3)**,** pp 315-30.

Nishiyama, A., Lin, X. H. & Stallcup, W. B. 1995. Generation of truncated forms of the NG2 proteoglycan by cell surface proteolysis. *Mol Biol Cell,* 6(12)**,** pp 1819-32.

Nishiyama, A. & Stallcup, W. B. 1993. Expression of NG2 proteoglycan causes retention of type VI collagen on the cell surface. *Mol Biol Cell,* 4(11)**,** pp 1097-108.

Nishiyama, A., Watanabe, M., Yang, Z. & Bu, J. 2002. Identity, distribution, and development of polydendrocytes: NG2-expressing glial cells. *J Neurocytol,* 31(6-7)**,** pp 437-55.

Niyibizi, C. & Eyre, D. R. 1989a. Bone type V collagen: chain composition and location of a trypsin cleavage site. *Connect Tissue Res,* 20(1-4)**,** pp 247-50.

Niyibizi, C. & Eyre, D. R. 1989b. Identification of the cartilage alpha 1(XI) chain in type V collagen from bovine bone. *FEBS Lett,* 242(2)**,** pp 314-8.

Onda, M., Wang, Q. C., Guo, H. F., Cheung, N. K. & Pastan, I. 2004. In vitro and in vivo cytotoxic activities of recombinant immunotoxin 8H9(Fv)-PE38 against breast cancer, osteosarcoma, and neuroblastoma. *Cancer Res,* 64(4)**,** pp 1419-24.

Ottaviani, G. & Jaffe, N. 2009. The epidemiology of osteosarcoma. *Cancer Treat Res,* 152(3-13.

Ozerdem, U., Grako, K. A., Dahlin-Huppe, K., Monosov, E. & Stallcup, W. B. 2001. NG2 proteoglycan is expressed exclusively by mural cells during vascular morphogenesis. *Dev Dyn,* 222(2)**,** pp 218-27.

Ozerdem, U., Monosov, E. & Stallcup, W. B. 2002. NG2 proteoglycan expression by pericytes in pathological microvasculature. *Microvasc Res,* 63(1)**,** pp 129-34.

Paoli, P., Giannoni, E. & Chiarugi, P. 2013. Anoikis molecular pathways and its role in cancer progression. *Biochim Biophys Acta,* 1833(12)**,** pp 3481-98.

Paulino, A. C. & Fowler, B. Z. 2005. Secondary neoplasms after radiotherapy for a childhood solid tumor. *Pediatr Hematol Oncol,* 22(2)**,** pp 89-101.

Pautke, C., Schieker, M., Tischer, T., Kolk, A., Neth, P., Mutschler, W. & Milz, S. 2004. Characterization of osteosarcoma cell lines MG-63, Saos-2 and U-2 OS in comparison to human osteoblasts. *Anticancer Res,* 24(6)**,** pp 3743-8.

Perry, J. A., Kiezun, A., Tonzi, P., Van Allen, E. M., Carter, S. L., Baca, S. C., Cowley, G. S., Bhatt, A. S., Rheinbay, E., Pedamallu, C. S., Helman, E., Taylor-Weiner, A., McKenna, A., DeLuca, D. S., Lawrence, M. S., Ambrogio, L., Sougnez, C., Sivachenko, A., Walensky, L. D., Wagle, N., Mora, J., de Torres, C., Lavarino, C., Dos Santos Aguiar, S., Yunes, J. A., Brandalise, S. R., Mercado-Celis, G. E., Melendez-Zajgla, J., Cardenas-Cardos, R.,

Velasco-Hidalgo, L., Roberts, C. W., Garraway, L. A., Rodriguez-Galindo, C., Gabriel, S. B., Lander, E. S., Golub, T. R., Orkin, S. H., Getz, G. & Janeway, K. A. 2014. Complementary genomic approaches highlight the PI3K/mTOR pathway as a common vulnerability in osteosarcoma. *Proc Natl Acad Sci U S A,* 111(51)**,** pp E5564-73.

Petrovici, K., Graf, M., Hecht, K., Reif, S., Pfister, K. & Schmetzer, H. 2010. Use of NG2 (7.1) in AML as a tumor marker and its association with a poor prognosis. *Cancer Genomics Proteomics,* 7(4)**,** pp 173-80.

Picci, P. 2007. Osteosarcoma (Osteogenic sarcoma). *Orphanet Journal of Rare Diseases*. Volume 2, Number 1, p1

Pluschke, G., Vanek, M., Evans, A., Dittmar, T., Schmid, P., Itin, P., Filardo, E. J. & Reisfeld, R. A. 1996. Molecular cloning of a human melanoma-associated chondroitin sulfate proteoglycan. *Proc Natl Acad Sci U S A,* 93(18)**,** pp 9710-5.

Poli, A., Wang, J., Domingues, O., Planaguma, J., Yan, T., Rygh, C. B., Skaftnesmo, K. O., Thorsen, F., McCormack, E., Hentges, F., Pedersen, P. H., Zimmer, J., Enger, P. O. & Chekenya, M. 2013a. Targeting glioblastoma with NK cells and mAb against NG2/CSPG4 prolongs animal survival. *Oncotarget,* 4(9)**,** pp 1527-46.

Poli, A., Wang, J., Domingues, O., Planagumà, J., Yan, T., Rygh, C. B., Skaftnesmo, K. O., Thorsen, F., McCormack, E., Hentges, F., Pedersen, P. H., Zimmer, J., Enger, P. & Chekenya, M. 2013b. Targeting glioblastoma with NK cells and mAb against NG2/CSPG4 prolongs animal survival. *Oncotarget,* 4(9)**,** pp 1527-46.

Poos, K., Smida, J., Maugg, D., Eckstein, G., Baumhoer, D., Nathrath, M. & Korsching, E. 2015. Genomic heterogeneity of osteosarcoma - shift from single candidates to functional modules. *PLoS One,* 10(4)**,** pp e0123082.

Price, M. A., Wanshura, L. E. C., Yang, J., Carlson, J., Xiang, B., Li, G., Ferrone, S., Dudek, A. Z., Turley, E. A. & McCarthy, J. B. 2011. CSPG4, a potential therapeutic target, facilitates malignant progression of melanoma. *Pigment Cell Melanoma Res,* 24(6)**,** pp 1148-57.

Risberg, K., Fodstad, O. & Andersson, Y. 2009. The melanoma specific 9.2.27PE immunotoxin efficiently kills melanoma cells in vitro. *Int J Cancer,* 125(1)**,** pp 23-33.

Risberg, K., Fodstad, O. & Andersson, Y. 2010. Anti-melanoma activity of the 9.2.27PE immunotoxin in dacarbazine resistant cells. *J Immunother,* 33(3)**,** pp 272-8.

Rivera, Z., Ferrone, S., Wang, X., Jube, S., Yang, H., Pass, H., Kanodia, S., Gaudino, G. & Carbone, M. 2012. CSPG4 As a Target of Antibody-Based Immunotherapy For Malignant Mesothelioma. *Clin Cancer Res,* 18(19)**,** pp 5352-63.

Rizvi, S. M., Qu, C. F., Song, Y. J., Raja, C. & Allen, B. J. 2005. In vivo studies of pharmacokinetics and efficacy of Bismuth-213 labeled antimelanoma monoclonal antibody 9.2.27. *Cancer Biol Ther,* 4(7)**,** pp 763-8.

Rosenberg, Z. S., Lev, S., Schmahmann, S., Steiner, G. C., Beltran, J. & Present, D. 1995. Osteosarcoma: subtle, rare, and misleading plain film features. *AJR Am J Roentgenol,* 165(5)**,** pp 1209-14.

Salanti, A., Clausen, T. M., Agerbaek, M. O., Al Nakouzi, N., Dahlback, M., Oo, H. Z., Lee, S., Gustavsson, T., Rich, J. R., Hedberg, B. J., Mao, Y., Barington, L., Pereira, M. A., LoBello, J., Endo, M., Fazli, L., Soden, J., Wang, C. K., Sander, A. F., Dagil, R., Thrane, S., Holst, P. J., Meng, L., Favero, F., Weiss, G. J., Nielsen, M. A., Freeth, J., Nielsen, T. O., Zaia, J., Tran, N. L., Trent, J., Babcook, J. S., Theander, T. G., Sorensen, P. H. & Daugaard, M. 2015. Targeting Human Cancer by a Glycosaminoglycan Binding Malaria Protein. *Cancer Cell,* 28(4)**,** pp 500-14.

Sanz, M. M., German, J. & Cunniff, C. 2016. Bloom's Syndrome.

Sasaki, H., Iyer, S. V., Sasaki, K., Tawfik, O. W. & Iwakuma, T. 2015. An improved intrafemoral injection with minimized leakage as an orthotopic mouse model of osteosarcoma. *Anal Biochem,* 486(70-4.

Sato, N., Funayama, N., Nagafuchi, A., Yonemura, S. & Tsukita, S. 1992. A gene family consisting of ezrin, radixin and moesin. Its specific localization at actin filament/plasma membrane association sites. *J Cell Sci,* 103 (Pt 1)(131-43.

Sato, S., Tang, Y. J., Wei, Q., Hirata, M., Weng, A., Han, I., Okawa, A., Takeda, S., Whetstone, H., Nadesan, P., Kirsch, D. G., Wunder, J. S. & Alman, B. A. 2016. Mesenchymal Tumors Can Derive from Ng2/Cspg4-Expressing Pericytes with beta-Catenin Modulating the Neoplastic Phenotype. *Cell Rep,* 16(4)**,** pp 917-27.

Sato, S., Tang, Y. J., Wei, Q., Hirata, M., Weng, A., Han, I., Okawa, A., Takeda, S., Whetstone, H., Nadesan, P., Kirsch, D. G., Wunder, J. S., Alman, B. A. & Canada, G. o. C. N. R. C. 2011. Mesenchymal tumors can derive from Ng2/Cspg4 expressing pericytes with β-catenin modulating the neoplastic phenotype.

Schlingemann, R. O., Rietveld, F. J., de Waal, R. M., Ferrone, S. & Ruiter, D. J. 1990. Expression of the high molecular weight melanoma-associated antigen by pericytes during angiogenesis in tumors and in healing wounds. *Am J Pathol,* 136(6)**,** pp 1393-405.

Schneider, S., Bosse, F., D'Urso, D., Muller, H., Sereda, M. W., Nave, K., Niehaus, A., Kempf, T., Schnolzer, M. & Trotter, J. 2001. The AN2 protein is a novel marker for the Schwann cell lineage expressed by immature and nonmyelinating Schwann cells. *J Neurosci,* 21(3)**,** pp 920-33.

Schoenfeld, A. J., Wang, X., Wang, Y., Hornicek, F. J., Nielsen, G. P., Duan, Z., Ferrone, S. & Schwab, J. H. 2016. CSPG4 as a prognostic biomarker in chordoma. *Spine J,* 16(6)**,** pp 722-7.

Schwarz, R., Bruland, O., Cassoni, A., Schomberg, P. & Bielack, S. 2009. The role of radiotherapy in oseosarcoma. *Cancer Treat Res,* 152(147-64.

Schwenkert, M., Birkholz, K., Schwemmlein, M., Kellner, C., Kugler, M., Peipp, M., Nettelbeck, D. M., Schuler-Thurner, B., Schaft, N., Dorrie, J., Ferrone, S., Kampgen, E. & Fey, G. H. 2008. A single chain immunotoxin, targeting the melanoma-associated chondroitin sulfate proteoglycan, is a potent inducer of apoptosis in cultured human melanoma cells. *Melanoma Res,* 18(2)**,** pp 73-84.

Scott, A. M., Allison, J. P. & Wolchok, J. D. 2012. Monoclonal antibodies in cancer therapy. *Cancer Immun.*

Sellers, D. L., Maris, D. O. & Horner, P. J. 2009. Post-injury niches induce temporal shifts in progenitor fates to direct lesion repair after spinal cord injury. *J Neurosci,* 29(20)**,** pp 6722-33.

Shan, L. Q., Qiu, X. C., Xu, Y. M., Ji, Z. G., Yang, T. T., Chen, X., Ma, B. A., Zhou, Y., Fan, Q. Y. & Yang, A. G. 2008. scFv-mediated delivery of truncated BID suppresses HER2-positive osteosarcoma growth and metastasis. *Cancer Biol Ther,* 7(11)**,** pp 1717-22.

Shapiro, F. D. & Eyre, D. R. 1982. Collagen polymorphism in extracellular matrix of human osteosarcoma. *J Natl Cancer Inst,* 69(5)**,** pp 1009-16.

Shefet-Carasso, L. & Benhar, I. 2015. Antibody-targeted drugs and drug resistance--challenges and solutions. *Drug Resist Updat,* 18(36-46.

Siitonen, H. A., Sotkasiira, J., Biervliet, M., Benmansour, A., Capri, Y., Cormier-Daire, V., Crandall, B., Hannula-Jouppi, K., Hennekam, R., Herzog, D., Keymolen, K., Lipsanen-Nyman, M., Miny, P., Plon, S. E., Riedl, S., Sarkar, A., Vargas, F. R., Verloes, A., Wang, L. L., Kaariainen, H. & Kestila, M. 2009a. The mutation spectrum in RECQL4 diseases. *Eur J Hum Genet,* 17(2)**,** pp 151-8.

Siitonen, H. A., Sotkasiira, J., Biervliet, M., Benmansour, A., Capri, Y., Cormier-Daire, V., Crandall, B., Hannula-Jouppi, K., Hennekam, R., Herzog, D., Keymolen, K., Lipsanen-Nyman, M., Miny, P., Plon, S. E., Riedl, S., Sarkar, A., Vargas, F. R., Verloes, A., Wang, L. L., Kaariainen, H. & Kestila, M. 2009b. The mutation spectrum in RECQL4 diseases. *Eur J Hum Genet,* 17(2)**,** pp 151-8.

Smith, F. O., Rauch, C., Williams, D. E., March, C. J., Arthur, D., Hilden, J., Lampkin, B. C., Buckley, J. D., Buckley, C. V., Woods, W. G., Dinndorf, P. A., Sorensen, P., Kersey, J., Hammond, D. & Bernstein, I. D. 1996. The human homologue of rat NG2, a chondroitin sulfate proteoglycan, is not expressed on the cell surface of normal hematopoietic cells but is expressed by acute myeloid leukemia blasts from poor-prognosis patients with abnormalities of chromosome band 11q23. *Blood,* 87(3)**,** pp 1123-1133.

Stallcup, W. B. 1981. The NG2 antigen, a putative lineage marker: immunofluorescent localization in primary cultures of rat brain. *Dev Biol,* 83(1)**,** pp 154-65.

Stallcup, W. B. 2017. NG2 Proteoglycan Enhances Brain Tumor Progression by Promoting Beta-1 Integrin Activation in both Cis and Trans Orientations. *Cancers (Basel),* 9(4)**,** pp.

Stallcup, W. B., Dahlin, K. & Healy, P. 1990. Interaction of the NG2 chondroitin sulfate proteoglycan with type VI collagen. *J Cell Biol,* 111(6 Pt 2)**,** pp 3177-88.

Stallcup, W. B. & Dahlin-Huppe, K. 2001. Chondroitin sulfate and cytoplasmic domain-dependent membrane targeting of the NG2 proteoglycan promotes retraction fiber formation and cell polarization. *J Cell Sci,* 114(Pt 12)**,** pp 2315-25.

Stallcup, W. B. & Huang, F. J. 2008. A role for the NG2 proteoglycan in glioma progression. *Cell Adh Migr,* 2(3)**,** pp 192-201.

Stegmuller, J., Schneider, S., Hellwig, A., Garwood, J. & Trotter, J. 2002. AN2, the mouse homologue of NG2, is a surface antigen on glial precursor cells implicated in control of cell migration. *J Neurocytol,* 31(6-7)**,** pp 497-505.

Stephens, P. J., Greenman, C. D., Fu, B., Yang, F., Bignell, G. R., Mudie, L. J., Pleasance, E. D., Lau, K. W., Beare, D., Stebbings, L. A., McLaren, S., Lin, M. L., McBride, D. J., Varela, I.,

Nik-Zainal, S., Leroy, C., Jia, M., Menzies, A., Butler, A. P., Teague, J. W., Quail, M. A., Burton, J., Swerdlow, H., Carter, N. P., Morsberger, L. A., Iacobuzio-Donahue, C., Follows, G. A., Green, A. R., Flanagan, A. M., Stratton, M. R., Futreal, P. A. & Campbell, P. J. 2011. Massive genomic rearrangement acquired in a single catastrophic event during cancer development. *Cell,* 144(1)**,** pp 27-40.

Sugiarto, S., Persson, A. I., Munoz, E. G., Waldhuber, M., Lamagna, C., Andor, N., Hanecker, P., Ayers-Ringler, J., Phillips, J., Siu, J., Lim, D. A., Vandenberg, S., Stallcup, W., Berger, M. S., Bergers, G., Weiss, W. A. & Petritsch, C. 2011. Asymmetry-defective oligodendrocyte progenitors are glioma precursors. *Cancer Cell,* 20(3)**,** pp 328-40.

Sulzbacher, I., Traxler, M., Mosberger, I., Lang, S. & Chott, A. 2000. Platelet-derived growth factor-AA and -alpha receptor expression suggests an autocrine and/or paracrine loop in osteosarcoma. *Mod Pathol,* 13(6)**,** pp 632-7.

Sun, M., Zhou, C., Zeng, H., Puebla-Osorio, N., Damiani, E., Chen, J., Wang, H., Li, G., Yin, F., Shan, L., Zuo, D., Liao, Y., Wang, Z., Zheng, L., Hua, Y. & Cai, Z. 2015. Hiporfin-mediated photodynamic therapy in preclinical treatment of osteosarcoma. *Photochem Photobiol,* 91(3)**,** pp 533-44.

Tao, J., Jiang, M. M., Jiang, L., Salvo, J. S., Zeng, H. C., Dawson, B., Bertin, T. K., Rao, P. H., Chen, R., Donehower, L. A., Gannon, F. & Lee, B. H. 2014. Notch activation as a driver of osteogenic sarcoma. *Cancer Cell,* 26(3)**,** pp 390-401.

Taran, S. J., Taran, R. & Malipatil, N. B. 2017. Pediatric Osteosarcoma: An Updated Review. *Indian J Med Paediatr Oncol.*

Terada, N., Ohno, N., Murata, S., Katoh, R., Stallcup, W. B. & Ohno, S. 2006. Immunohistochemical study of NG2 chondroitin sulfate proteoglycan expression in the small and large intestines. *Histochem Cell Biol,* 126(4)**,** pp 483-90.

Tillet, E., Gential, B., Garrone, R. & Stallcup, W. B. 2002. NG2 proteoglycan mediates beta(1) integrin-independent cell adhesion and spreading on collagen VI. *Journal of Cellular Biochemistry,* 86(4)**,** pp 726-736.

Tillet, E., Ruggiero, F., Nishiyama, A. & Stallcup, W. B. 1997. The membrane-spanning proteoglycan NG2 binds to collagens V and VI through the central nonglobular domain of its core protein. *J Biol Chem,* 272(16)**,** pp 10769-76.

Troisi, R., Masters, M. N., Joshipura, K., Douglass, C., Cole, B. F. & Hoover, R. N. 2006. Perinatal factors, growth and development, and osteosarcoma risk. *Br J Cancer.*

Trotter, J., Karram, K. & Nishiyama, A. 2010. NG2 cells: Properties, progeny and origin. *Brain Res Rev,* 63(1-2)**,** pp 72-82.

Tschernia, N., Orentas, R. & Mackall, C. 2014. Chondroitin sulfate proteoglycan 4 specific chimeric antigen receptor therapy for pediatric solid tumors. *J Immunother Cancer.*

Unniyampurath, U., Pilankatta, R. & Krishnan, M. N. 2016. RNA Interference in the Age of CRISPR: Will CRISPR Interfere with RNAi? *Int J Mol Sci,* 17(3)**,** pp 291.

Van Sinderen, M., Cuman, C., Winship, A., Menkhorst, E. & Dimitriadis, E. 2013. The chrondroitin sulfate proteoglycan (CSPG4) regulates human trophoblast function. *Placenta,* 34(10)**,** pp 907-12.

Vander Griend, R. A. 1996. Osteosarcoma and its variants. *Orthop Clin North Am,* 27(3)**,** pp 575-81.

Veres, A., Gosis, B. S., Ding, Q., Collins, R., Ragavendran, A., Brand, H., Erdin, S., Cowan, C. A., Talkowski, M. E. & Musunuru, K. 2014. Low incidence of off-target mutations in individual CRISPR-Cas9 and TALEN targeted human stem cell clones detected by whole-genome sequencing. *Cell Stem Cell,* 15(1)**,** pp 27-30.

Vial, D. & McKeown-Longo, P. J. 2008. PAI-1 stimulates fibronectin matrix assembly in osteosarcoma cells through crosstalk between the αvβ5 and α5β1 integrins. *J Cell Sci,* 121(Pt 10)**,** pp 1661-70.

Vial, D., Monaghan-Benson, E. & McKeown-Longo, P. J. 2006. Coordinate regulation of fibronectin matrix assembly by the plasminogen activator system and vitronectin in human osteosarcoma cells. *Cancer Cell Int.*

Viguet-Carrin, S., Garnero, P. & Delmas, P. D. 2006. The role of collagen in bone strength. *Osteoporos Int,* 17(3)**,** pp 319-36.

Vihinen, P., Riikonen, T., Laine, A. & Heino, J. 1996. Integrin alpha 2 beta 1 in tumorigenic human osteosarcoma cell lines regulates cell adhesion, migration, and invasion by interaction with type I collagen. *Cell Growth Differ,* 7(4)**,** pp 439-47.

Wang, J., Svendsen, A., Kmiecik, J., Immervoll, H., Skaftnesmo, K. O., Planaguma, J., Reed, R. K., Bjerkvig, R., Miletic, H., Enger, P. O., Rygh, C. B. & Chekenya, M. 2011a. Targeting the NG2/CSPG4 proteoglycan retards tumour growth and angiogenesis in preclinical models of GBM and melanoma. *PLoS One,* 6(7)**,** pp e23062.

Wang, J., Svendsen, A., Kmiecik, J., Immervoll, H., Skaftnesmo, K. O., Planaguma, J., Reed, R. K., Bjerkvig, R., Miletic, H., Enger, P. O., Rygh, C. B. & Chekenya, M. 2011b. Targeting the NG2/CSPG4 proteoglycan retards tumour growth and angiogenesis in preclinical models of GBM and melanoma. *PLoS One,* 6(7)**,** pp e23062.

Wang, L. L., Levy, M. L., Lewis, R. A., Chintagumpala, M. M., Lev, D., Rogers, M. & Plon, S. E. 2001. Clinical manifestations in a cohort of 41 Rothmund-Thomson syndrome patients. *Am J Med Genet,* 102(1)**,** pp 11-7.

Wang, X., Katayama, A., Wang, Y., Yu, L., Favoino, E., Sakakura, K., Favole, A., Tsuchikawa, T., Silver, S., Watkins, S. C., Kageshita, T. & Ferrone, S. 2011c. Functional characterization of an scFv-Fc antibody that immunotherapeutically targets the common cancer cell surface proteoglycan CSPG4. *Cancer Res,* 71(24)**,** pp 7410-22.

Wang, X., Osada, T., Wang, Y., Yu, L., Sakakura, K., Katayama, A., McCarthy, J. B., Brufsky, A., Chivukula, M., Khoury, T., Hsu, D. S., Barry, W. T., Lyerly, H. K., Clay, T. M. & Ferrone, S. 2010. CSPG4 protein as a new target for the antibody-based immunotherapy of triple-negative breast cancer. *J Natl Cancer Inst,* 102(19)**,** pp 1496-512.

Wang Y., Sabbatino F., Yu L., Favoino E., Wang X., Ligorio M., Ferrone S., Schwab J.H., Ferrone C.R. 2013. Tumor antigen-specific monoclonal antibody-based immunotherapy, cancer initiating cells and disease recurrence. B. Bonavida (Ed.), Resistance to Targeted Anti-Cancer Therapeutics, Springer-Verlag New York, New York, NY, pp. 25-47

Wanshura L.E.C., Yang J., M.A., J.H., Dudek A.Z., McCarthy J.B. CSPG4 mediates melanoma cell survival in response to BRAFV600E inhibition. [abstract]. In: Proceedings of the 104th Annual Meeting of the American Association for Cancer Research; 2013 Apr 6-10; Washington, DC. Philadelphia (PA): AACR; Cancer Res 2013;73(8 Suppl):Abstract nr 4058. doi:10.1158/1538-7445.AM2013-4058

Warta, R., Herold-Mende, C., Chaisaingmongkol, J., Popanda, O., Mock, A., Mogler, C., Osswald, F., Herpel, E., Kustner, S., Eckstein, V., Plass, C., Plinkert, P., Schmezer, P. & Dyckhoff, G. 2014. Reduced promoter methylation and increased expression of CSPG4 negatively influences survival of HNSCC patients. *Int J Cancer,* 135(11)**,** pp 2727-34.

Wei, L., Yang, Y., Zhang, X. & Yu, Q. 2002. Anchorage-independent phosphorylation of p130(Cas) protects lung adenocarcinoma cells from anoikis. *J Cell Biochem,* 87(4)**,** pp 439-49.

Wen, Y., Makagiansar, I. T., Fukushi, J., Liu, F. T., Fukuda, M. N. & Stallcup, W. B. 2006. Molecular basis of interaction between NG2 proteoglycan and galectin-3. *J Cell Biochem,* 98(1)**,** pp 115-27.

Whelan, J., McTiernan, A., Cooper, N., Wong, Y. K., Francis, M., Vernon, S. & Strauss, S. J. 2012. Incidence and survival of malignant bone sarcomas in England 1979-2007. *Int J Cancer,* 131(4)**,** pp E508-17.

Wilson, B. R., Giovanna. Ferrone, Soldano. 2017. Immunochemical characterization of a human high molecular weight — melanoma associated antigen identified with monoclonal antibodies | SpringerLink.

Wilson, B. S., Imai, K., Natali, P. G. & Ferrone, S. 1981. Distribution and molecular characterization of a cell-surface and a cytoplasmic antigen detectable in human melanoma cells with monoclonal antibodies. *Int J Cancer,* 28(3)**,** pp 293-300.

Winship, A., Van Sinderen, M., Heffernan-Marks, A. & Dimitriadis, E. 2017. Chondroitin sulfate proteoglycan protein is stimulated by interleukin 11 and promotes endometrial epithelial cancer cell proliferation and migration. *Int J Oncol,* 50(3)**,** pp 798-804.

Wolf, P. & Elsasser-Beile, U. 2009. Pseudomonas exotoxin A: from virulence factor to anti-cancer agent. *Int J Med Microbiol,* 299(3)**,** pp 161-76.

Wong, F. L., Boice, J. D., Jr., Abramson, D. H., Tarone, R. E., Kleinerman, R. A., Stovall, M., Goldman, M. B., Seddon, J. M., Tarbell, N., Fraumeni, J. F., Jr. & Li, F. P. 1997. Cancer incidence after retinoblastoma. Radiation dose and sarcoma risk. *Jama,* 278(15)**,** pp 1262-7.

Xiao, W., Mohseny, A. B., Hogendoorn, P. C. & Cleton-Jansen, A. M. 2013. Mesenchymal stem cell transformation and sarcoma genesis. *Clin Sarcoma Res,* 3(1)**,** pp 10.

Yang, J., Price, M. A., Neudauer, C. L., Wilson, C., Ferrone, S., Xia, H., Iida, J., Simpson, M. A. & McCarthy, J. B. 2004a. Melanoma chondroitin sulfate proteoglycan enhances FAK and ERK activation by distinct mechanisms. *J Cell Biol,* 165(6)**,** pp 881-91.

Yang, J. B., Price, M. A., Neudauer, C. L., Wilson, C., Ferrone, S., Xia, H., Iida, J., Simpson, M. A. & McCarthy, J. B. 2004b. Melanoma chondroitin sulfate proteoglycan enhances FAK and ERK activation by distinct mechanisms. *Journal of Cell Biology,* 165(6)**,** pp 881-891.

Yi, E. S., Shmookler, B. M., Malawer, M. M. & Sweet, D. E. 1991. Well-differentiated extraskeletal osteosarcoma. A soft-tissue homologue of parosteal osteosarcoma. *Arch Pathol Lab Med,* 115(9)**,** pp 906-9.

Yu, L., Favoino, E., Wang, Y., Ma, Y., Deng, X. & Wang, X. 2011. The CSPG4-specific monoclonal antibody enhances and prolongs the effects of the BRAF inhibitor in melanoma cells. *Immunol Res,* 50(2-3)**,** pp 294-302.

Yuan, P., Zhang, H., Cai, C., Zhu, S., Zhou, Y., Yang, X., He, R., Li, C., Guo, S., Li, S., Huang, T., Perez-Cordon, G., Feng, H. & Wei, W. 2015. Chondroitin sulfate proteoglycan 4 functions as the cellular receptor for Clostridium difficile toxin B. *Cell Res,* 25(2)**,** pp 157-68.

Zanotti, S. & Canalis, E. 2016. Notch Signaling and the Skeleton. *Endocr Rev,* 37(3)**,** pp 223-53.

Zeng, H., Zhang, Z., Dai, X., Chen, Y., Ye, J. & Jin, Z. 2016. Increased Expression of microRNA-199b-5p Associates with Poor Prognosis Through Promoting Cell Proliferation, Invasion and Migration Abilities of Human Osteosarcoma. *Pathol Oncol Res,* 22(2)**,** pp 253-60.

Zhang, J., Walsh, M. F., Wu, G., Edmonson, M. N., Gruber, T. A., Easton, J., Hedges, D., Ma, X., Zhou, X., Yergeau, D. A., Wilkinson, M. R., Vadodaria, B., Chen, X., McGee, R. B., Hines-Dowell, S., Nuccio, R., Quinn, E., Shurtleff, S. A., Rusch, M., Patel, A., Becksfort, J. B., Wang, S., Weaver, M. S., Ding, L., Mardis, E. R., Wilson, R. K., Gajjar, A., Ellison, D. W., Pappo, A. S., Pui, C. H., Nichols, K. E. & Downing, J. R. 2015. Germline Mutations in Predisposition Genes in Pediatric Cancer. *N Engl J Med,* 373(24)**,** pp 2336-46.

Zhao, S., Lu, N., Chai, Y. & Yu, X. 2015. Rapamycin inhibits tumor growth of human osteosarcomas. *J buon,* 20(2)**,** pp 588-94.

Zhou, W. Y., Zheng, H., Du, X. L. & Yang, J. L. 2016. Characterization of FGFR signaling pathway as therapeutic targets for sarcoma patients. *Cancer Biol Med,* 13(2)**,** pp 260-8.

Zhu, L. B., Jiang, J., Zhu, X. P., Wang, T. F., Chen, X. Y., Luo, Q. F., Shu, Y., Liu, Z. L. & Huang, S. H. 2014. Knockdown of Aurora-B inhibits osteosarcoma cell invasion and migration via modulating PI3K/Akt/NF-κB signaling pathway. *Int J Clin Exp Pathol,* 7(7)**,** pp 3984-91.

Zhu, X., Hill, R. A. & Nishiyama, A. 2008. NG2 cells generate oligodendrocytes and gray matter astrocytes in the spinal cord. *Neuron Glia Biol,* 4(1)**,** pp 19-26.